UPPSALA
UNIVERSITET

FYSMAS1053

Examensarbete 30 hp
Februari 2017

A Measurement Level Module for a Pellet Tracking System

Jenny Regina

Masterprogrammet i fysik
Master Programme in Physics

UPPSALA
UNIVERSITET

Teknisk- naturvetenskaplig fakultet
UTH-enheten

Besöksadress:
Ångströmlaboratoriet
Lägerhyddsvägen 1
Hus 4, Plan 0

Postadress:
Box 536
751 21 Uppsala

Telefon:
018 – 471 30 03

Telefax:
018 – 471 30 00

Hemsida:
http://www.teknat.uu.se/student

Abstract

A Measurement Level Module for a Pellet Tracking System

Jenny Regina

This report concerns a detection module used for a pellet tracking system. Spheres of frozen hydrogen known as pellets can be used as internal targets in hadron physics experiments. Pellets are created some distance above the accelerator beam and directed in a pellet beam pipe to intersect the accelerator beam. To determine the position of a pellet in the interaction region in the case of an interaction, the pellets need to be tracked. This is done using tracking sections along the pellet beam pipe with measurement levels containing lasers illuminating the pellets and cameras, detecting the light. The pellet position in the interaction region can be reconstructed with an accuracy of 0.1 mm. To reach this accuracy there are high demands on the alignment of the cameras and lasers. Alignment by a pellet beam pipe is generally difficult so a solution enabling alignment elsewhere is desired. Therefore a detection module consisting of a plate with cameras and lasers mounted to it has been constructed. These cameras and lasers can be aligned in an alignment bench setup before being transported to a pellet beam pipe. The alignment of the cameras and lasers on the detection module must be maintained under certain conditions e.g. transportation, temperature changes, exposure to vibrations. This report covers investigations regarding the mechanical stability of the detection module under these conditions. Different alignment bench targets are investigated. The effects of the optics of the cameras and lasers and the functionality of the detection module are investigated.

Handledare: Hans Calén
Ämnesgranskare: Tord Johansson
Examinator: Andreas Korn
FYSMAS1053

Contents

Chapter 1

Populärvetenskaplig Sammanfattning

Syftet med projektet som presenteras i denna rapport är att undersöka stabiliteten och andra effekter hos en mätmodulsprototyp som används för att spåra pelletar. Pelletar är små, frysta vätekulor som används som mål för kollisioner med partiklar i acceleratorer vid hadronfysikexperiment. Pelletar planeras att användas som mål vid det kommande PANDA (anti-Proton ANnihilation at Darmstadt) experimentet vid HESR (High Energy Storage Ring) i Darmstadt, Tyskland och de har tidigare använts vid WASA (Wide Angel Shower Apparatus) experimentet vid CELSIUS vid TSL (The Svedberg Laboratoriet), Uppsala och senare vid COSY (COoler SYnchrotron), Jülich, Tyskland. Pelletstrålen skapas några meter från kollisionsområdet och riktas ner mot acceleratorstrålen där pelletarna växelverkar med strålens partiklar. Detektorsystemet måste placeras närmst partikelstrålen, därför måste pelletarna skapas en bit bort. För att veta om en viss pellet befann sig i kollisionsområdet och dess exakta position vid en kollision måste de individuella pelletarna spåras. Denna spårning görs med hjälp av ett optiskt spårningssystem bestående av en spårningssektion ovanför och en under kollisionsområdet där varje spårningssektion innehåller mätnivåer bestående av lasrar som belyser pelletstrålen och kameror som registrerar ljuset från pelletarna. Kamerornas siktlinje och laserstrålarna på en mätnivå måste sammanfalla inom ett smalt område vid pelletstrålen. Spårningssystemet för pelletar testas vid en teststation för pelletar, UPTS (Uppsala Pellet Test Station) vid TSL, här har även tekniken för att skapa pelletar utvecklats.

Upplinjeringen av kameror och lasrar i ett plan måste göras mekaniskt medan upplinjeringen av planen relativt varandra görs i spårrekonstruktionen. Upplinjeringen av planen med acceleratorstrålen görs genom att inkludera reaktionsfrekvensen som en funktion av pelletpositionen. Brist på utrymme vid detektorer och svårigheter med siktförhållanden gör det lämpligare att sköta den mekaniska upplinjeringen av kameror och lasrar på en arbetsbänk. Bland annat på grund av detta har en mätmodul skapats på vilken två kameror, två lasrar för mätning av pelletar samt en laser för upplinjeringssyfte är monterade. Dessa kameror och lasrar kan linjeras upp vid en arbetsbänk och sedan kan mätmodulen relativt enkelt förflyttas och monteras vid mätnivån vid teststationen för pelletar. Kamerorna och lasrarna är placerade på kamera- och laser-plattor på modulplattan vilka kan finjusteras i höjdled samt

roteras vid upplinjering med hjälp av justeringsskruvar, också kallade mikrometerskruvar eftersom de i princip har mikrometerprecision. En upplinjeringsprocedur för båda kamerorna och alla tre lasrarna har utvecklats. En annan fördel med mätmodulen är att dess kameror och lasrar kan upplinjeras med ett mål som är mycket enklare att ställa upp än att sätta igång en pelletkörning. Dessutom har en pelletsstråle en rumsutsträckning i det vertikala kamera- och laser-planet vilken gör den olämpliga att använda för upplinjering. Vid arbetsbänken kan ett mål med liten utsträckning i det vertikala planet, tex fiskelinor placerade i behållare, användas för upplinjering vid arbetsbänken. För upplinjering kan ett konstant laserljus användas för belysning av fiskelinorna. För att undersöka egenskaper hos modulen samt optiken hos kamerorna och lasrarna som används kan laserljus pulseras så att fiskelinorna mer liknar pelletar.

Upplinjeringen av mätmodulens kameror och lasrar måste vara stabil under vissa förhållanden så som transport tex mellan arbetsbänken och mätnivån vid pelletstrålen, mindre förändringar i rumstemperatur samt exponering för vibrationer från vakuumpumpar som förekommer vid pågående experiment. Stabiliteten hos upplinjeringen av kameror och lasrar under dessa förhållanden har testats och visat sig vara stabil under dessa. Eftersom det används magnetfält vid partikel detektorerna under pågående experiment måste optiken hos kamerorna och lasrarna förbli oförändrad vid exponering för magnetfälten. Optiken hos kamerorna och lasrarna har tidigare testats för detta och inte visat några tecken på att påverkas av magnetiska fält.

Kamerorna som används läser ut en linje pixlar åt gången med en exponeringscykel på 12.5 μs. Denna exponeringscykel innefattar en dödtid på ca 2.5 μs som behövs för elektronisk överföring av signaler. Under denna tid samlar inte kamerorna något ljus vilket leder till en teoretisk ineffektivitet på runt 20% eftersom mycket korta ljussignaler inte detekteras under denna tid. I verkligheten har ljussignalerna en tidsutsträckning men dödtiden bidrar ändå med en viss ineffektivitet för väldigt korta ljussignaler. Detta måste kunna hanteras. Genom att placera två kameror mitt emot varandra (som kamerorna på mätmodulen är placerade) och förskjuta exponeringscykeln hos en kamera relativt exponeringscykeln hos den andra kameran så dötiden hos den senare hamnar i den första kamerans exponeringstid kan man garantera ett minst en kamera alltid detekterar ljussignaler, dvs. förbipasserande pelletar. Hur stor andel av de detekterade pelletarna som detekteras av bara en kamera, båda kamerorna i samma exponeringscykel eller av båda kamerorna i olika exponeringscykler beror på den relativa förskjutningen mellan exponeringscyklerna. Detta har undersökts som ett test av upplinjeringen av kamerorna och lasrarna på mätmodulen eftersom denna typ av analys ställer höga krav på upplinjeringen. Detta har både undersökts med pelletar och med en fiskelina vid arbetsbänken där signallängden på lasrarna kan justeras. Andra effekter som påverkar mätningarna är kamerainställningar så som fokus och bländare. Inställningarna av dessa kan enkelt optimeras vid arbetsbänken.

Vid mätningar av pelletar är det viktigt att kamerornas exponeringscykler är synkroniserade. Detta kan kontrolleras med hjälp av så kallade synkroniseringsdioder som placeras framför vardera kameran. Synkroniseringsdioderna är ljusdioder som mottar samma signal från en pulsgenerator för att försäkra att de lyser samtidigt. Genom att under en mätning kontrollera vilken exponeringscykel kamerorna ser samma synkroniseringsdiod signal i kan det kontrolleras att exponeringscyklerna är

synkroniserade. Ovan beskrivna synkroniseringsdioder har installerats på mätmodulen.

I framtiden kommer en ny nivå placeras 60 mm ovanför den befintliga DM plattan vid testbänken. Dessa kommer sedan kunna monteras isär för separat förflyttning till och montering vid teststationen för pelletar. Det finns också en möjlighet att reducera vikten på mätmodulen som för närvarande är ca 8 kg genom att hål borras på lämpliga ställen på modulplattan. Dessa hål kommer att möjliggöra visuell inspektion av komponenter på tex den undre nivån av mätmodulen utan att de monteras isär. En reduktion av vikten är även bra för att förenkla hanteringen av mätmodulen vid transport.

Chapter 2

Introduction

The aim of the project presented in this report is to investigate the possibilities of improvements of a DM (Detection Module[1]) used for pellet tracking. Pellets are small spheres of frozen hydrogen which are planned to be used as internal targets in the hadron physics experiment PANDA (anti-Proton ANnihilation at DArmstadt) at the future accelerator HESR (High Energy Storage Ring) at FAIR (Facility for Antiproton and Ion Research), Darmstadt, Germany [1]. Anti-protons will be accelerated and interact with a target. One such target is a stream of pellets which is created some distance away from, approximately 2.7 m above the accelerator beam and directed via a pellet beam pipe to intersect the anti-proton beam in an interaction region. In order to accurately reconstruct and analyze the hadronic events, the pellets need to be properly tracked and the exact position of a single pellet in the interaction region at the time of an interaction needs to be determined. Pellets have previously been used as target at WASA (Wide Angel Shower Apparatus) first at the CELSIUS storage ring at TSL (The Svedberg Laboratoriet), Uppsala and later at COSY (COoler SYnchrotron), Jülich, Germany.

Pellets and the pellet tracking system are currently being developed and tested at the UPTS (Uppsala Pellet Test Station). The tracking system consists of lasers illuminating the pellets at different positions in the pellet beam pipe and cameras detecting the light. The cameras and lasers are to be placed in several measurement levels in one tracking section above the accelerator beam and one tracking section below. LS (Line-Scan) cameras reading out one line of pixels at the time are used as well as STR (Structured-Light-Pattern diode) lasers, which can be set to have a very thin horizontal beam line profile in the pellet beam region. The alignment between the cameras and lasers in one plane must be done mechanically. In order to reconstruct the pellet position in the interaction region with the desired accuracy there are high demands on the pellet detection efficiency and the alignment of the cameras and lasers. Because of lack of space and poor sight conditions at the pellet beam pipe at experiments, the mechanical alignment of the cameras and lasers is difficult and sometimes impossible to perform on site, by the pellet beam pipe. Hence, there is a need to be able to align cameras and lasers elsewhere. The DM (Detection Module) consists of a DM plate with two cameras and three

[1]Project supported by the "Carl Tryggers Stiftelse för Vetenskaplig Forskning" under contract CTS 14:225.

lasers mounted to it. Two lasers are optimized for pellet detection and one laser is optimized for alignment purposes. The cameras and lasers of the DM can be aligned in an alignment bench setup and the DM can be transported to the tracking section a pellet beam pipe for pellet measurements. This requires the alignment to be stable throughout the transportation. During experiments slight changes in the room temperature are expected as well as vibrations from the vacuum pumps and machinery. The stability of the alignment under these conditions has been examined. Additional reasons for needing a construction such as the DM are the possibilities it provides to perform the alignment of cameras and lasers as well as testing the optics of the cameras and lasers with a more simple target to set up than starting a pellet run. The pellet stream have a slight spread in the horizontal plane making it unfit for alignment purposes where the position of the target should be quite accurately known. Another, simpler and more easily controlled, type of target can be set up in the alignment bench setup.

2.1 Background

The PANDA project is a hadron physics experiment designed to investigate physics of the strong interaction using antiprotons. PANDA is currently under construction at the HESR accelerator at FAIR in Darmstadt, Germany. In order to expand and improve the theory, QCD (Quantum Chromodynamics) will be investigated in the regime in between perturbative high energy QCD and the more unknown low energy regime. [2]

States of all quantum numbers can be created in $p\bar{p}$ collisions which makes it an advantage colliding anti-protons with hydrogen spheres containing protons. This will enable spectroscopy of charmonium which is a state containing a charm and an anti-charm quark, other states containing a charm quark such as the D-meson as well as strange and charmed baryons. Spectroscopy for double hypernuclei (where a hypernucleus is a nucleus containing at least one hyperon which is a baryon with at least one strange quark as well as nucleons) will also be possible. It will also enable searching for hybrids consisting of quark, anti-quark and excited glue as well as glueballs entirely consisting of glue, which are yet to be confirmed experimentally. [2] [3]

2.2 Pellets

Pellets are small spheres of frozen hydrogen with a diameter of $20 - 35\ \mu m$. The pellet stream as viewed from a monitor can be seen in the right photo of figure 2.1. Pellets constitute a good target due to their high density of target material of well above 10^{15} atoms/cm^2 [4], typically $2{\cdot}10^{15}{-}6{\cdot}10^{15}$ atoms/cm^2 of an individual pellet. Another pro of using pellets as internal targets is that they provide the possibility to know the position of a single pellet in the interaction region very accurately.

Pellets are created some distance above the accelerator beam (approximately 2.7 m in the PANDA experiment) due to the space needed for the detector system closer to

the accelerator beam and the interaction region. The pellets travel through thin vacuum pipes, the pellet beam pipe, towards the interaction region where interactions with the beam particles take place. The Pellets then continue a similar distance where they are finally collected in a dump where they evaporate and the hydrogen gas is removed by vacuum pumps. This prevents the pellets from scattering back into the interaction region.

Pellets are created from a hydrogen gas which is cooled to 14.1 K at which temperature it liquefies. For the cooling, helium in a closed cycle in a cold head is used. This works as a cryogenic refrigerator. The hydrogen liquid is broken up into droplets by a thin nozzle with an opening diameter of 11 μm vibrating at a frequency of 40-100 kHz. The driving pressure before the nozzle is around 400 mb or slightly higher. The pressure in the droplet chamber is around 18 mb. The velocity of the droplets is 20-30 m/s inside the droplet chamber. The droplets travel through a DC (Droplet Chamber) and reach a VIC (Vacuum Injection capillary) about 7 mm below the nozzle where they freeze due to a high pressure gradient. The pressure before the VIC is roughly 20 mb and the pressure after is of the order of 10^{-4} mb. This pressure gradient accelerates the droplets. The droplets in the droplet chamber before entering the VIC can be seen in the left photo in figure 2.1. The length of the VIC is roughly 70 mm and its inner diameter is 1.4 mm. Upon exiting the VIC the droplets have become frozen and are now pellets. The pellet velocity is then roughly 70 m/s and they travel a few mm apart. A slight spread in velocity, however, arises at the VIC. [2]

Figure 2.1: Droplets observed on a monitor during a pellet run (left). The pellet stream observed on a monitor during a pellet run, (right).

2.3 The Uppsala Pellet Test Station

Pellets and the PTR (pellet tracking system) are being tested and developed at the UPTS at TSL in Uppsala. The UPTS consists of a pellet generator and a pellet beam pipe with observation levels and a tracking section with two levels along the pipe. Regular CCD (Charge Coupled Device) cameras can be used to observe the pellet stream at the observation levels including at the tracking section. The pellet beam pipe with the pellet generator at the top can be seen in the photos of figure

2.2. The pellet stream has an angular divergence which makes the spatial spread of the pellet stream increase along the pellet beam pipe. The skimmer is a conical collimator, which can be seen in figure 2.4, designed to "filter" away pellets with a too big angular divergence from the center of the stream. The skimmer has an opening with a diameter of 2 mm and is located roughly 1.5 m below the VIC exit. The two levels of the tracking section, PTRup and PTRlow, are located around 1.9 m below the VIC exit with a spacing of roughly 60 mm. Example distributions *e.g.* the position distributions from measurements of the pellet stream at these levels can be seen in appendix A. The pellet stream has been collimated by the skimmer when it reaches this point. The six observation levels positioned along the beam pipe are;

1. The DC level is located by the droplet chamber. This observation level contains 4 observation windows every 90° in a plane and is located 76.5 mm above the VIC exit. The left image in figure 2.1 shows the image of droplets from the droplet chamber.

2. The VIC level is located directly below the VIC exit. This observation level contains 4 observation windows every 90° in a plane. The right image in 2.1 shows the image of the pellet stream at this level.

3. The PTRgen level is located 271.5 mm below the VIC exit and contains 4 observation windows every 90° in a plane as well as 2 windows for illumination between the observation windows opposite each other.

4. An observation level is located directly above the skimmer and contains 4 observation windows every 90° in a plane. 4 windows for illumination are located between the observation windows. This level is located 1513 mm below the VIC exit. Images of the pellet stream illuminated by lasers at this level can be seen from two different angles in the two bottom images on the bottom monitor in figure 2.3. The skimmer itself is also visible in these images.

5. The PTRup is the first level of the tracking chamber and is located 35 cm below the skimmer. This level contains 4 observation windows every 90° in a plane as well as 4 windows for illumination between the observation windows. This level is located 1860.2 mm below the VIC exit.

6. The PTRlow is the second level of the tracking chamber. This level contains 4 observation windows every 90° in a plane and 4 windows for illumination between the observation windows. This level is located 1940 mm below the VIC exit.

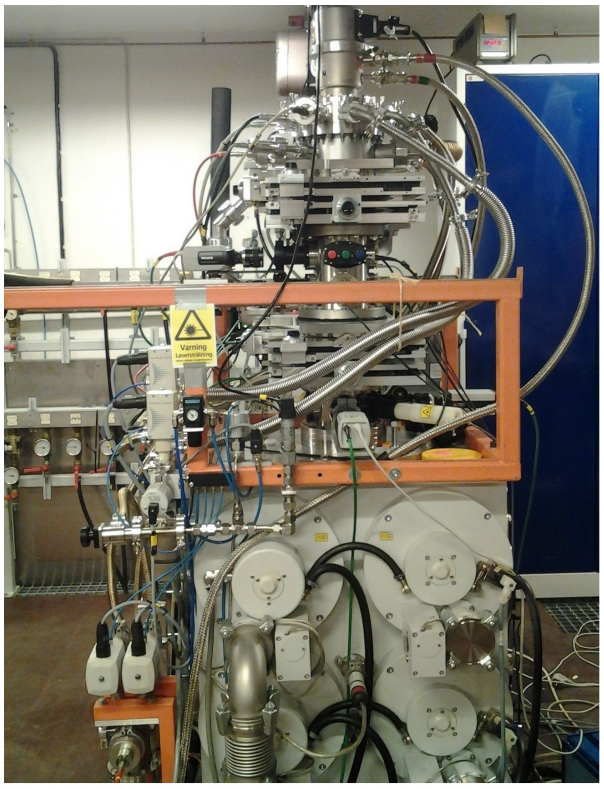

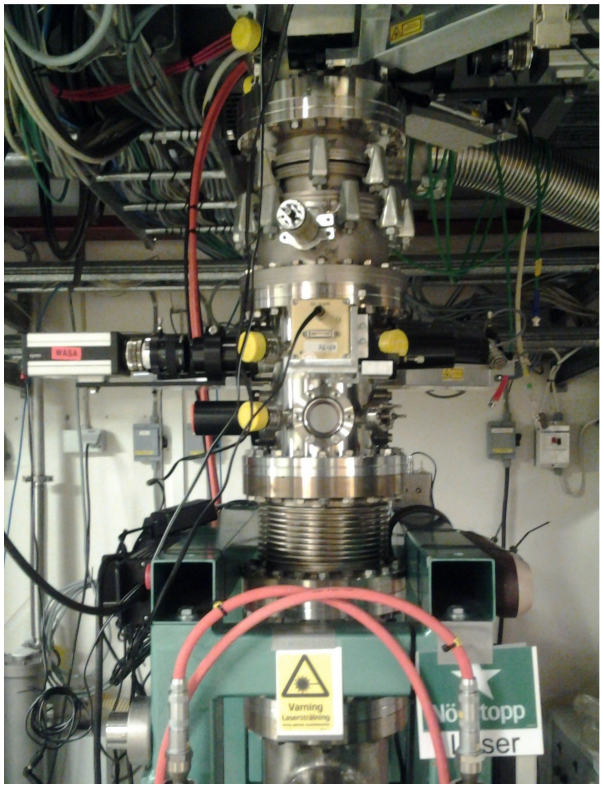

Figure 2.2: The UPTS. The upper photo shows the upper level of the UPTS with the pellet generator at the top and the upper part of the pellet beam pipe. The three uppermost observation levels are located here. The lower photo shows the lower part of the pellet beam pipe. The tracking section and the skimmer are located here.

Figure 2.3: The two monitors at the top show images from two different angles of the droplet chamber, the two monitors directly below these show images of the VIC exit from two different angles. The top two of the images on the fifth monitor show the pellet stream from two different angles at PTRgen. The two bottom images on the fifth monitor show the pellet stream directly above the skimmer. To the right of the fifth monitor the control panel for the pellet target gas and vacuum system can be seen.

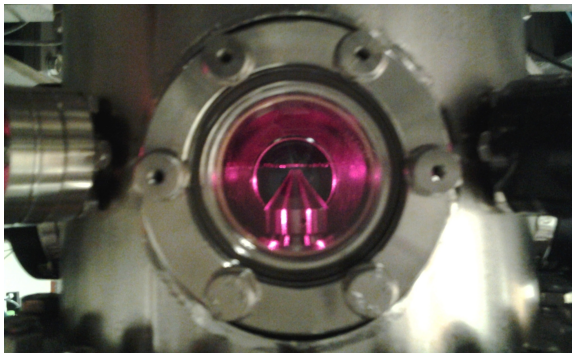

Figure 2.4: The skimmer. The pellet stream is illuminated by lasers directly above the skimmer where a large deviation from the central line of the stream can be observed for some pellets.

2.4 The Pellet Tracking System

The pellets need to be tracked before and after the interaction region by the accelerator beam. The track of each individual pellet from the production point to the interaction point is needed in order to determine the position of the pellet in the interaction region. This is done using an optical tracking system, referred to as the PTS (Pellet Tracking System), with lasers illuminating the pellets and cameras detecting the scattered light. A sketch of a pellet tracking system can be seen in figure 2.5. The cameras and lasers are positioned in consecutive levels of two cameras and two lasers in each level. The camera line of sight and the laser beam line profile in one level span a plane perpendicular to the pellet beam pipe. The distance between the measurement levels is desired to be as short as possible for the best pellet identification for the track reconstruction. However, due to the space needed for the cameras in between the levels, a spacing of 60 mm have been chosen. The cameras are facing each other in order to deal with the camera exposure cycle dead time discussed in section 6.5 for a full pellet detection efficiency. LS (Line-Scan) CCD cameras [13] are used for detection of the light from the lasers illuminating the pellets. This means that only one line of pixels is read out at the time. This gives an advantage in speed and there is no need for a two dimensional picture which would contain many empty and unnecessary pixels. One readout line consists of 512 pixels. Even and odd pixels are read out separately. One pixel is 14×14 μm^2 corresponding to an effective image size of 35×35 μm^2 at the working distance. One pixel has a light signal amplitude resolution of 12 bits. The lasers are placed at 135° with respect to the cameras since this angle gives the maximum illumination and optimizes the pellet detection efficiency. STR(Structured-Light-Pattern) diode lasers [14] are used for illumination. These lasers can be set to have a thin horizontal beam line profile with a width of roughly 3 mm and a height of less than 50 μm at the position corresponding to the pellet stream region where the lasers are also focused.

The pellet tracking system will be optimized to reconstruct the pellet position in the interaction region with a precision of 0.1 mm [7]. To reach this precision, the pellet detection efficiency in one level of a tracking section must be better than 20 μm and the camera line of sight must coincide with the laser beam line profile in a plane within 10 μm in height in the pellet beam region. This puts very high demands on the alignment of the cameras and lasers with respect to each other within a plane but also on the alignment between the planes. The alignment of the cameras and lasers with respect to each other within a plane is done mechanically. The alignment between the different levels is done in the track reconstruction procedure. The levels also need to be aligned with respect to the accelerator beam. This alignment is done by including the frequency of reactions as a function of the pellet position.

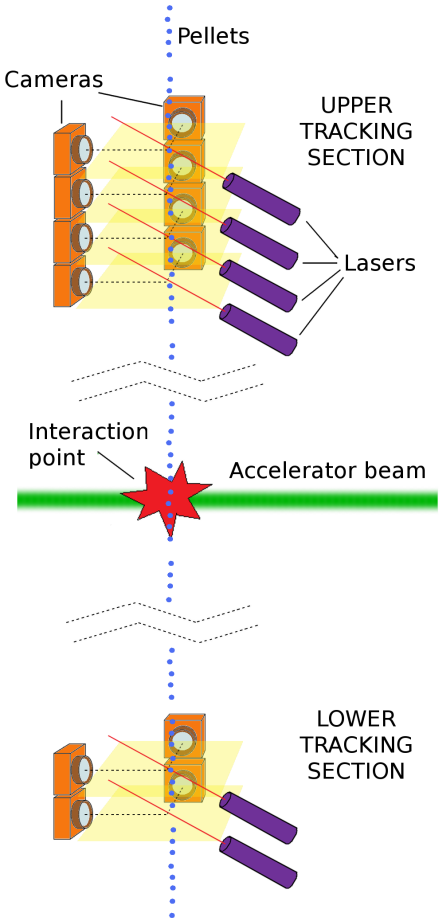

Figure 2.5: Sketch of tracking sections above and below the accelerator beam [2]. The upper tracking section contains four measurement levels with one laser and two cameras in each level. The lower tracking section contains two such levels.

Chapter 3

The Detection Module

There are three main reasons why a construction of the DM (Detection Module) was initially designed;

1. The cameras and lasers in one measurement level need to be aligned at a position away from the pellet beam pipe. At PANDA it will be impossible to perform an alignment at the pellet beam pipe due to a lack of space. At the UPTS it is also rather difficult to perform such an alignment.

2. The cameras and lasers need to be aligned with a simpler target to set up and more stable target than a pellet stream. By stable meaning that the position of the target should be fairly well known. Since a pellet stream has a spatial spread in the horizontal plane making it an unfit target for careful alignment of the cameras and lasers.

3. The optics of the cameras and lasers need to be examined with a target which is simpler to set up and more easily controllable than a pellet stream.

A construction of a DM provides a solution to all three of these needs. It provides a possibility to easily align cameras and lasers in an alignment bench setup for later use at the tracking section at the pellet beam pipe. At the alignment bench setup another target than a pellet stream can be used for alignment purposes and for testing the optics of the cameras and lasers.

The DM can be seen in figure 3.1 at the alignment bench setup and in figure 3.2 at the tracking section of the pellet beam pipe at the UPTS. The latter photo illustrates how much more difficult the alignment of the cameras and lasers is in this type of environment as compared to the alignment bench setup seen in figure 3.1. The DM consists of an aluminum plate mounted to a base plate by a dummy window-flange with a window to allow for illumination in the same position as a window on the tracking section of the PTS. There are two cameras and three lasers mounted to the DM plate. The cameras and lasers are labeled (from left to right in the half circle in figure 3.1) CamA, LasB, LasC (under installation in the photo), LasA and CamB. Two of the lasers, LasA and LasB have been optimized for pellet detection. CamA is situated at 135° relative to LasA and CamB is situated at 135° relative to LasB. This angle is chosen to give a sufficient illumination and the highest possible pellet detection efficiency. With this configuration CamA detects refracted light

from LasA and reflected light from LasB. CamB detects refracted light from LasB and reflected light from LasA. LasC is situated at 90° relative both cameras. This laser is optimized for alignment purposes and the angle has been chosen such that a similar image from an illuminated object can be obtained in both cameras. The angle at which it is positioned with respect to the lasers allows for measurements of refracted light as well as reflected light from the same laser in both cameras which in turn allows for a better and more precise comparison of the camera images. The cameras are situated opposite each other and facing each other in order to deal with the dead time in the camera exposure cycle discussed in chapter 6. The cameras and lasers are all facing a virtual center, corresponding to the pellet stream region which is also the measurement region where both the cameras and lasers should be focused. The distance between the cameras focal plane and the central position is 250 mm and the distance between the front of the lasers and the central position is 185 mm. The focal plane of the cameras and the laser beams meet 36 mm above the DM plate. The plane spanned by the laser beams and the line of sight of the cameras is referred to as the horizontal plane. The direction perpendicular to this is called the vertical direction.

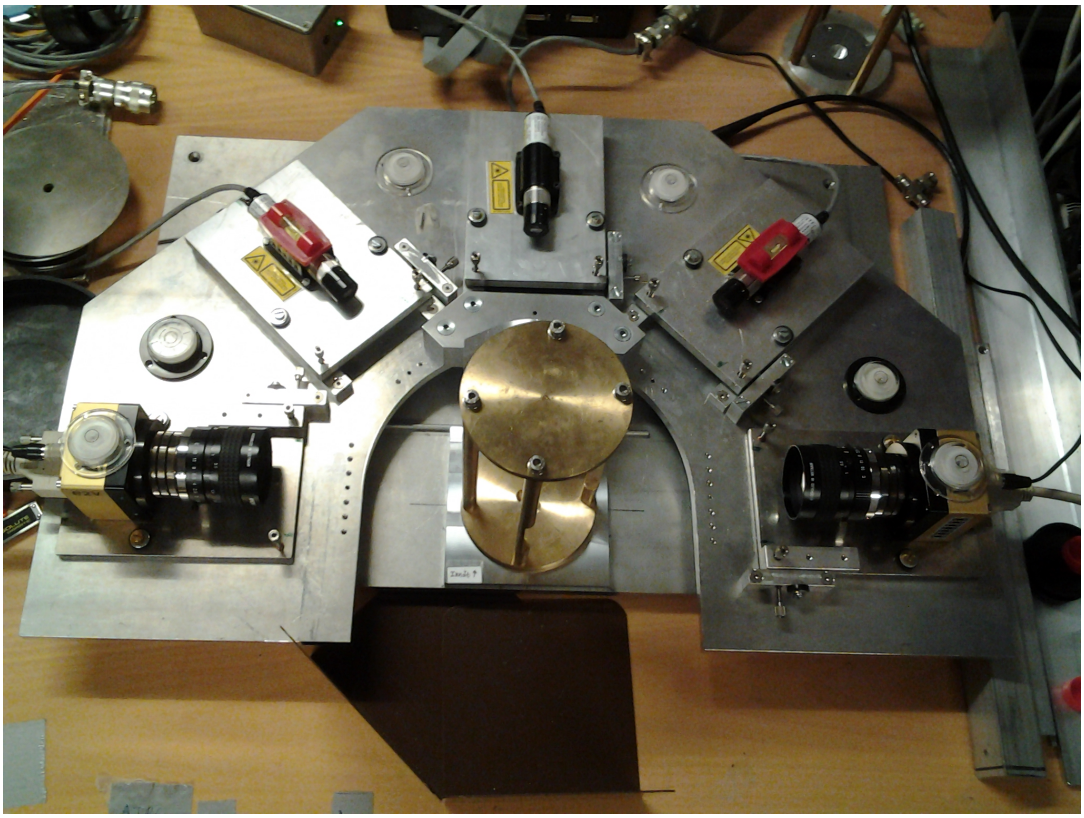

Figure 3.1: The DM. The cameras and lasers are placed in a half circle on the DM plate facing a center and they are labeled (from left to right) CamA, LasB, LasC , LasA and CamB. A target holder with five fishing lines is placed in the central position. Round spirit levels are placed at four positions on the DM plate and on both cameras for the alignment of the support structure. Two red spirit levels are placed on the two installed lasers.

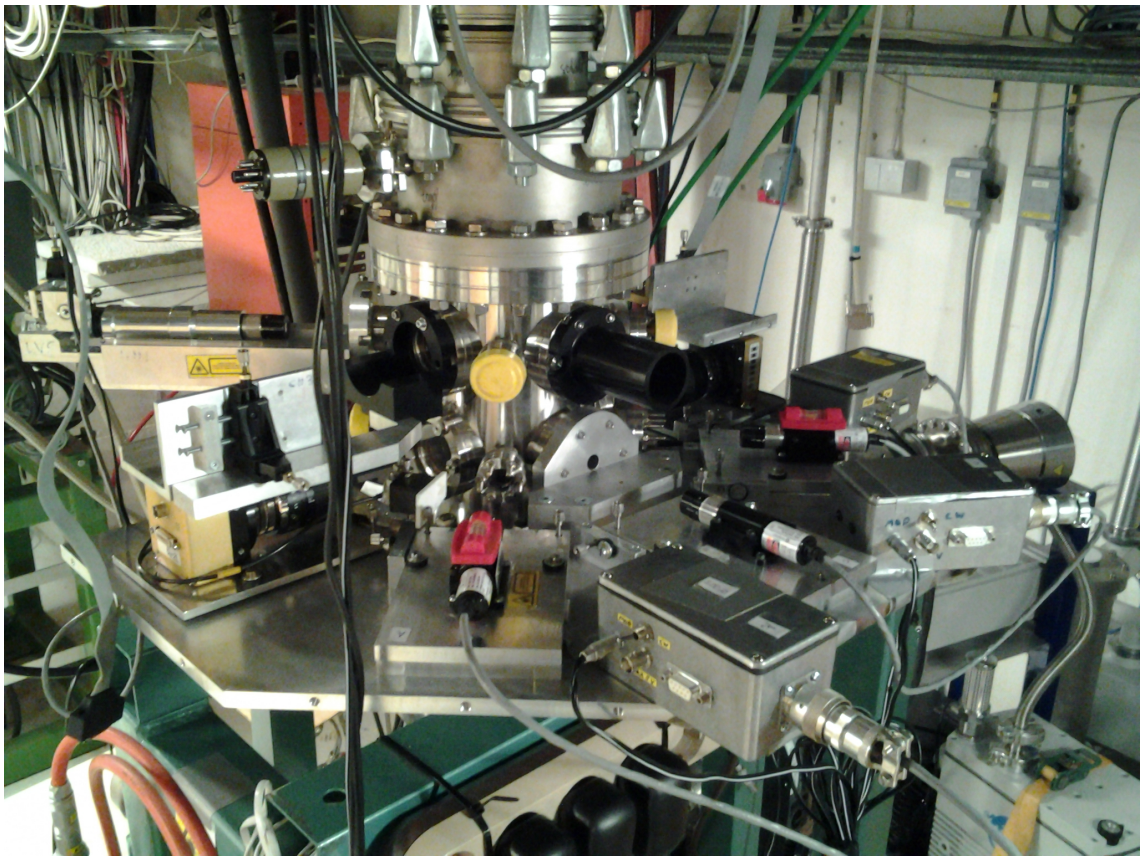

Figure 3.2: The DM at the UPTS in preparation for a pellet run. The DM is mounted to the measurement level PTRlow in the photo. Due to lack of space, connection boxes for the lasers are fastened to the DM plate which they are not in the alignment bench setup.

The alignment bench targets used are fishing lines in sets of two or five fishing lines placed in a row in a target holder. The target holder for five fishing lines can be seen in the leftmost photo of figure 3.3. Both target holders are constructed for convenient rotation as well as right/left and forward/backward displacement. A plate in which the target holder can be placed, as can be seen in the center photo of figure 3.3, has been constructed to make sure the rotations and translations as mentioned above can be done separately. Five fishing lines illuminated by a laser can be seen in the rightmost photo of figure 3.3.

Figure 3.3: A target holder with five fishing lines (left), a plate used to simplify the rotation of the target holder without making any other spatial displacements (center) and a close up on the five fishing lines illuminated with a laser beam (right).

3.1 Cameras and Lasers

The cameras used on the DM are LS cameras and the lasers are STR lasers as described in section 2.4. These can be seen in figure 3.4. Each laser is placed in a heat sink clamp which keeps the laser in position. The cameras and lasers are mounted to camera- and laser-plates to enable precision height adjustment and rotations. There are two support plates between the laser plates and the DM plate as can be seen in figure 3.4. Each camera- and laser-plate has three micrometer screws for height adjustment and rotations, two at the front corners of each plate and one at the back in the center. One turn of these micrometer screws corresponds to a 0.20 mm change in height. Half a turn of only the rear adjustment screw corresponds to a change in height of 125 μm of the laser beam line profile or the camera line of sight in the central position. There is also one micrometer screw for horizontal position adjustment at the front right side of each plate. The power setting for the lasers can be varied in order to obtain different intensities of the laser beam so that the best camera image can be obtained.

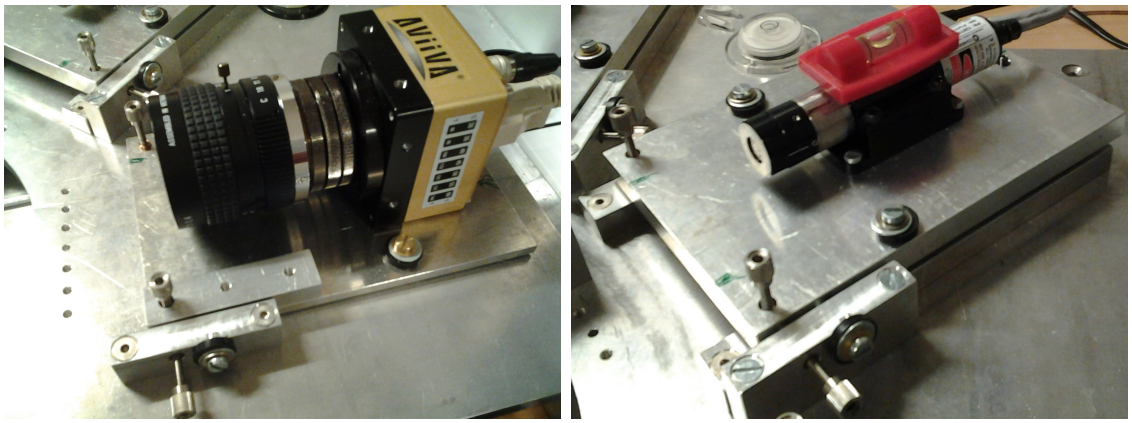

Figure 3.4: A camera (left) mounted to a camera plate and laser (right) mounted to a laser plate on the DM. The two front micrometer screws for height adjustment and the micrometer screw for horizontal adjustment can be seen in both photos. The rear micrometer screw can be seen on the laser plate in the right photo of the laser under the connection cable.

3.2 Electronics

The cameras operate continuously with an exposure cycle consisting of an exposure time during which the cameras collect light and the pixel content is filled and a dead time for the readout, to transfer the collected charge. The dead time also works as a restore time. The cameras are continuously provided their camera cycle structure via modules in a NIM (Nuclear Instrument Module) crate where the signals are set and controlled. The signals are monitored on an oscilloscope. The NIM crate and the oscilloscope can be seen in figure 3.5. For all measurements presented and discussed in this report, except where stated, the exposure cycle is 12.5 μs with an exposure time of 10 μs and a dead time of 2.5 μs. The exposure cycle signal will in the following be called the CYC signal. A positive trigger signal, TRIG, roughly of length 1 μs is placed in the dead time. The TRIG signal triggers the start of a readout frame. One readout frame consists of data from a certain set number of exposure cycles. For all measurements presented and discussed in this report, the number of exposure cycles (readout lines) in one readout frame is 2024. Each camera receives a separate CYC and TRIG signal. Having separate signals allows for making relative shifts of the exposure cycles of the cameras. These signals need to be synchronized for the proper operation of the cameras. The pixel content for each camera is read out by a FG (Frame Grabber) which in turn is read out by a PC (Personal Computer) after data for one readout frame has been collected.

The lasers receive their signal from a pulse generator via connection boxes, one connection box for each laser. The lasers can be set to continuous wave or pulsing light at these connection boxes. It is only possible to connect two connection boxes at the same time directly via cables to the pulse generator. Therefore, if three lasers are to be used simultaneously, one signal needs to be split between to two connection boxes. The connection box connected directly to the pulse generator needs a resistance of 50 Ω, the connection boxes receiving the split signal need a

resistance of 100 Ω.

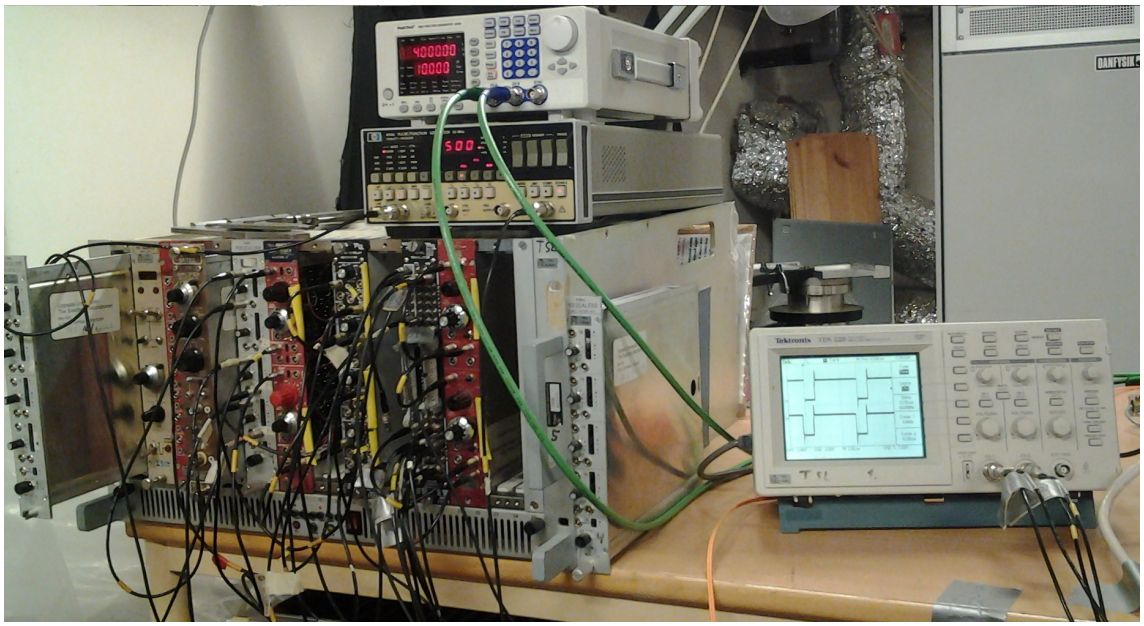

Figure 3.5: The electronics. The NIM crate can be seen to the left in the photo positioned on the desk. The pulse generator for the lasers is the white top box. The pulse generator below is used to pulse the synchronization diodes. An oscilloscope monitoring the camera exposure cycles can be seen to the right in the photo.

Chapter 4

Alignment Procedure

In order for the cameras and lasers on the DM to detect pellets with the required accuracy, they need to be properly aligned. Before the installation of LasC on the DM, an alignment procedure based on LasA and LasB was used. This is an extended version of the older alignment procedure modified to make use of the new laser simplifying the alignment. Before the alignment procedure is described, some differences between the alignment bench targets and pellets will be noted.

4.1 Differences between the Alignment Bench Targets and a Pellet Stream

Alignment bench targets are used for alignment in the alignment bench setup. Fishing lines in sets of two or five can be used for alignment purposes in the alignment bench setup. There are some differences between the fishing lines and the pellets/pellet stream which are of importance in the data analysis. Some of these aspects such as the position distribution of the fishing lines and the strong transmitted light from these are important for the alignment. For measurements and data analysis, a ROOT [10]-based program called PelletCounter is used. Some plots however are made using MATLAB Version R2015a [11]. For alignment purposes, a camera monitoring program called wxPropView [12] is used.

4.1.1 The Position Distribution

The most apparent difference between the fishing lines and the pellet stream in the analysis is the position distributions. Examples of the position distribution for two fishing lines and for the pellet stream can be seen in the plots in figure 4.1. Relatively narrow peaks corresponding to the positions of each fishing line appear in the case of measurements with fishing lines. For most practical purposes concerning measurements with fishing lines, a light distribution with a similar appearance as the position distribution have been found to be better to use and more well behaved for slight changes in the intensity of the laser beam. The peaks in the position distribution to the fishing lines are of great importance in the alignment procedure,

in particular the distribution obtained in a camera monitoring program. The pellet stream gives rise to a wider distribution. The width depends on the level of measurement along the pellet beam pipe. In the example in the right plot in figure 4.1 from a measurement at PTRlow, the measured width is roughly 70 pixels corresponding to 2.5 cm.

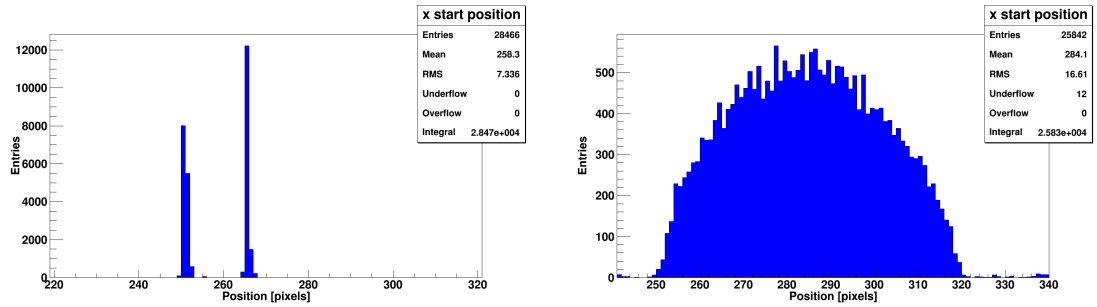

Figure 4.1: Examples of the position distribution from measurements with two fishing lines (left) and from measurements with pellets (right). The x-scales on the plots are different but the same size.

4.1.2 The Light Integral

The light signals from the fishing lines detected in the cameras are quite different from the light signals from pellets. The light signals from fishing lines originate from the lasers pulsing on the fishing lines and the light scattering into the cameras whereas the light from pellets originate from a pellet passing the laser beam with a constant light and the light is scattered into the cameras. The cameras detect a much stronger light from fishing lines so a much lower laser beam intensity is used when fishing lines are used as compared to when pellets are measured. The strong light from fishing lines enables and simplifies the use of camera monitoring programs for low intensities of the laser beam in the alignment bench setup. A power setting of around 2.7 mW is used for measurements of fishing lines and a power setting of 10-100 mW are used for pellet measurements. The cameras detect both refracted and reflected light depending on which laser is used. For transparent fishing lines, the refracted light is about 40 times stronger than reflected light whereas for pellets, the refracted light is about 3 times stronger than the reflected light [6].

The light integral is a measure of the collected light from one light signal either from a pellet or a laser pulse on a fishing line. The light integral is given by the integral of the overlap function (of the pellet or light signal and the camera sensor line) in time coordinate space multiplied by the brightness per unit of time. The general appearance of the light integral for measurements with two fishing lines can be seen in the left plot of figure 4.2. In this case, two distinct peaks corresponding to the fishing lines appear in the light integral plot. This means that the light from one fishing line is stronger than the light from the other. The general appearance of the light integral for measurements with pellets can be seen in the right plot of figure 4.2. This light integral peaks at low values and has the appearance of a very steep hill. This implies that most light signals from pellets are very weak. As expected, the light integral is heavily affected by the intensity of the laser beam. More examples

of light integrals from measurements with pellets for different intensities of the laser beam can be seen in appendix A. At very low values of the light integral plot, a peak corresponding to noise appears. The hint of such a peak can be seen in the left plot of figure 4.2. A cut (threshold) can be applied on the light integral only letting light signals with an amount of light above a certain value be part of the analysis. This way the noise can be reduced. In the analysis discussed in this report, this cut is 13.

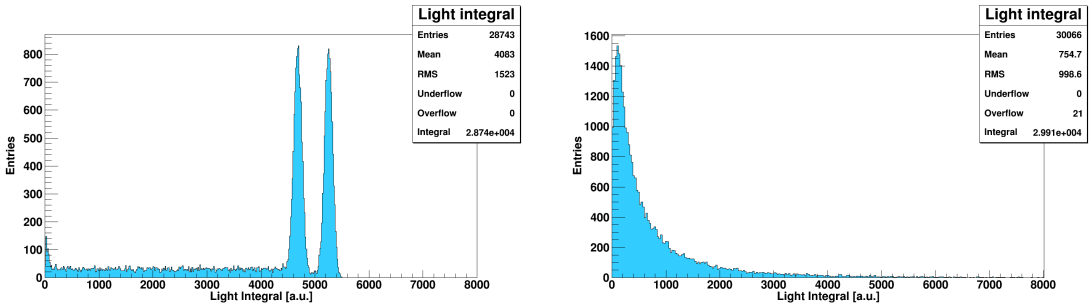

Figure 4.2: Examples of the light integral from measurements with two fishing lines (left) and from measurements with pellets (right).

4.2 Initial Rough Alignment

The DM plate needs to be placed roughly in a horizontal position. It can be checked if the plate is horizontal by placing spirit levels on different positions on the DM plate as well as on the cameras and lasers. Such spirit levels can be seen in figure 3.1.

There are two adjustment micrometer screws on each camera- and laser-plate in the front corners and one at the center at the back for vertical adjustment and rotation of the camera line of sight. These can be seen in both photos of figure 3.4. One turn of a micrometer screw corresponds to a change in distance of 0.20 mm. There are two screws with springs on both sides of the plates used for more rough adjustments and to adjust the tension over the micrometer screws. The screws need to be adjusted if the camera- or laser-plate needs to be raised or lowered greater distances, greater distances meaning more than a few of turns of the micrometer screw. There is also a micrometer screw for horizontal adjustment at the front left side of each plate. Initially, the laser plates are placed at a nominal height of 21.8 mm above the DM plate and the camera plates are placed at a nominal height of 6 mm above the DM plate. This makes the focal plane of the cameras and the laser beams meet about 36 mm above the DM plate and about 66.5 mm above the base plate. The height above the DM plate can be measured using a vernier caliper.

4.3 Focusing and Rotation of the Lasers

The next step is to focus the lasers in the central position corresponding to the pellet beam region. By observing the laser beam line profile in the central position

on a slightly transparent mm paper, the focus can be roughly set. The back of a mm paper placed in the central position can be seen in figure 4.3. The laser beam line profile needs to be roughly horizontal and to get it this way, the laser can be loosened from the heat sink clamp and turned by hand. The rotation should be done after the focusing since the focusing slightly rotates the laser beam line profile.

It should also be checked that the laser beam is roughly horizontal at different places along the laser beam so there is no inclination of the laser. This is done by observing the laser beam on a mm paper at different positions from the laser. A complication when doing this is that the laser beam line profile rotates along the laser beam so the center of the beam needs to be estimated. The beam line profile is vertical at the laser and rotates to become horizontal at the focus. If the laser beam is not horizontal, the inclination of the laser can be set using the rear micrometer screw.

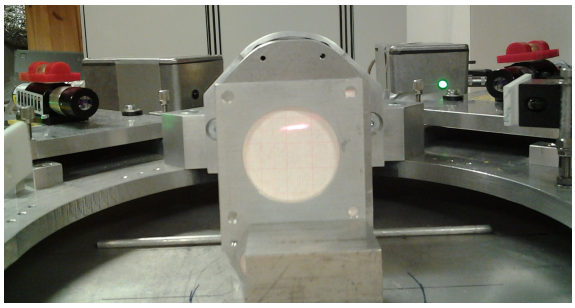

Figure 4.3: The laser beam as observed on a mm paper. All three lasers are used.

4.4 Usage of the Camera Monitoring Program and Placement of the Alignment Target

For setting the height and relative rotations between the cameras and lasers, a camera monitoring program can be used. The rear adjustment screw can be used to raise or lower the laser beam or the line of sight of the cameras at the central position by adjusting the inclination of the camera- or laser-plate instead of adjusting the height of entire camera- or laser-plate. This can be used to check relative positions during the alignment. Half a turn of the rear adjustment screw corresponds to 125 μm change in height at the central position of the camera line of sight or the laser beam. The overlap region between the camera line of sight and the laser beam is checked with the help of a camera monitoring program, in this case wxPropView, which can be seen in figure 4.4. The peaks correspond to the positions of the fishing lines. In the left photo of figure 4.4, the left window shows the camera image from CamA and the right window shows the camera image from CamB. In this case LasA is used so CamA detects refracted light and CamB reflected light. The camera analogue gain for CamA is set to the lowest possible and the camera analogue gain is set to 700 for CamB. The latter corresponds to a gain increase in the camera image of roughly 40. Due to the positions of the cameras (facing each other) the camera images are mirrored with respect to each other. In the right photo of figure 4.4, only LasB is used so in this case CamA detects reflected light and CamB detects

refracted light. The windows on the computer screen correspond to the same camera as in the left photo but in this case the camera analogue gain is set to 700 for CamA and CamB has the lowest gain set.

By changing the height of the camera line of sight or the laser beam in the central position, the overlap between these can be determined from where the camera image disappears. The overlap region should be $\pm 1/4$ turn of the rear adjustment screw on both the camera- and the laser-plate corresponding to a change in height of $\pm 62.5\ \mu m$ of the camera line of sight or the laser beam in the central position. The optimal vertical position can be determined from the vertical center position of the distribution in the camera monitoring program to a precision of 10 μm.

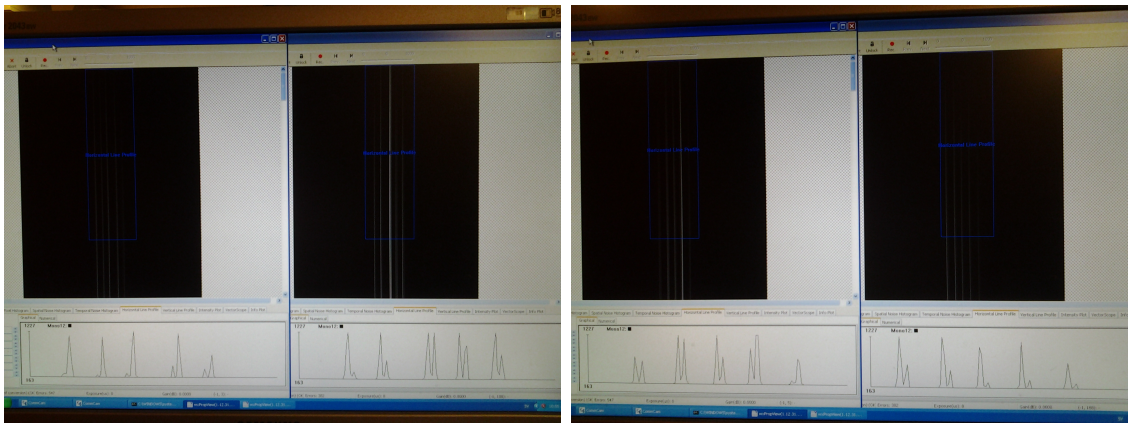

Figure 4.4: Example of an alignment check using five fishing lines with the camera monitoring program wxPropView. In the left photo, CamA detects refracted light and CamB detects reflected light from LasA. In the right photo, CamA detects reflected light and CamB detects refracted light from LasB.

The fishing lines are placed consecutively in a row in the target holders as depicted in figure 4.5 for the case of five fishing lines. An angle of the target holder which gives a sharp image in the camera monitoring program can be chosen, preferably with 45° between the row of fishing lines and the laser beam as can be seen in configurations *b*) and *c*) in figure 4.5 when LasC is used or the line of sight of LasA or LasB (configuration *b*) for LasB and configuration *c*) for LasA) is varied. Configuration *a*) is preferable when the height of the line of sight of the cameras is varied when LasA or LasB is used.

When varying the height of the camera line of sight or the laser beam in the central position, relative rotations between the camera line of sight and laser beam line profile can be detected by observation of the disappearance of the peaks in the camera image. If the peaks disappear simultaneously, there is no relative rotation, otherwise, the rotation of one of the cameras or lasers needs to be slightly adjusted.

A complication when checking the alignment using LasC is that the row of fishing lines must be placed at a certain angle with respect to the laser beam in order to get a good signal from all fishing lines. From observation, the best signal in both cases is obtained when the row of fishing lines is placed at a 45° angle with respect to the laser beam as depicted in configurations *b*) and *c*) in figure 4.5. This places the fishing lines at different distances from the laser and the cameras which means that the peaks in the camera image corresponding to the fishing lines might disappear

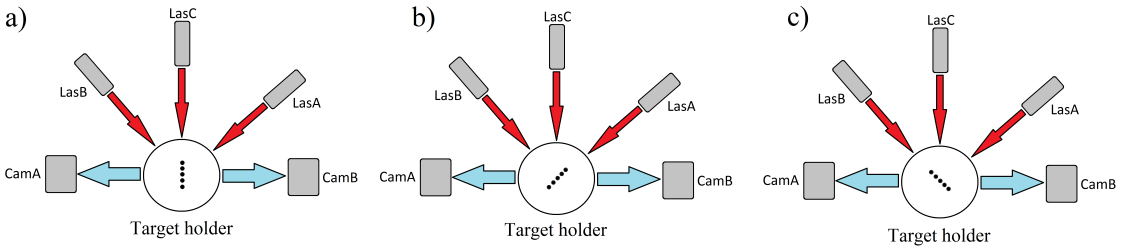

Figure 4.5: Sketch of the experimental setup as seen from above. The five dots in the target holder represent the positions of the fishing lines in the case of the target holder for five fishing lines. Configuration *a*) of fishing lines is suitable for using LasA and LasB. Configuration *b*) is suitable for using LasB and LasC. Configuration *c*) is suitable for using LasA and LasC.

slightly uneven when raising or lowering the laser, uneven meaning not at the same time. This might falsely imply a relative rotation between the laser beam line profile and the camera line of sight. In the case of LasA and LasB, the fishing lines can be placed on a row perpendicular to the cameras line of sight and the alignment can be checked by varying the height of the camera line of sight. The target holder can also be placed such that the row of fishing lines is perpendicular to the laser beam so that no fishing line is closer or further away from the laser than the other fishing lines as is displayed in figure 4.5 and the alignment can be checked by variation of the height of the laser beam line profile. This is not possible in the case of LasC due to its placement relative the cameras as is illustrated in figure 4.5. One solution to this problem is to observe the central fishing line and make sure its camera image of it disappears after $\pm 1/4$ turn of the rear screw of the camera- or laser-plates and make sure that the camera images of the other fishing lines disappear as expected depending on their position. However, the effect is generally so small it is hardly noticeable.

4.5 Adjustment of the Line of Sight and Focus of the Cameras

The cameras need to be aligned with respect to the lasers and focused. Since LasC is positioned symmetrically with respect to both cameras, the best choice is to initially align both cameras with respect to this laser. This can be done by observing the transmitted or reflected light from one laser illuminating the target fishing lines and check the camera images in a camera monitoring program.

The camera height above the DM plate should first be adjusted. If there is initially no image in the camera monitoring program the rear micrometer screw of the camera plate can be rotated so that the height of the camera line of sight is varied in the central position in order to investigate if the camera plate needs to be raised or lowered. Even if there is initially an image this should still be done in order to find out if the camera image gets sharper at higher or lower positions and the height of the camera plate needs to be adjusted a small bit. From this variation of the height

of the line of sight of the cameras and laser beam it can be calculated how much the camera plate needs to be raised or lowered.

After finding the optimal vertical position for the cameras, the three micrometer screws for height adjustment can be used to set the cameras in this position. Once the optimal vertical position has been set for both cameras, the focus of the cameras should be checked and adjusted if needed. This is done by changing the focus and trying to get as sharp of an image as possible of the fishing lines. If configuration *a*) from figure 4.5 is used, the focus is just set using all fishing lines since all fishing lines are at the same distance from the cameras. If the outer fishing lines are at different distances to the cameras as compared to the central fishing line (e.g. as in the case when LasC is used in configurations *b*) and *c*) in figure 4.5) the cameras should be focused on the central fishing line. Once this is done the overlap region between the camera line of sight and the laser beam should be checked once again and the optimal vertical position should be checked. Some small adjustments might be needed.

4.6 Fine Adjustment of the Lasers

Once the cameras are aligned with respect to LasC as described in section 4.4, refracted light from LasA can be used to align it with CamA and refracted light from LasB to align it with CamB. The best configuration of the fishing lines in this case is to have them placed on a row perpendicular to the line of sight of the camera or the laser beam of the laser used as depicted in figure 4.5 depending on which object is moved. However the difference between these configurations is negligible for alignment purposes. The lasers can be aligned with respect to the cameras in a similar way as the cameras are aligned with respect to LasC. Once the alignment of both lasers has been performed, the alignment can be checked using reflected light from LasA in CamB and reflected light from LasB in CamA. This is done once again by checking the overlap region by moving camera line of sight and the laser beam using the rear micrometer screws as described in section 4.4. Both cameras and LasA and LasB should be fairly aligned but some minor adjustments may need to be done after this last crosscheck. The lasers can be adjusted slightly by rotation of the laser plates using the front micrometer screws. An alternative approach to performing the rotation of the laser is to monitor the image of the alignment target in the camera monitoring program while performing the rotation of the laser by hand as described in section 4.2. This way the rotation of the laser will not need much adjustment using the adjustment screws ensuring the space between the laser plate and the support plates is enough.

4.7 Alignment Checks with Pellets

Alignment checks with a pellet stream are needed in order to determine if the alignment of cameras and lasers is still good after transportation from the alignment bench setup to the pellet beam pipe. Also, at the alignment bench setup a power

setting of roughly 3 mW is used for the lasers whereas at the pellet beam pipe, a setting of 50-100 mW is used. It is interesting to know how well aligned the cameras and lasers are for different intensities of the laser beam and if the value of the power setting affects the alignment. The alignment is checked for pellets a with power setting for the lasers of 10-100 mW. With pellets, the alignment cannot be checked using the camera monitoring program because the light signal from pellets is too weak. The alignment checks need to be performed using discrete points of measurements in PelletCounter. For example, the mean value of the light integral can be plotted as a function of the height of the line of sight of one camera. The alignment is not performed with pellets, only checked. Examples of results of these alignment checks can be seen in the plots in figure 4.6 for a power setting of 10 mW for the lasers. The mean value of the light integral for both cameras is plotted as a function of the height of the camera line of sight in the central position of one camera for all three lasers separately. In the figure, 0 denotes the nominal height of the line of sight and the other values are vertical displacements of the camera line of sight from this position. The mean value of the light integral for the stationary camera is slightly affected by the inclination of the other camera, probably due to reflections between the cameras. The best alignment is found within the limits of investigation in the vertical direction for all plots since the maximal mean value of the light integral is obtained within these limits. The results in the bottom plots in figure 4.6 indicate that the pellet stream is slightly closer to CamB than to CamA since both cameras should detect equally strong light from LasC but CamB seems to detect stronger light. This is in agreement with the result in figure 5.3. In the cases when LasA and LasB is used, the refracted light is about twice as strong as the reflected light in the vertical position where the maximal value of the mean value of the integral is obtained.

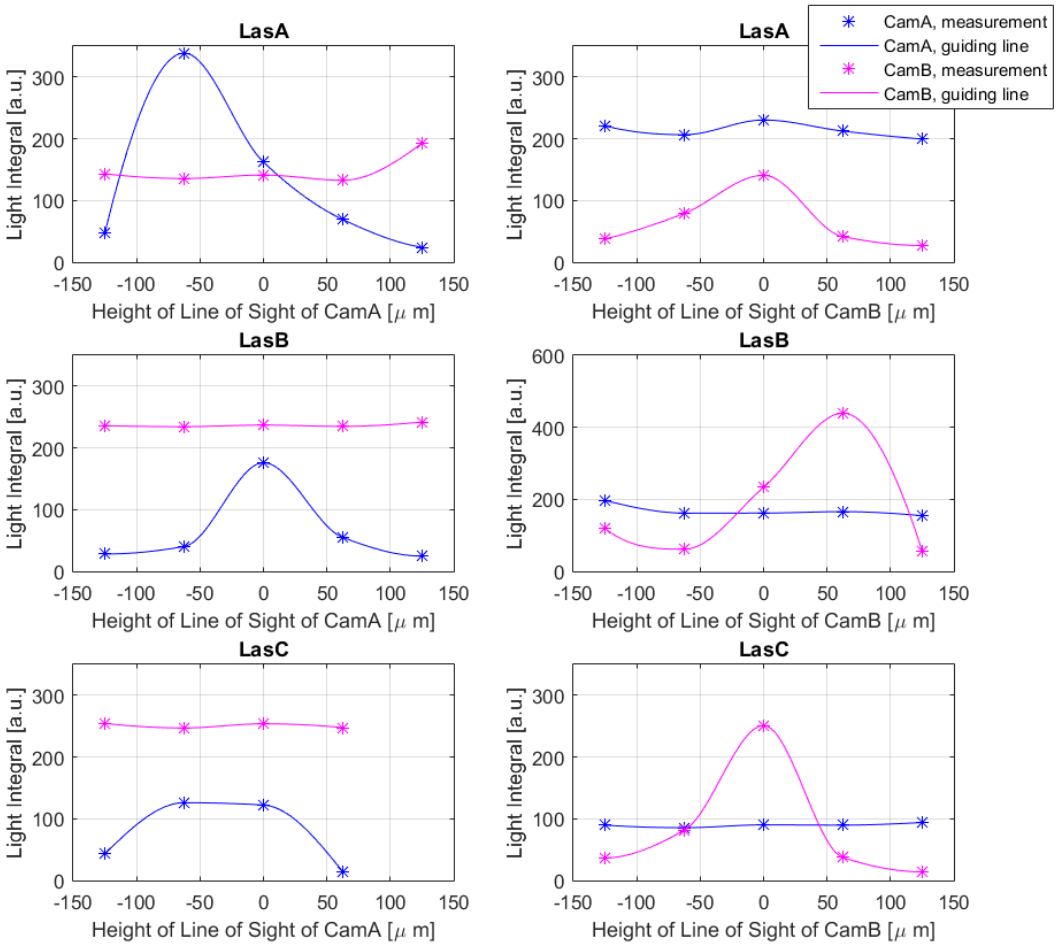

Figure 4.6: Alignment with pellets for different lasers and with a power setting of 10 mW for all lasers. The results from changing the height of the line of sight of CamA are seen in the left plots and the results from changing the height of the line of sight of CamB is seen in the right plots. The vertical position 0 indicates the nominal height of the camera line of sight in the central position. The other values indicate the distance from the nominal value in the vertical direction.

4.8 Investigations of Alignment Bench Targets

In order to obtain the best alignment possible, a good alignment bench target is needed. A good alignment bench target should give a clear signal in both cameras and give a good light integral meaning that the collected light should be sufficient in both cameras for both refracted and reflected light for a certain intensity of the laser beam. The alignment bench target should also be simple to set up and it should remain stable for longer times. Theoretically, anything refracting and reflecting the light from the lasers can be used as an alignment bench target. In the past *e.g.* different liquids at room temperature have been used for testing droplet nozzles. Such a setup could have been considered. However, a more stable and convenient solution is preferable, *e.g.* different types of fishing lines. These are stable and simple to set up in target holders. Different fishing lines of different

thickness and transparency are examined in order to find properties concerning reflected and refracted light. From the results, it is determined which fishing line or lines are the best alignment bench target or targets.

The fishing lines examined are two fishing lines with diameters of 0.08 mm, one transparent and one braided, non-transparent fishing line. Further, some transparent fishing lines with diameters of 0.27 mm, 0.24 mm, 0.18 mm, 0.125 mm and 0.10 mm are examined. All these fishing lines are examined together with a transparent reference fishing line with a diameter of 0.12 mm in a target holder for two fishing lines. The distance between the outer edges of the fishing lines in this target holder is approximately 0.5 mm. However, this may differ along the vertical direction.

The results of the investigations of alignment bench targets can be seen in figures 4.7-4.13 where the light distribution from CamA and CamB for refracted and reflected light are shown. The camera image of the reference fishing line can be seen as the light blue peak to the right in the image from CamA and to the left in the image from CamB in all these figures. LasA is used in all measurements except in figure 4.12 where LasB is used. The values for the power setting are the values giving the best position distributions and light integrals in both cameras simultaneously. A power setting of 3 mW is used for LasA in all measurements except for the measurement with the braided fishing line in figure 4.7, which is the only non-transparent fishing line examined, where a slightly higher value of the power setting (3.02 mW) is used. A higher value of the power setting (3.10 mW) is used for LasB which is used in figure 4.12 in order to get an equally good position distribution and light integral in both cameras as for LasA. The figures 4.7-4.13 show that in general the distance between the peaks as read off from CamA is slightly smaller than the distance as read off from the distribution from CamB. This indicates that the target holder with the fishing lines is slightly closer to CamB. The thickness of the peaks depends on the intensity of the laser beam. Therefore, it is only interesting to compare relative widths of the peaks rather than the individual ones.

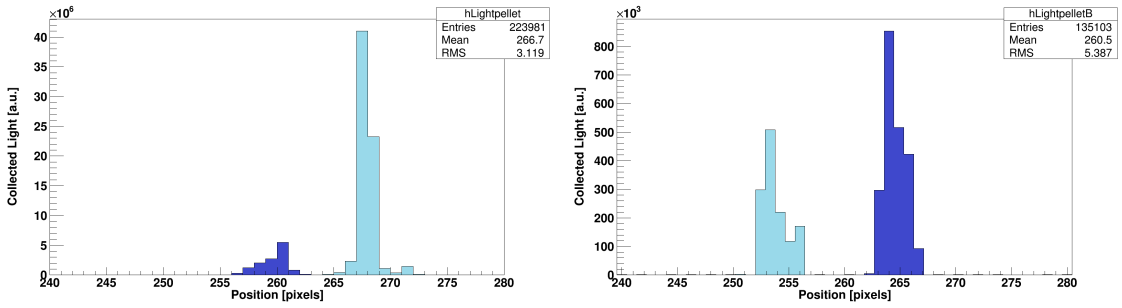

Figure 4.7: Light distribution in CamA (left) and in CamB (right). Only LasA is used with a power setting of 3.02 mW. The detected light from the braided 0.08 mm diameter fishing line is seen as the dark blue peak. The detected light from the 0.12 mm diameter reference fishing line is seen as the light blue peak. The scale is roughly 50 times larger in the left plot.

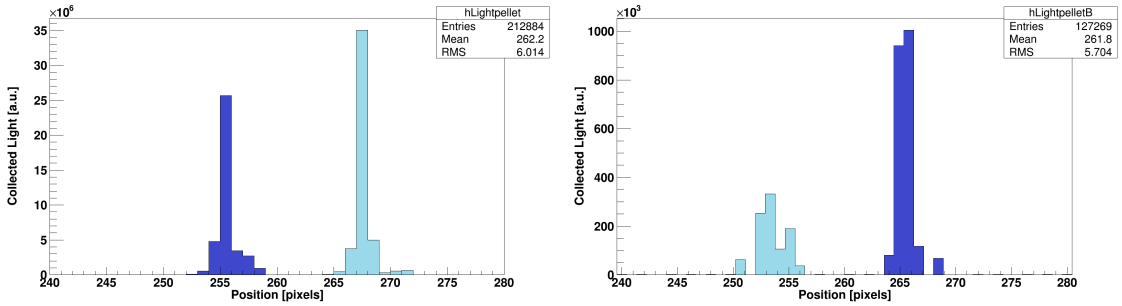

Figure 4.8: Light distribution in CamA (left) and in CamB (right). Only LasA is used with a power setting of 3 mW. The detected light from the transparent 0.08 mm diameter fishing line is seen as the dark blue peak. The detected light from the 0.12 mm diameter reference fishing line is seen as the light blue peak. The scale is roughly 35 times larger in the left plot.

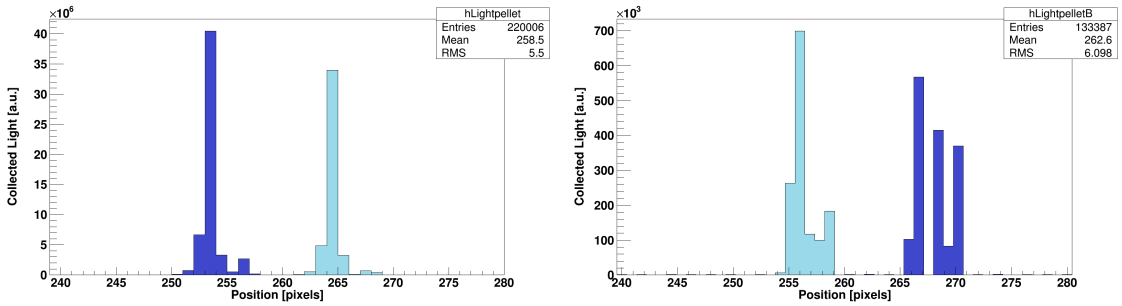

Figure 4.9: Light distribution in CamA (left) and in CamB (right). Only LasA is used with a power setting of 3 mW. The detected light from the transparent 0.10 mm diameter fishing line is seen as the dark blue peak. The detected light from the 0.12 mm diameter reference fishing line is seen as the light blue peak. The scale is roughly 57 times larger in the left plot.

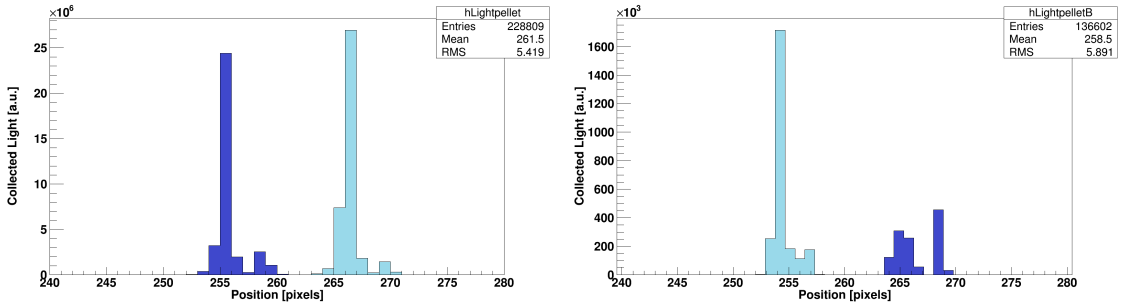

Figure 4.10: Light distribution in CamA (left) and in CamB (right). Only LasA is used with a power setting of 3 mW. The detected light from the transparent 0.125 mm diameter fishing line is seen as the dark blue peak. The detected light from the 0.12 mm diameter reference fishing line is seen as the light blue peak. The scale is roughly 16 times larger in the left plot.

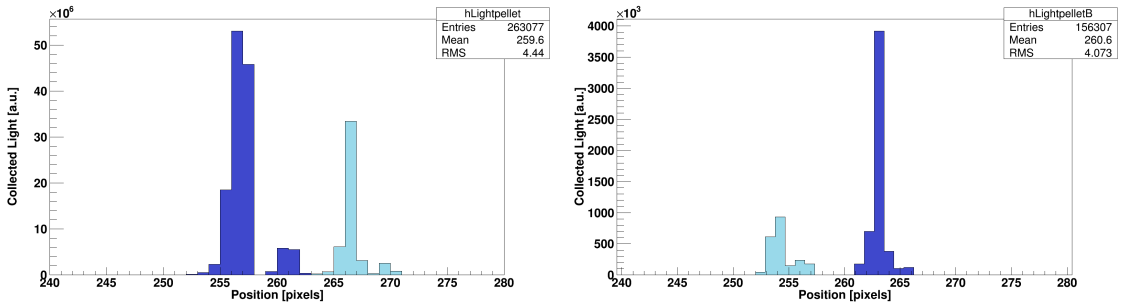

Figure 4.11: Light distribution in CamA (left) and in CamB (right). Only LasA is used with a power setting of 3 mW. The detected light from the transparent 0.18 mm diameter fishing line is seen as the dark blue peak. The detected light from the 0.12 mm diameter reference fishing line is seen as the light blue peak. The scale is roughly 13 times larger in the left plot.

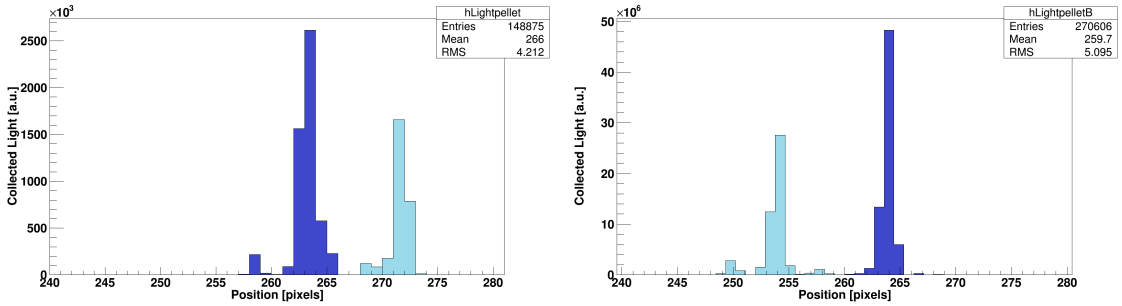

Figure 4.12: Light distribution in CamA (left) and in CamB (right). Only LasB is used with a power setting of 3.1 mW. The detected light from the 0.24 mm diameter fishing line is seen as the dark blue peak. The detected light from the 0.12 mm diameter reference fishing line is seen as the light blue peak. Note that LasB is used in this case so the reflected and refracted light is shown in the opposite camera as compared to the other figures. The scale is roughly 20 times larger in the left plot.

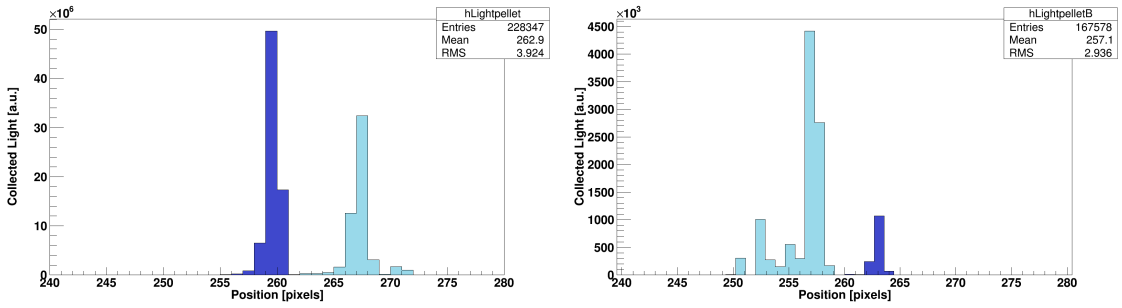

Figure 4.13: Light distribution in CamA (left) and in CamB (right). Only LasA is used with a power setting of 3 mW. The detected light from the transparent 0.27 mm diameter fishing line is seen is seen as the dark blue peak. The detected light from the 0.12 mm diameter reference fishing line is seen as the light blue peak. The scale is roughly 11 times larger in the left plot.

A description of each fishing line follows;

- **The braided 0.08 mm diameter, braided fishing line.** This is the only non-transparent fishing line examined. The distance between the center of the peaks corresponding to this fishing line and the reference fishing line is roughly 7 pixels for refracted light and 11 pixels for reflected light. The intensity of the laser beam used to illuminate this fishing line is slightly greater than the intensity used to illuminate the other fishing lines. The signal from this fishing line for refracted light is smaller than the signals from refracted light from all other fishing lines examined. This is expected due to the non-transparency of this fishing line. From refracted light, no width can be read off due to the smearing. The width of the peak as read off from reflected light is 0.14 mm (4 pixels).
- **The transparent 0.08 mm diameter, transparent fishing line.** The distance between the center of the peaks corresponding to this fishing line and the reference fishing line is roughly 0.42 mm (12 pixels) for refracted light and for reflected light. The width of the peak as read off from refracted light is roughly 0.035 mm (1 pixel) and as read off from reflected light 0.07 mm (2 pixels).
- **The 0.10 mm diameter fishing line.** The distance between the center of the peaks corresponding to this fishing line and the reference fishing line is roughly 0.385 mm (11 pixels) for refracted light and 0.385-0.525 mm (11-15 pixels) for reflected light. In the case of reflected light it is hard do estimate due to the smearing of both peaks in that plot. The reflected light from this fishing line gives a very smeared signal. The width of the peak as read off from refracted light is roughly 0.035 mm (1 pixel) and as read off from reflected light 0.175 mm (5 pixels). However the latter is very uncertain due to the smearing.
- **The 0.12 mm diameter fishing line.** The reference fishing line.
- **The 0.125 mm diameter fishing line.** The distance between the center of the peaks corresponding to this fishing line and the reference fishing line is roughly 0.42 mm (11 pixels) for refracted light and 0.42-0.49 mm (11-14

pixels) for reflected light but in the latter case it is harder to estimate due to the two smaller peaks constituting the right peak. The reflected light from this fishing line gives a very small and smeared signal. The width of the peak as read off from refracted light is roughly 0.035 mm (1 pixel). From reflected light, no width can be read off due to the smearing.

- **The 0.18 mm diameter fishing line.** The distance between the center of the peaks corresponding to this fishing line and the reference fishing line is roughly 0.35 mm (10 pixels) for both refracted light and 0.315 mm (9 pixels) reflected light. The width of the peak as read off from refracted light is roughly 0.07-0.105 mm (2-3 pixels) and as read off from reflected light 0.035 mm (1 pixel).
- **The 0.24 mm diameter fishing line.** The distance between the center of the peaks corresponding to this fishing line and the reference fishing line is roughly 0.35 mm (10 pixels) for refracted light and 0.28 mm (8 pixels) for reflected light. The width of the peak as read off from refracted light is roughly 0.07 mm (2 pixels) and as read off from reflected light 0.035 mm (1 pixel).
- **The 0.27 mm diameter fishing line.** The distance between the center of the peaks corresponding to this fishing line and the reference fishing line is roughly 0.28 mm (8 pixels) for refracted light and 0.21 mm (6 pixels) for reflected light but in the latter case it is harder to estimate due to the smearing of the left peak. This fishing line gives a very small signal and it affects the camera image of the reference fishing line making this image very smeared for reflected light. The width of the peak as read off from refracted light is roughly 0.035-0.07 mm (1-2 pixels) and as read off from reflected light 0.035 mm (1 pixel).

The best fishing line to use for alignment purposes is the transparent 0.08 mm diameter fishing line. This fishing line gives a better signal than the braided, non-transparent one with the same diameter or the thicker ones.

Chapter 5

Stability of the Alignment

The alignment of the cameras and lasers on the DM (Detection Module) must be maintained under certain conditions. The alignment must remain stable under transportation, under temperature changes and during exposure to vibrations which occur during pellet runs. The stability of the alignment under these conditions has been examined. The behavior of the camera and laser optics under exposure to magnetic fields which may affect the camera image has previously been checked and is only briefly discussed here. The support structure consisting mainly of aluminum is not magnetic so it has not been tested for effects of magnetic fields. It is important for later measurements and usage of the DM to know if the alignment is stable or how it changes under these different conditions which are the expected main sources of distortions of the alignment. Also the alignment bench targets must be stable to make possible careful optimization of the alignment. The stability over time of the fishing lines used as alignment bench targets in the target holders has therefore been examined.

5.1 Checking the Alignment

The alignment of the cameras and lasers need to be verified in both the vertical direction and horizontal plane on a regular basis or when needed. Different means of investigation is needed for these checks. For the vertical alignment checks, the camera monitoring program wxPropView is used in the alignment bench setup. Discrete points of measurements in the vertical direction are used for measurements with pellets since the light from these is too weak for being visible in wxPropView. Using this software is otherwise preferred since this is simpler and less time consuming. Using alignment bench targets is also preferred since these can be chosen such that relative rotations between the lasers and cameras can be detected. For investigating changes in alignment in the horizontal plane in between two measurements, the camera pixel correlation is used. Using this, it can be determined if the cameras have changed their position relative each other in the horizontal plane in between the measurements. This is the only way to detect small relative changes in the alignment in the horizontal plane (pixel scale).

5.1.1 Usage of the Camera Monitoring Program

In order to check how the alignment has changed under the above mentioned conditions, the camera monitoring program wxPropView is used when it is possible, *i.e.* in the alignment bench setup. Using this program, the vertical alignment can be checked by observation of the overlap region between the camera line of sight and the laser beam. The vertical position of the camera line of sight or a laser beam is varied in the central position by rotation of the rear adjustment screws of the camera- or laser-plates. By doing this for all lasers and cameras separately for both refracted and reflected light, the alignment between all lasers and cameras can be checked. The overlap region between the camera line of sight and the laser beam can be determined and the center of the distribution seen on the computer screen in the camera monitoring program can be estimated with 10 μm accuracy. By using more than one fishing line, relative rotations can be detected by observation of how the camera images of the fishing lines disappear at the boundaries of the vertical distribution when the height of the camera line of sight or the laser beam is varied. If the height of the peaks do not decrease simultaneously it implies there is a relative rotation.

When it is not possible to use this program *i.e.* in pellet measurements, discrete points of measurements using PelletCounter is used and the light integral is plotted as a function of the height of the camera line of sight when the laser beams are kept at a constant height. This method is less accurate and more time consuming and it is practically impossible to detect small relative rotations between cameras and lasers using a pellet stream.

5.1.2 Usage of the Pixel Correlation

In order to determine if the cameras have moved relative each other in the horizontal plane, the pixel correlation plot can be used. A sketch displaying how the experimental setup translates to the pixel correlation plot can be seen in figure 5.1 in the case of measurements with fishing lines. By comparing the pixel correlation plot for two different measurements it can be determined if the target has moved in between these measurements or if the cameras have moved relative each other or if a combination of the two has occurred. The dotted line in the pixel correlation plot in figure 5.1 represents the line along which the distribution in the pixel correlation plot has moved in between two measurements if the target has moved in between the measurements. The dotted line does not need to have slope -1. The slope depends on the apparent size of the target as seen by the cameras. The closer the target is to one camera the larger the target will appear in the camera, this affects the slope of the dotted line. This means that if the target moves away from or towards a camera in between two measurements, the slope of the line is affected. If the cameras have moved relative each other, the distribution in the pixel correlation plot will have moved outside the dotted line. The slope is extracted from the pixel correlation plot. In the case of pellets, the pellet stream translates to a narrow distribution along the dotted line in the sketch of the pixel correlation plot in figure 5.1 since the pellet stream has a larger spatial spread than the fishing lines. There are several pixel correlation plots available but the most appropriate to use is a plot

with a condition that both cameras see the same signal in the same readout line which ensures that all signals in the pixel correlation plot is seen by both cameras. Usage of the pixel correlation is currently the only way to detect small changes in the alignment in the horizontal plane at the pixel level.

When comparing two pixel correlation plots, a mean value is set for the camera image in CamA and CamB which are chosen from a position distribution in one of the measurements. The deviation of the distribution in the pixel correlation plot from these mean values is then plotted for both measurements and the mean values of these latter plots can be compared. When possible (and needed), the fitted slope of the dotted line is used when making these latter plots. The difference between these mean values indicates how much the cameras have moved relative each other horizontally.

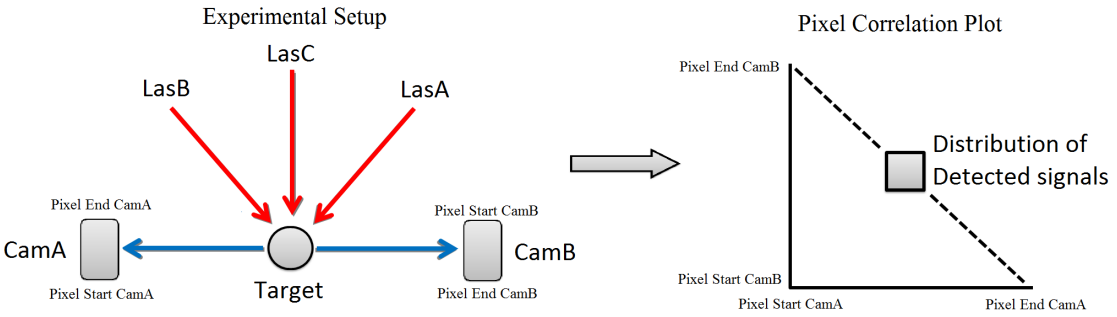

Figure 5.1: Sketch of a comparison between the experimental setup as seen from above and the pixel correlation plot in the case of measurements with fishing lines.

5.2 Stability against Vibrations

The alignment of the cameras and lasers on the DM needs to be stable when the DM is subjected to vibrations. This is tested with pellets during a pellet run during which the DM is exposed to vibrations from the vacuum pumps. Alignment checks are performed in the vertical direction using discrete points of measurements at two different occasions and in between is the DM subjected to vibrations. As mentioned previously, using discrete points of measurement is the only way to investigate the alignment using pellets since pellets give too weak light signals for using wxPropView.

The plots in figure 5.2 show the results from the investigations of the alignment in the vertical direction. The mean value of the light integral is plotted as a function of the height of the camera line of sight. In each plot, the mean value of the light integral as measured in both cameras is plotted but the line of sight is only varied for one camera in each plot. This is done for two different series of measurements performed roughly 19 h of pellet run time apart. During the time in between, the DM is subjected to vibrations. The plots for the early and later measurements look very similar and the alignment for all cameras and lasers can be estimated to have changed less than 30 μm in the vertical direction in between the measurements.

The difference in height of the curves from the earlier and later measurements can be explained by the pellet beam being slightly closer to one camera at the early measurement and further away from this camera at a later measurement. This also accounts for the difference in height of the curves for both cameras at the point where the camera whose line of sight is varied measures its largest value of the light integral in the bottom plots in figure 5.2. The results in the two lower plots of figure 5.2 indicate that the pellet stream is slightly closer to CamB than to CamA since both cameras should detect equally strong light from LasC. This is in agreement with the results in figure 5.3.

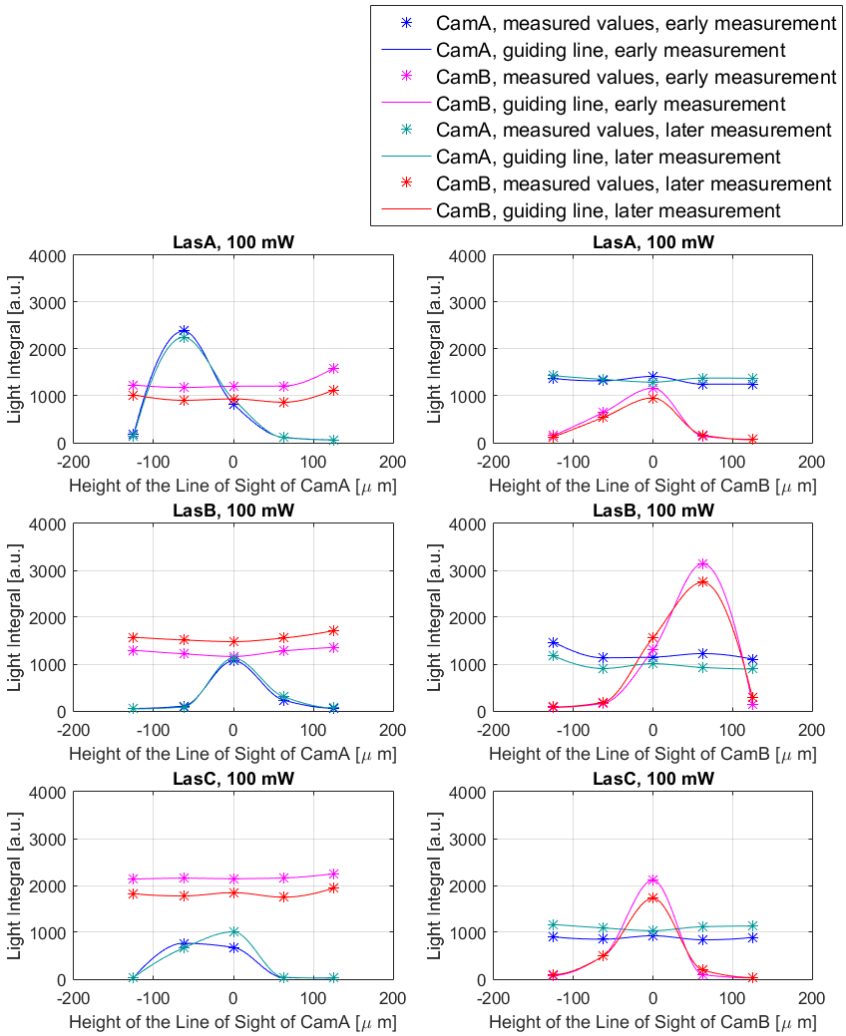

Figure 5.2: Light from LasA, LasB and LasC individually with a 100 mW power setting. The results from changing the height of the line of sight of CamA are seen in the left plots and the corresponding results from changing the height of the line of sight of CamB is seen in the right plots. The vertical position 0 indicates the nominal height of the camera line of sight in the central position. The other values indicate the distance from the nominal value in the vertical direction. The mean value of the light integral in both cameras is plotted for comparison even though the line of sight of only one camera is varied. During the time in between the early and later measurements the DM is subjected to vibrations.

The only way to check carefully if the alignment has changed in the horizontal

plane in between two measurements is to compare the pixel correlations between the cameras and see if the cameras have changed their position relative each other. This is done for measurements in between which the DM is subjected to vibrations. The pixel correlation from two different measurements with pellets can be seen in the plots of figure 5.3 when only LasA is used. The right plot in this figure is from a measurement made roughly 24 h after the first measurement where the left pixel correlation plot is from. In the time in between the measurements the DM is subjected to vibrations. A power setting of 10 mW is used for the measurements and for similar measurements involving the other lasers. By comparing how the pixel correlation has changed in between these measurements it can be determined how the cameras have moved relative each other horizontally along the pixel line direction. The fact that the line formed by the distribution does not have slope -1 but is less steep than expected if the pellet stream would be in the central position, indicates that the pellet stream is slightly closer to CamB than to CamA. The most accurate way to determine if the cameras have moved relative each other is to extract a mean value in the x- and y-direction from position distribution plots for CamA and CamB for the first measurement and plot the deviation of the distribution from this mean value for both cases of the pixel correlation. This deviation for both measurements can be seen in figure 5.4. The difference in deviation between the measurements gives a measure of how much the cameras have moved relative each other. The deviation from zero for both distributions is due to the fact that the mean value is calculated using position distributions and may end up outside the distribution in the pixel correlation plot. This does not matter since only the difference between the mean values between the plots is interesting. The slope of the lines need to be taken into account in this type of analysis since if the slope changes it means that the pellet stream has moved closer or further away from the cameras. Using the wrong slope could lead to a result which misleadingly indicates that the cameras have moved relative each other when in reality the pellet stream has moved relative the cameras. The difference in mean value between the left plot and right plot of figure 5.4 where LasA is used is 1.41 pixels and it is 0.457 pixels in similar plots where LasB is used. From similar measurements when only LasC is used, a difference of 4.4 pixels between the early and late measurement is found. This difference is larger than that for the measurements where one of the other lasers is used. This might be because there is only reflection involved in this measurement. The light is also reflected at a larger angle in this case, at 90° as opposed to the reflection at 45° for LasA and LasB. This means that the behavior of the light is more unpredictable in the case of LasC and reflections between the cameras affect the camera image more easily.

The conclusion is that the alignment of the cameras and lasers on the DM seems to be stable when the DM is exposed to vibrations.

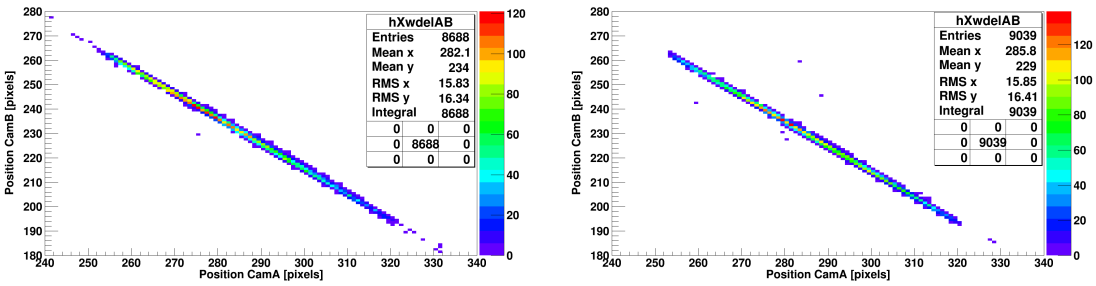

Figure 5.3: Pixel correlation with only LasA. The left plot is from a measurement approximately 24 h before the measurement which the right plot is from. During the time in between the DM was subjected to vibrations. The slope of the line formed by the distribution is approximately -0.962 in the right plot and -0.968 in the left plot.

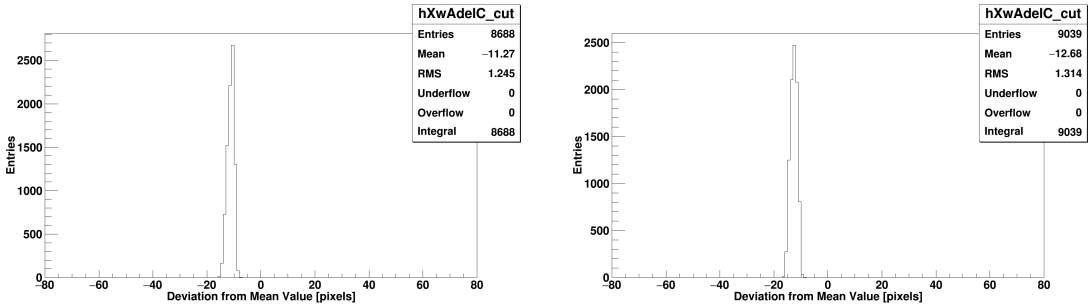

Figure 5.4: Deviation from the mean value with only LasA. The left plot is from a measurement approximately 24 h before the measurement which the right plot is from. During the time in between the DM was subjected to vibrations. The difference in mean value of the distributions in the left and right plot is 1.41 pixels.

5.3 Stability under Transportation

Since the DM should be aligned in an alignment bench setup and moved to the pellet tracking chamber, the alignment must remain stable under such transportations. This is examined by performing an alignment check and doing measurements in the alignment bench setup before and after transporting the DM to the pellet test station and back in order to examine the differences.

The alignment in the vertical direction is checked using wxPropView. The same results of the alignment checks are obtained before and after the transportation. The peaks in the camera images disappear evenly after $\pm 1/4$ turn of the rear adjustment screw on both camera plates and the laser plates of LasA and LasB. $\pm 1/4$ turn of the rear adjustment screw on all camera plates and laser plates means that the overlap region between the camera line of sight and the laser beam line profile is 125 μm in the vertical direction. The center of the distributions in the cameras is located within 10 μm of the center of this distribution. This means that the maximal change in vertical alignment between the alignment checks is 20 μm. The even appearance/disappearance of the peaks implies that there is no relative rotation between the laser and camera planes before or after transportation.

The pixel correlation between the cameras is examined in order to determine if any relative change in the horizontal positions of the cameras have occurred. The fishing lines used for the measurements are a transparent fishing line of diameter 0.12 mm and a braided, non-transparent fishing line of diameter 0.08 mm. A 2.9 mW power setting is used for LasA and a 3.1 mW setting is used for LasB. A frequency of the laser pulses of 4 kHz is used for laser pulses of 2.5 μs length. At the time of these investigations, LasC has not been installed so it is not included. The pixel correlation for measurements before and after transportation is shown in figure 5.5. Both LasA and LasB are used in both measurements since only one laser gave a too inhomogeneous illumination with the setup of fishing lines used. In order to check if any change in the pixel correlation has occurred, a mean value is obtained from the position distribution in both cameras from the earlier measurement. The deviation of the distribution in both pixel correlation plots from these mean values is plotted. The difference in mean value of these distributions gives the relative change in the pixel correlation plots in between the measurements. These plots are shown in figure 5.6. The distributions in the pixel correlation plots show no spatial change in the distribution which can be attributed to the cameras changing their horizontal position relative each other as measured in the plots in figure 5.6. The difference in mean value of the distributions in the left and right plot in figure 5.6 is 0.4 pixel which is not detectable in the camera image.

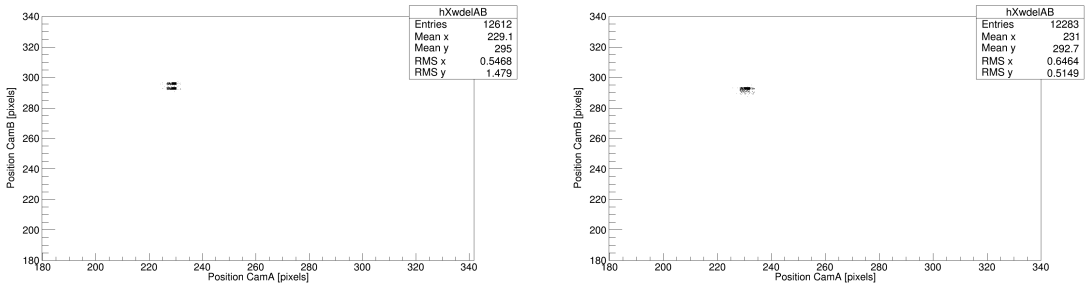

Figure 5.5: Pixel correlation with both LasA and LasB used before transportation (left) and after transportation (right).

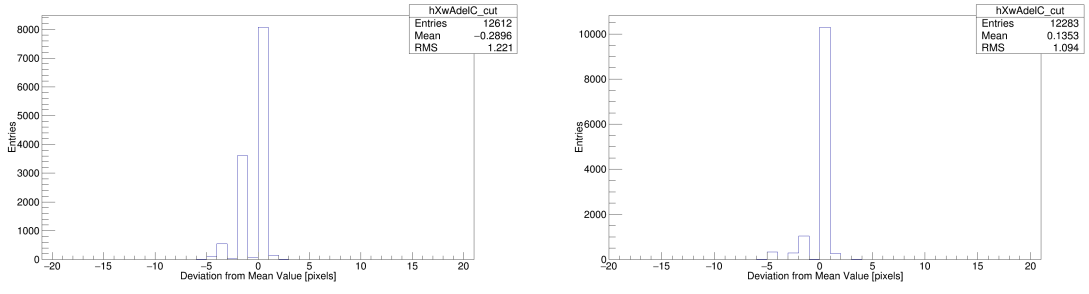

Figure 5.6: Deviation from the mean value with both LasA and LasB used before transportation (left) and after transportation (right). The difference in mean value in between these two plots is 0.425 pixels.

5.4 Stability under Temperature Changes

The alignment of the cameras and lasers on the DM must be maintained under smaller changes in the room temperature. At PANDA, temperature changes of about 5°C can be expected. There are two main effects to look for at different temperatures, changes in the alignment originating from thermal expansion or contraction of the support material and optical effects originating from the cameras or lasers or both.

5.4.1 Mechanical Stability under Temperature Changes

The support material of the DM plate expands or contracts at different temperatures which directly affects the alignment. Because of the position at which the DM is mounted to the pellet beam pipe or to the base plate at the alignment bench setup, four possible changes in the alignment can occur from expansion or contraction of the support material;

1. The cameras can move away from or towards the point where the DM is mounted. The latter means that the cameras will also slightly move away from LasC. In this case, both cameras move an equal distance in the same direction.

2. The cameras can move away from or towards each other. Only this effect, the relative change in position between the cameras, if large enough, is detectable. The expected effect however is very small. The support material is made of aluminum with an expansion coefficient of $23.2 \cdot 10^{-6}\ K^{-1}$ [8]. The height and width of the DM plate is 410 mm and 620 mm respectively in the horizontal plane. A temperature change of 5°C (the maximal change in room temperature obtained during the tests) leads to a change in width of 0.072 mm of the DM. This means that both cameras change their distance to the target with 0.035 mm. Since the distance between the focal plane of the camera and the target is 250 mm, this change in distance corresponds to 0.014% change in distance to the target. Such a change is not detectable.

3. Another effect from the expansion or contraction of the material is that LasA and LasB might rotate slightly with respect to the cameras line of sight since the expansion of the DM plate is not the same in both directions in the horizontal plane due to slightly different height and width of the DM plate. However, because of the broad width of the laser beam line profile in the central position (roughly 3 mm) this effect is not detectable at the small scale of expansion and contraction in question.

4. The DM-plate and the camera and laser-plates may expand or contract in the vertical direction. The camera- and laser-plates are of different thickness so for a given temperature change they expand or contract differently. However, there are also empty space and support plates (for the laser plates) and screws in this direction and it is hard to predict how the entire system reacts to a temperature change.

In order to investigate the mechanical stability of the DM, alignment checks using the camera monitoring program are performed for each laser and camera individually in the vertical direction for different temperatures. Alignment checks are performed at 18°C and 23°C in order to check the overlap between the camera line of sight and the laser beam. In these checks, the camera line of sight of both cameras and the laser beam line profile of all lasers are varied in height in the central position individually for the check of the overlap region. The same result is obtained in both checks, the peaks in the camera image disappear simultaneously after $\pm 1/4$ turn of the rear adjustment screw of the camera- and laser-plates. This implies that the center of the vertical distribution is located within 10 μm of the center of this interval for both alignment checks. This in turn implies that the alignment in the vertical direction differ less than 20 μm for each camera and laser at 18°C and 23°C. The fact that the peaks disappear evenly implies that there is no relative rotation between the laser and camera planes.

The pixel correlation plot is used to determine if any relative change in the horizontal position between the cameras occurs at different temperatures. LasA is used in both measurements for the pixel correlation plots with a power setting of 2.96 mW at the temperatures 18°C and 23°C. The power setting is chosen such that the position distributions look fairly similar at both temperatures and the light integral is more than noise for both reflected and refracted light at both temperatures. The pixel correlation plots are shown in figure 5.7. The plots showing the deviation of one cameras pixel content for both cameras in different directions from a set mean value for the pixel correlation plots are shown in figure 5.8. The figure 5.8 shows that in the measurement at 23°C, the pixel content of the cameras deviate less than 0.8 pixels compared to the measurement at 18°C.

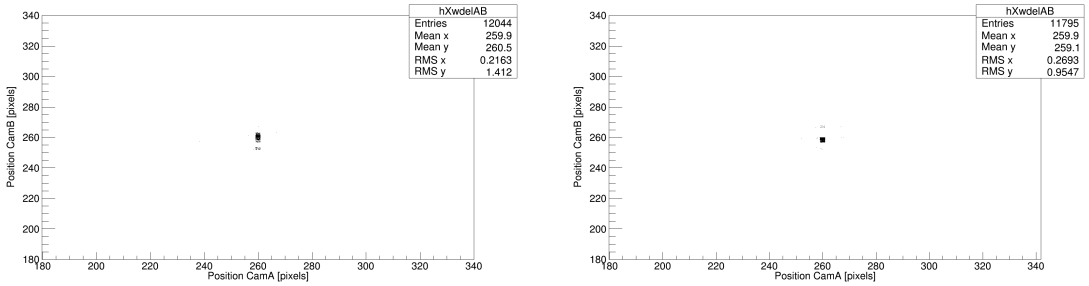

Figure 5.7: Pixel correlation with only LasA at 18°C (left) and 23°C (right).

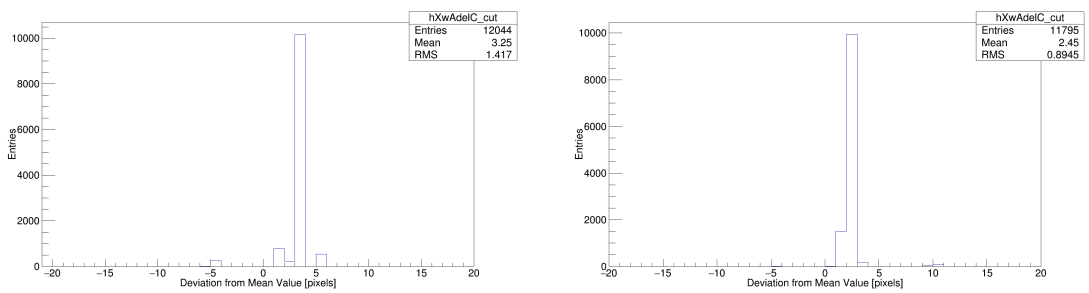

Figure 5.8: Deviation from the mean value with only LasA at 18°C (left) and 23°C (right).

5.4.2 Optical Effects at Different Temperatures

The optics of the cameras and lasers may also be affected by changes in the room temperature and changes of the temperature of the cameras and lasers. In order to investigate how the optics is affected by changes in temperatures, measurements of the light integral and the number of detected light signals are made for different intensities of the laser beam and at two different room temperatures, 18°C, and 23°C. The temperatures of the cameras and lasers are roughly the same as the room temperature for these measurements. The results from these investigations can be seen in figures 5.9-5.12, with plots for refracted light from LasA and LasB (figures 5.9-5.10) and reflected light from LasA and LasB (figures 5.11-5.12). Figures 5.9-5.10 show that the mean value of the light integral increases faster with increasing intensity of the laser beam at lower temperatures. For reflected light the plot for the mean value of the light integral exhibits a small peak at certain values of the power setting. This peak marks the value of the power setting at which so called additional peaks (discussed in section 6.1) start appearing in the spatial distribution. These peaks are called additional since they do not correspond to the position of a fishing line. This peak appears at roughly a 2.98 mW power setting for LasA at 18°C and at a 3.05 mW power setting for LasA at 23°C. For LasB the peak appears at a 3.05 mW power setting for 18°C and at a 3.15 mW power setting at 23°C. The number of detected light signals also exhibits a peak at slightly higher intensities of the laser beam than at which the additional peaks start appearing. The plots of the mean value of the light integral in 5.11-5.12 show that itl increases faster with increasing power setting at lower temperatures. However, this pattern can be seen to be broken in the left plot of figure 5.11 for power settings larger than 3.1 mW. The plot of the number of entries, *i.e.* detected light signals in figure 5.12 shows peaks which appear at lower values of the power setting for lower temperatures.

The fact that the number of detected light signals increases at higher values of the power setting for the laser at higher temperatures implies that the detection efficiency of the cameras is temperature dependent in the region investigated, a 2.7-3.3 mW power setting for the lasers and temperatures of 18°C to 23°C. A similar behavior of the mean value of the light integral shows that the detected light in the cameras get weaker for increasing temperatures and is therefore temperature dependent in the investigated regions of the intensity of the laser beam and temperature.

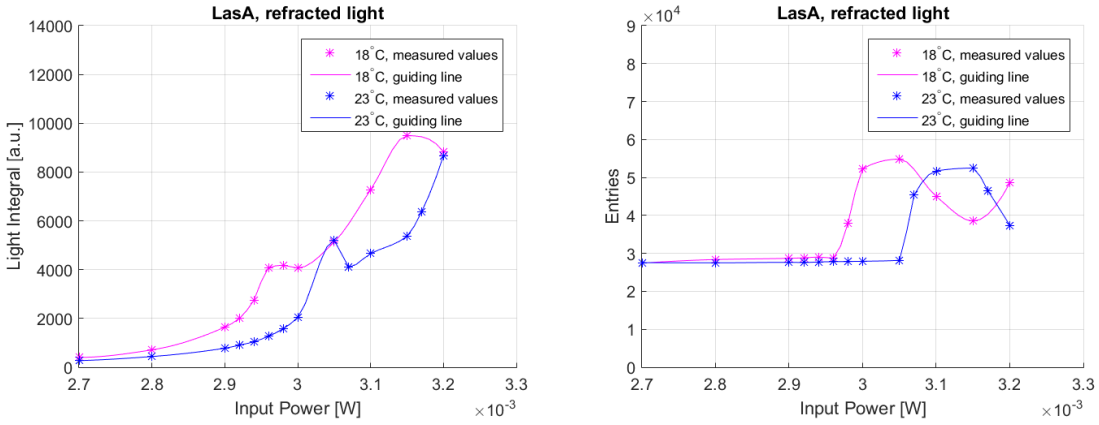

Figure 5.9: Refracted light from LasA detected in CamA. The mean value of the light integral at 18°C and 23°C as a function of the power setting is shown in the left plot. The corresponding number of entries is shown in the right plot.

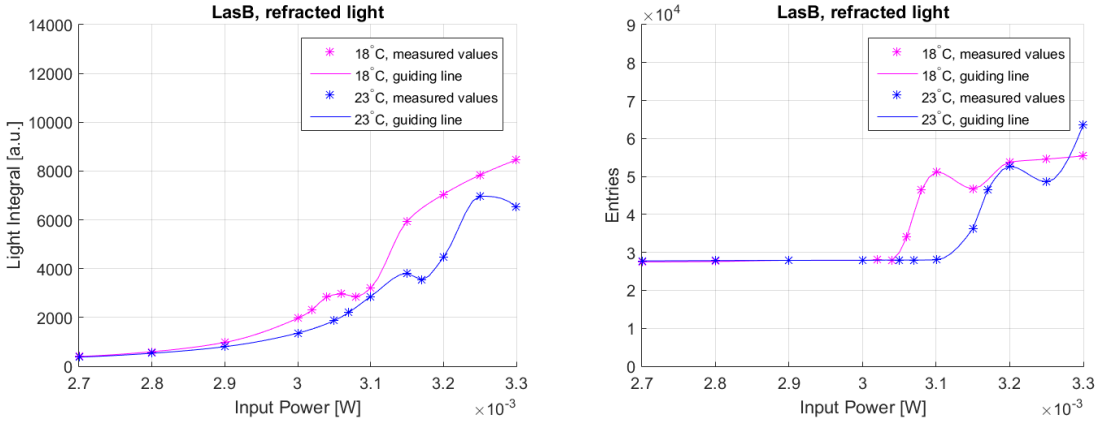

Figure 5.10: Refracted light from LasB detected in CamB. The mean value of the light integral at 18°C and 23°C as a function of the power setting is shown in the left plot. The corresponding number of entries is shown in the right plot.

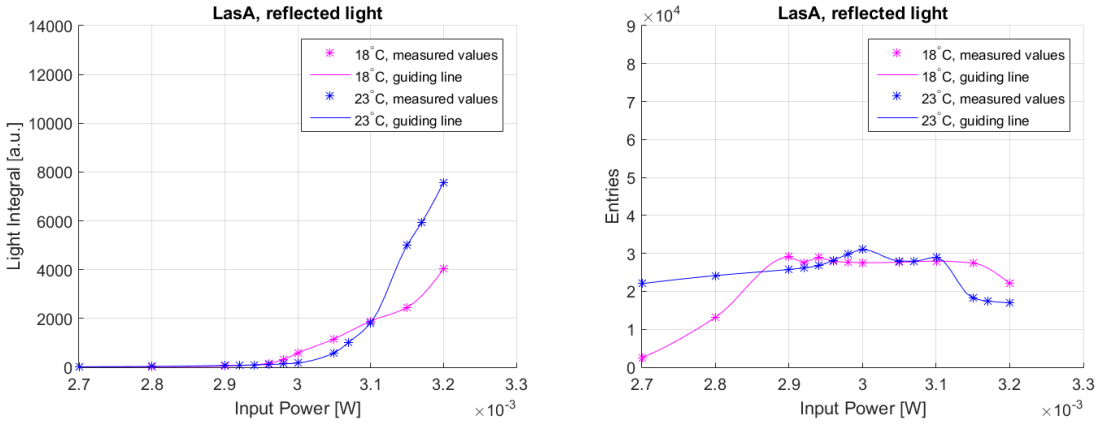

Figure 5.11: Reflected light from LasA detected in CamB. The mean value of the light integral at 18°C and 23°C as a function of the power setting is shown in the left plot. The corresponding number of entries is shown in the right plot.

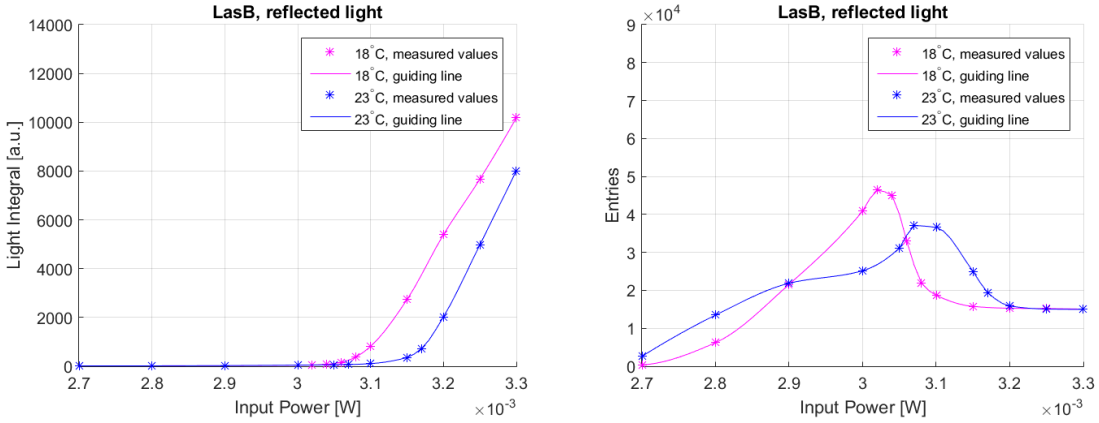

Figure 5.12: Reflected light from LasB detected in CamA. The mean value of the light integral at 18°C and 23°C as a function of the power setting is shown in the left plot. The corresponding number of entries is shown in the right plot.

5.5 Sensitivity to Magnetic Fields

The sensitivity to magnetic fields of the DM has previously been evaluated at the PTS. Since the support material, which is made of aluminum, is not magnetic, the only expected change in alignment between the cameras and lasers is from the optics of the cameras and lasers. How the optics is affected by the presence of magnetic fields has been tested by observing the camera image of a laser beam and bringing a magnet of 100 Gauss close to cameras and lasers. The camera image did not change in the presence of the magnetic field indicating that the optics was not affected. The maximum expected magnetic field the DM would be exposed to at PANDA is 50 Gauss [9].

5.6 Stability over Time

One problem with the setup when left for a longer time is that the tension of the fishing lines tends to decrease. This can be fixed by fastening weights to the fishing lines as can be seen in the photos of figure 5.13, this is, however, very unpractical for two reasons. First, the fishing lines are fastened with tape at the bottom and at the top of the target holder, and if weights are fastened to the fishing lines the tape is not enough to stop the fishing lines from sliding upwards in the holder. Since the fishing lines are not perfectly homogeneous, this affects the camera image. If needed, this problem could be solved using strong glue instead of tape. Second, the weights also need to be fastened to the holder since they destabilize the holder by swinging making the target holder swing. This makes the setup with weights quite unpractical. The best and simplest way to keep the tension in the fishing lines is to adjust them when needed.

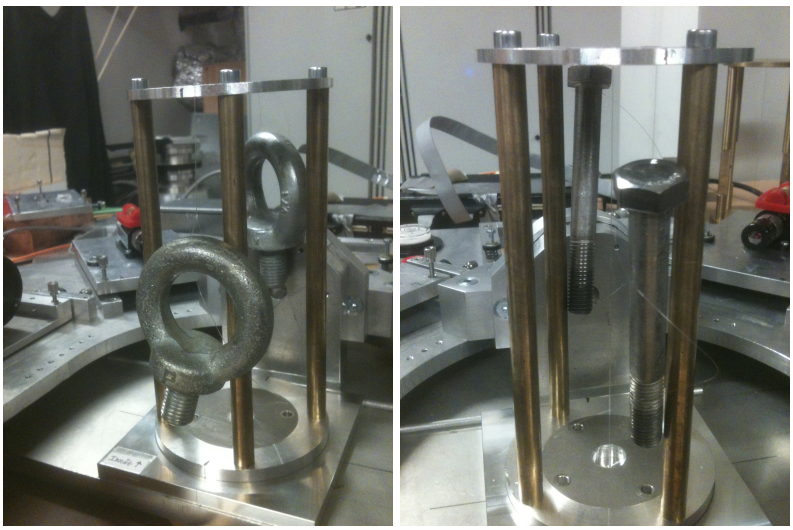

Figure 5.13: A target holder with two fishing lines with heavier weights (left) and lighter weights (right).

Chapter 6

Camera Effects

The DM (Detection Module) can be used for examining and optimizing the optics of the lasers and cameras as well as the effects of the camera settings such as the focus and apertures. This can be done with an alignment bench target in the alignment bench setup as well as with a pellet stream by a pellet beam pipe. Since the light signals from pellets differ from the light signals from the alignment bench target both in amplitude and length the effects must be examined for both cases.

6.1 Light Intensity

In the alignment bench setup, a low intensity of the laser beam is desired firstly for safety reasons, there is less risk of eye damages with lower intensity and secondly, effects such as reflections between the cameras appear for higher intensities of the laser beam. However, optical effects appear at higher values of the power setting ($\gtrsim$ 3.1 mW) for the lasers with measurements with fishing lines at the alignment bench setup. This is troubling because it needs to be known that the lasers behave the same way for different values of the power setting. It also needs to be known how the detected images of the fishing lines behave for different values of the power setting and thereby the intensity of the laser beam. The optical effects in question heavily affect the detected image of the fishing lines and the collected light.

When the power setting for the lasers is around the area of the small peak in the left plots in figures 5.9 and 5.10, additional peaks (one for each fishing line), one pixel wide appear in the position distribution plot. These peaks are referred to as additional peaks because they do not correspond to the positions of fishing lines and have a different appearance as compared to the wider peaks corresponding to the positions of fishing lines. Two such additional peaks can be seen in the left plot of figure 6.1 roughly one pixel to the left of the wider peaks corresponding to the positions of the fishing lines. The new, additional peaks follow at a constant distance from the original peaks in the position distribution when the target holder is moved in the direction perpendicular to the line of sight of the camera. This implies it is some optical effect originating from the camera. The new peaks are only seen in refracted light, probably because the light signals from the refracted light carry a larger amount of light. The additional peaks contribute to the light integral with

peaks at low values as can be seen in the left plot of figure 6.3, since they carry a low amount of light as compared to the signals giving rise to the regular peaks. This naturally lowers the mean value of the light integral spectra. This is the reason for the small peaks in the left plots in figures 5.9 and 5.10. For a power setting of the laser larger than the power setting for which the peak in the light integral vs the power setting plot in figures 5.9 and 5.10 appears, an additional effect of smearing of the original peaks appear in the position distribution. Such a smearing can be seen in the right plot of figure 6.1. The smearing increases with increasing intensity of the laser beam and the distance between the original peaks increases and eventually gets impossible to read off. The light distribution plots are affected to a lesser extent by high values of the power setting ($\gtrsim 3.1$ mW). The peaks in the light distribution get slightly thicker for larger power settings. An example of this can be seen in figure 6.2. The light integral plot also exhibits smearing for larger power settings as can be seen in the right plot in figure 6.3. These effects of smearing at higher intensities of the laser beam appear to be partly due to reflections between the cameras. The cluster width for the same two values of the power setting for the laser can be seen in figure 6.4. The cluster width also gets wider for higher values of the power setting for the laser.

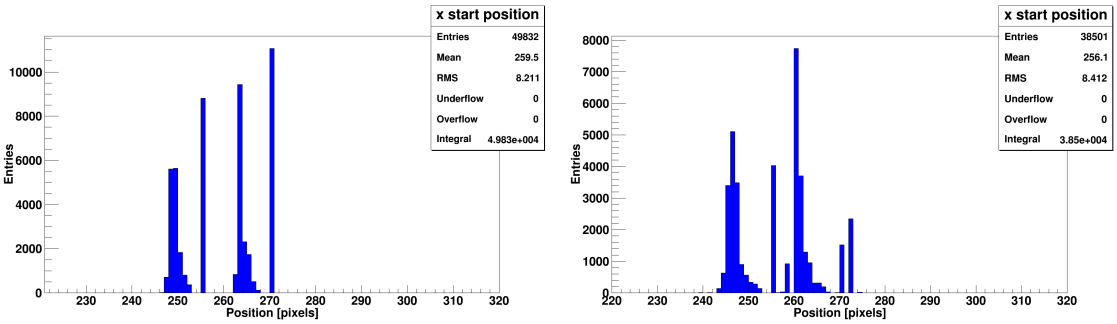

Figure 6.1: Position distributions for the cases of a 3 mW power setting for LasA (left) and a 3.15 mW power setting (right). In the left plot, two additional peaks one pixel wide appear to the right of the wider original peaks. In the right plot the smearing of the position distributions has become prominent.

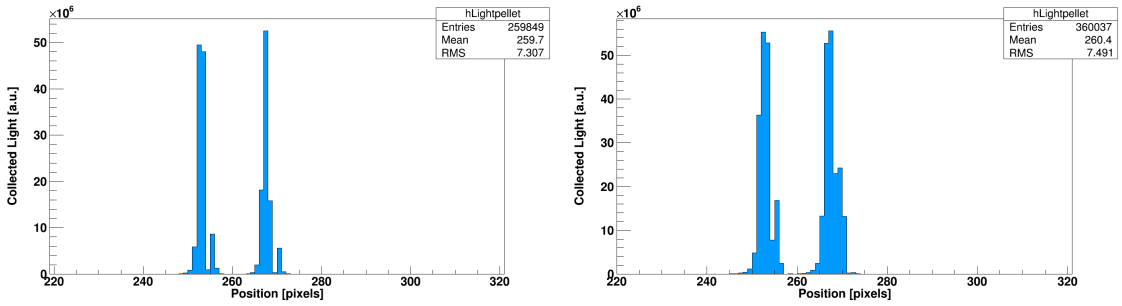

Figure 6.2: Light distribution for the cases of a 3 mW power setting for LasA (left) and a 3.15 mW power setting (right).

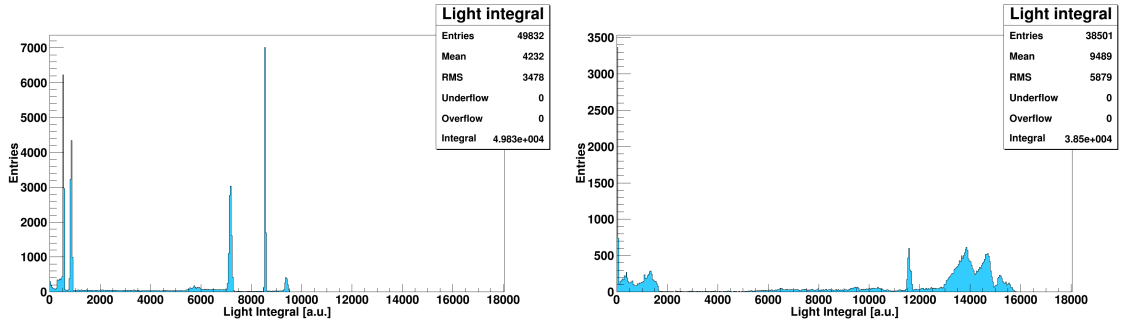

Figure 6.3: Light integral for the cases of a 3 mW power setting for LasA (left) and a 3.15 mW power setting (right).

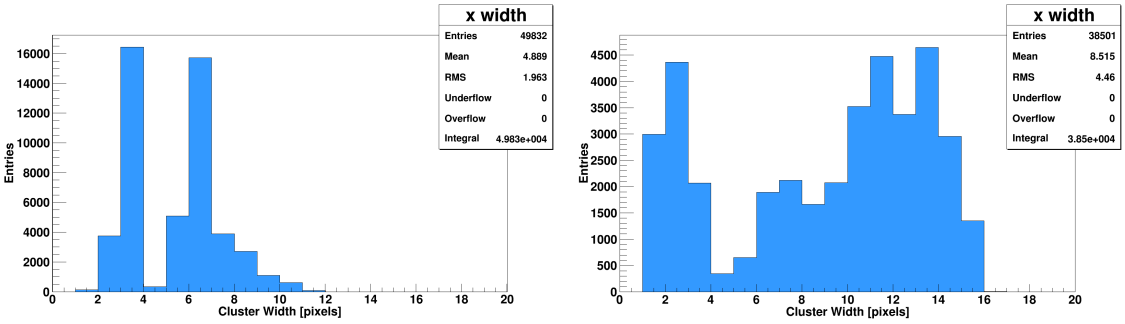

Figure 6.4: Cluster width for the cases of a 3 mW power setting for LasA (left) and a 3.15 mW power setting (right).

6.2 Focus

In order to investigate the focus of the cameras in the horizontal direction along the camera line of sight, one transparent fishing line of diameter 0.08 mm is used and it is displaced to the right and to the left (in the direction of the line of sight of the cameras) with respect to the central position (as is depicted in the sketch in figure 6.5). The line of sight of the cameras is also raised and lowered at the central position in order to investigate the dependence of the focus in the vertical direction. For these investigations, LasC is used with a power setting of 6 mW, a frequency of the laser pulses of 4 kHz and a pulse length of 2.5 μm. Since both cameras detect similar light signals from this laser, this assures that the only differences appearing between the two camera images originate from the focus of the cameras. For these investigations, the camera not used is covered in order to prevent any reflections between the cameras affecting the light integral.

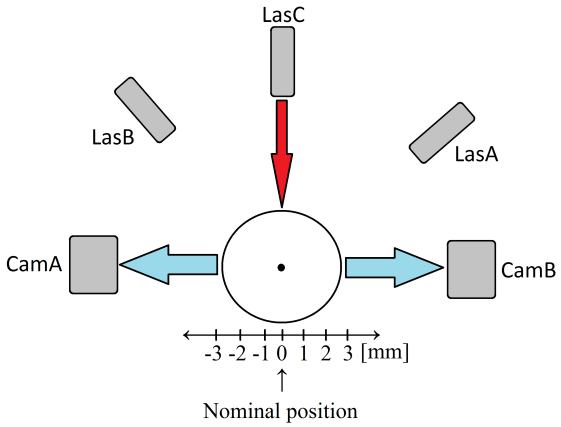

Figure 6.5: Schematic sketch of the experimental setup is seen from above indicating the displacement of the fishing line in the horizontal direction along the line of sight of the cameras. Note that the distances in the sketch are not to scale, the distance between the focal planes of the cameras and the central position is 250 mm in the real setup.

The results from the investigations of the focus of the cameras using a fishing line can be seen in figure 6.6 and 6.7. In figure 6.6 the mean value of the light integral and the number of entries, *i.e.* detected light signals, are plotted as a function of the distance of the fishing line from the central position where the camera is focused. The mean value of the light integral and the number of entries is plotted as a function of the height of the line of sight of the cameras in 6.7. The mean value of the light integral for both cameras is rather constant throughout the expected overlap region between the laser beam and camera line of sight in the horizontal direction along the line of sight of the cameras, which is slightly more than 3 mm. The number of entries is very constant over the expected overlap region and slightly outside the region. The same is true for the results in the plots in figure 6.7 where the expected overlap region is roughly 50 μm in the vertical direction at the central position. Here however, the mean value of the light integral display a clear peak centered at the nominal height of the line of sight of the camera. The figures 6.6 and 6.7 show that the focus of both cameras is centered roughly in the nominal position in both directions.

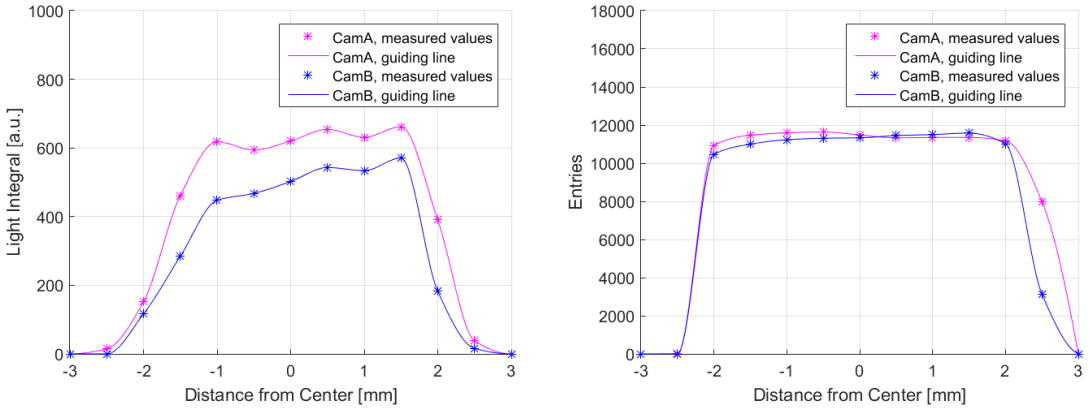

Figure 6.6: The mean value of the light integral (left) and the number of entries (right) as a function of the distance between the fishing line and the central position where the cameras are focused. The camera not used is covered in order to prevent reflections between the cameras.

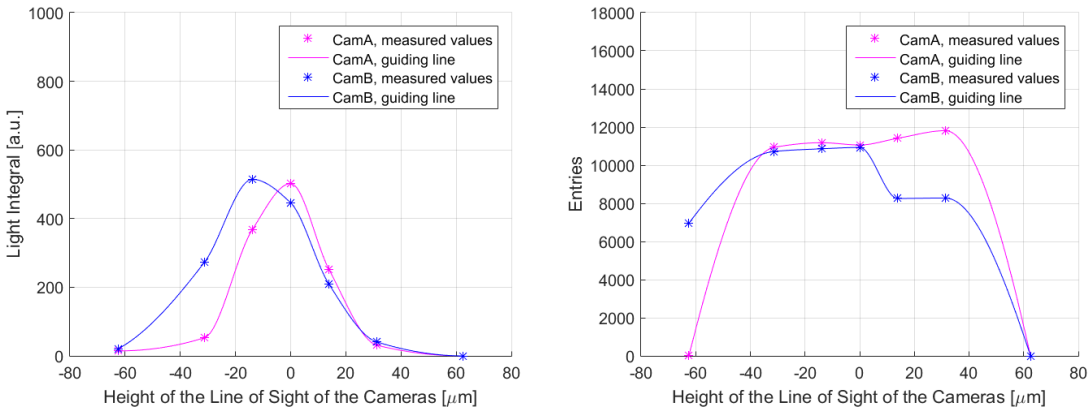

Figure 6.7: The mean value of the light integral (left) and the number of entries (right) as a function of the height of the camera line of sight as measured from the nominal position determined to be the best in the alignment. The camera not used is covered in order to prevent reflections between the cameras.

The conclusion is that the camera line of sight is located within $\pm 20\ \mu m$ of the nominal position in the vertical direction set using wxPropView. The mean value of the light integral and the number of entries is quite constant over the expected overlap region between the camera line of sight and the laser beam in the horizontal plane.

The effects of the camera focus settings were also examined with pellets by doing measurements for different focus settings. These measurements are performed individually for all lasers with a power setting of 100 mW for all lasers. The number of entries detected in the cameras for different lasers and focus settings is presented in table 6.1.

Table 6.1: The number of entries at different focus settings of both cameras.

Focus		1	1.2	1.3	1.7
LasA	CamA	$67{\cdot}10^3$	–	$46{\cdot}10^3$	$34{\cdot}10^3$
	CamB	$50{\cdot}10^3$	$33{\cdot}10^3$	$44{\cdot}10^3$	–
LasB	CamA	$40{\cdot}10^3$	–	$41{\cdot}10^3$	$31{\cdot}10^3$
	CamB	$43{\cdot}10^3$	$31{\cdot}10^3$	$42{\cdot}10^3$	–
LasC	CamA	$44{\cdot}10^3$	–	$42{\cdot}10^3$	$32{\cdot}10^3$
	CamB	$40{\cdot}10^3$	$33{\cdot}10^3$	$41{\cdot}10^3$	–

The number of entries peaks at a focus setting of 1 and 1.3.

6.3 Apertures

For fishing lines, aperture setting bl:5.6 is in general used and for pellets, from which the cameras do not detect as strong light signals, aperture setting bl:1.4, corresponding to the biggest aperture, is used. It is important to know how the amplitude of the detected light behaves for different aperture settings, both for pellets and for fishing lines in order to find the best settings possible and to get the best results.

Effects of the apertures are examined at higher intensities of the laser beam in the alignment bench setup. Results from the investigations with different aperture settings with fishing lines can be seen in figures 6.8-6.10. Five transparent fishing lines of diameter 0.12 mm roughly 1 mm apart are used in the investigations with fishing lines. The figures are from measurements made with LasA with a 3.2 mW power setting. These measurements are a part of a test to investigate if the effects of smearing and the additional peaks (discussed in section 6.1) at higher intensities of the laser beam can be decreased by changing the aperture setting of the camera. The aperture setting of CamB is bl:5.6 throughout the measurements. The plots show the position distributions, the light distributions and the light integral for CamA for two different aperture settings of CamA; bl:5.6 and bl:16. The high peaks, one pixel wide, in the position distribution, most prominent in the left plot of figure 6.8, are additional peaks. The left plot of the light integral in figure 6.9 is completely unreadable whereas the right plot display (some) peaks corresponding to the peaks in the position distribution. This behavior is quite expected since increasing the aperture setting decreases the amount of light collected by the camera. The height of left peaks in the light distribution drastically decreases and the peaks get narrower for higher aperture settings as can be seen by comparing the plots in figure 6.10. In the light distribution, the peaks corresponding to the fishing lines are sometimes divided into two peaks. The gap in between these probably corresponds to a position in the center of a fishing line from where no light reaches the camera.

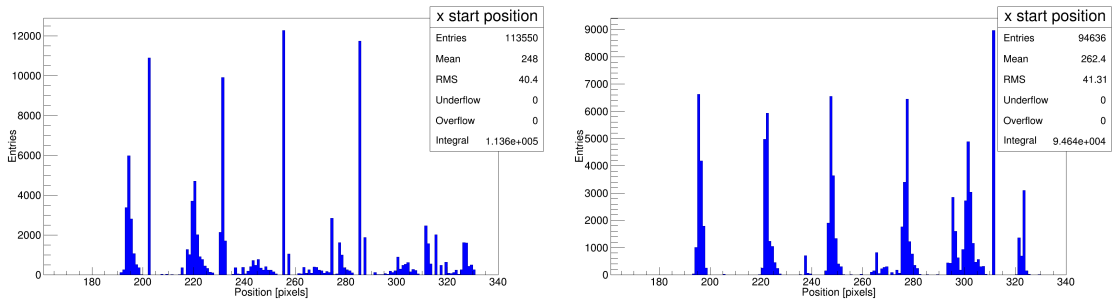

Figure 6.8: The position distribution as measured in CamA for an aperture setting of CamA of bl:5.6 (left) and bl:16 (right).

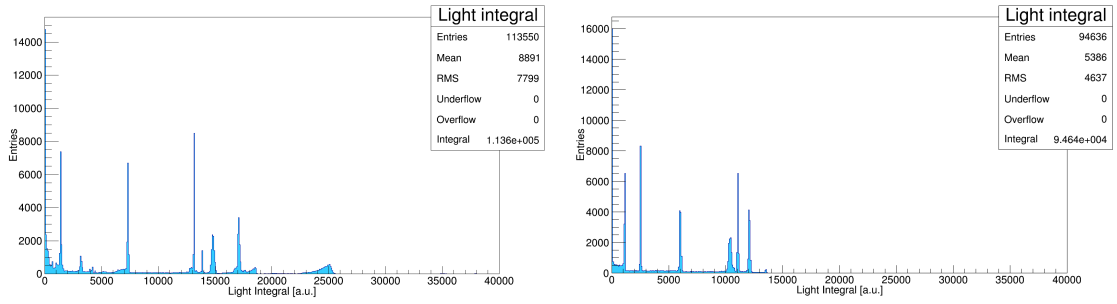

Figure 6.9: The light integral as measured in CamA for an aperture setting of CamA of bl:5.6 (left) and bl:16 (right). The left plot is quite unreadable whereas the right plot displays some peaks corresponding to the peaks in the position distribution.

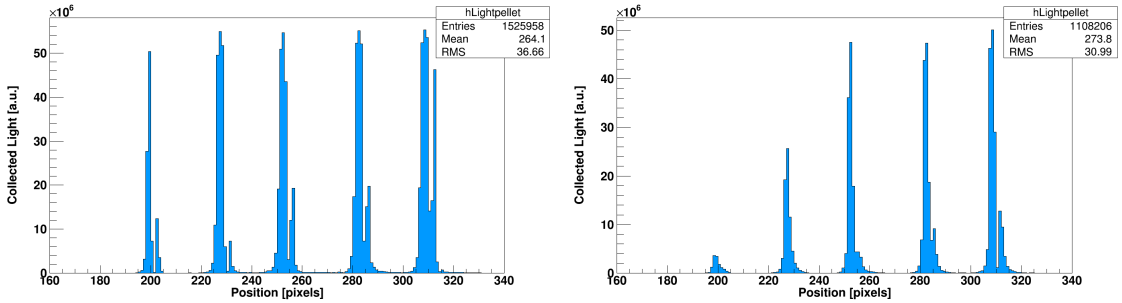

Figure 6.10: Light distribution as measured in CamA. The left plot shows the light distribution for an aperture setting of bl:5.6 and the right plot for an aperture setting of bl:16.

Figure 6.11 shows how the mean value of the light integral as measured in both cameras depends on the aperture settings of CamA. The results are from measurements with five fishing lines with a diameter of 0.12 mm roughly 1 mm apart and with a power setting of 3.2 mW for LasA in the alignment bench setup. The mean value of the light integral decreases heavily for CamA as the value of the aperture setting of this camera is increased. The collected light should decrease by half between two values of the aperture setting when going to higher from lower values in the figure. However, this is not the case, sometimes the mean value of the light integral decreases more and sometimes less. This might be because five fishing lines are used in the tests and that the light integral have an unpredictable behavior for five fishing lines and for higher intensities of the laser beam. The mean value of the light integral of CamB is also affected slightly even if the aperture setting of this camera is kept constant. This effect is probably due to reflections between the cameras which depend on the aperture setting.

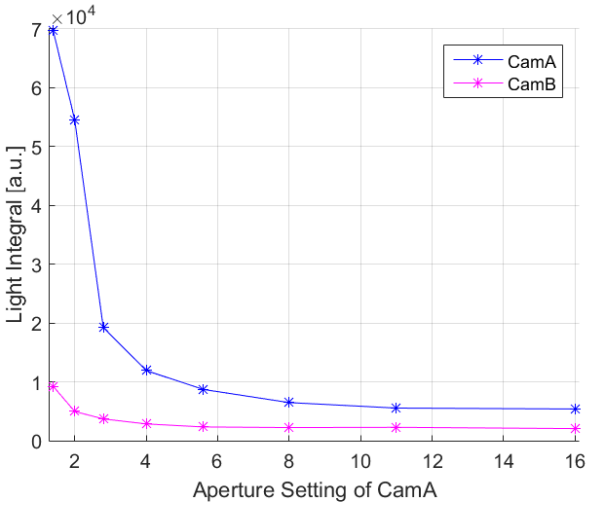

Figure 6.11: The aperture setting of CamA vs the light integral as detected in both cameras. The mean value of the light integral detected in CamA decreases drastically and the light integral of CamB decreases slightly for increasing aperture setting of CamA.

The investigations of the effects of the apertures of the cameras with pellets is made by comparing the light signal from one laser (LasA, LasB and Las C respectively) as well as the light signal when all three lasers are used simultaneously at different aperture settings of CamB. The aperture setting of CamA is bl:1.4 for reference. Different intensities of the laser beam are also used in order to investigate the differences. Results from the investigations of the effects of the aperture setting with pellets are presented in tables 6.2-6.4 where the number of light signals in each camera is presented for different aperture settings of CamB. Together with schematic sketches of the setup used for the measurements (figures 6.12-6.14) the results are divided into parts according to if refracted light, reflected light or both at the same time is used since this affects how the number of light signals is affected by the aperture setting. The results show a greater sensitivity for the number of light signals and the collected light from LasA (reflected light at 45° angle) and LasC (reflected light at 90° angle) of the aperture settings of CamB than for the number of light signals and the collected light from LasB (refracted light at 135° angle). This is the case for all values of the power setting used. For an aperture setting of bl:11 CamB do not detect any signals from LasA or LasC with a power setting of 10 mW.

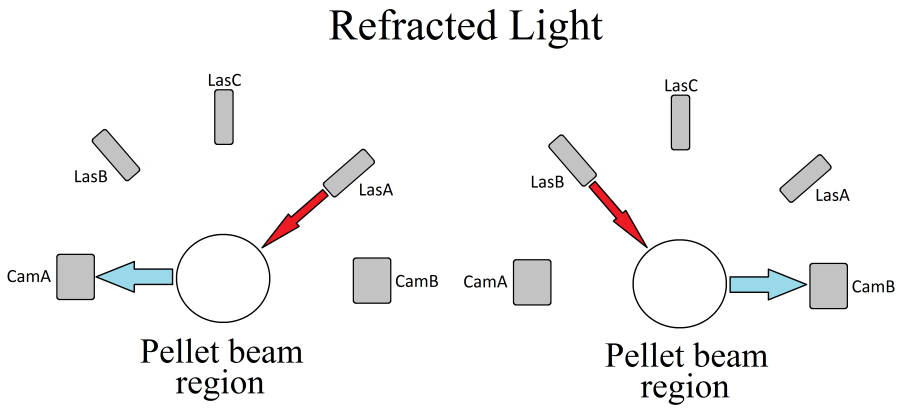

Figure 6.12: Schematic sketch of how light is refracted from LasA and LasB.

Table 6.2: The number of light signals detected in both cameras for different aperture settings of CamB. Only refracted light is used.

Aperture setting, CamB	1.4	5.6	11	16
LasA, 10 mW, CamA	$13 \cdot 10^3$	$13 \cdot 10^3$	$14 \cdot 10^3$	–
LasB, 10 mW, CamB	$12 \cdot 10^3$	$1 \cdot 10^3$	$0.5 \cdot 10^3$	–
LasA, 50 mW, CamA	$19 \cdot 10^3$	$16 \cdot 10^3$	$14 \cdot 10^3$	–
LasB, 50 mW, CamB	$14 \cdot 10^3$	$10 \cdot 10^3$	$3 \cdot 10^3$	–
LasA, 100 mW, CamA	$29 \cdot 10^3$	$16 \cdot 10^3$	–	$14 \cdot 10^3$
LasB, 100 mW, CamB	$28 \cdot 10^3$	$7 \cdot 10^3$	–	$5 \cdot 10^3$

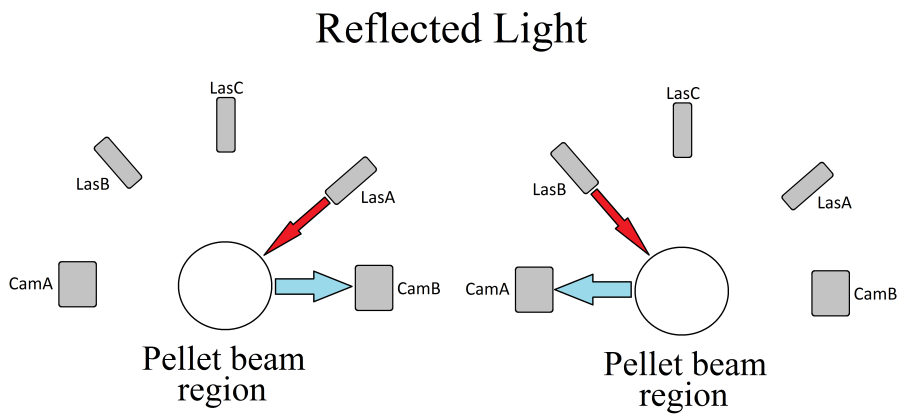

Figure 6.13: Schematic sketch of how light is reflected light from LasA and LasB.

Table 6.3: The number of light signals detected in both cameras for different values of the aperture of CamB. Only reflected light is used.

Aperture setting, CamB	1.4	5.6	11	16
LasA, 10 mW, CamB	$13 \cdot 10^3$	$1 \cdot 10^3$	0	–
LasB, 10 mW, CamA	$11 \cdot 10^3$	$9 \cdot 10^3$	$10 \cdot 10^3$	–
LasA, 50 mW, CamB	$18 \cdot 10^3$	$2 \cdot 10^3$	$0.03 \cdot 10^3$	–
LasB, 50 mW, CamA	$14 \cdot 10^3$	$14 \cdot 10^3$	$12 \cdot 10^3$	–
LasA, 100 mW, CamB	$28 \cdot 10^3$	$11 \cdot 10^3$	–	$0.2 \cdot 10^3$
LasB, 100 mW, CamA	$28 \cdot 10^3$	$13 \cdot 10^3$	–	$14 \cdot 10^3$

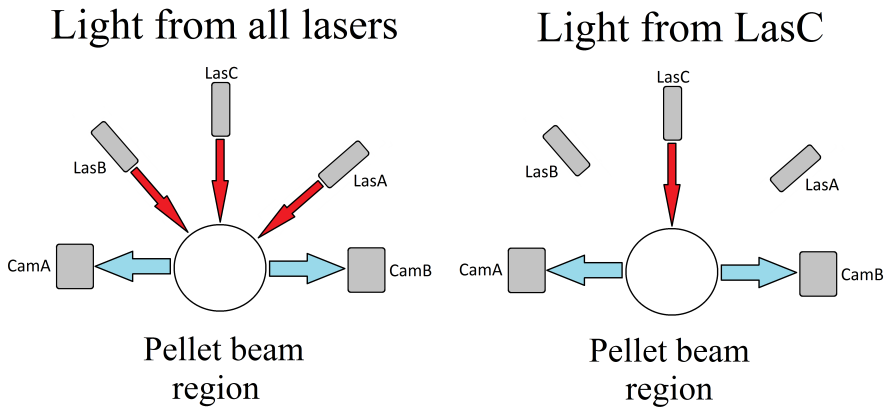

Figure 6.14: Schematic sketch of how light is scattered into the cameras from all lasers simultaneously and from only LasC.

Table 6.4: The number of light signals detected in both cameras for different aperture settings of CamB. Only light from all lasers simultaneously or from only LasC is used. This type of light gives a similar signal in both cameras.

Aperture setting, CamB	1.4	5.6	11	16
LasA, LasB and LasC 10 mW, CamA	$16 \cdot 10^3$	$15 \cdot 10^3$	$14 \cdot 10^3$	$13 \cdot 10^3$
LasA, LasB and LasC 10 mW, CamB	$16 \cdot 10^3$	$7 \cdot 10^3$	$0.7 \cdot 10^3$	0
LasA, LasB and LasC 50 mW, CamA	–	$15 \cdot 10^3$	$16 \cdot 10^3$	–
LasA, LasB and LasC 50 mW, CamB	–	$11 \cdot 10^3$	$4 \cdot 10^3$	–
LasA, LasB and LasC 100 mW, CamA	–	$17 \cdot 10^3$	–	$16 \cdot 10^3$
LasA, LasB and LasC 100 mW, CamB	–	$15 \cdot 10^3$	–	$7 \cdot 10^3$
LasC, 10 mW, CamA	$9 \cdot 10^3$	$9 \cdot 10^3$	$10 \cdot 10^3$	–
LasC, 10 mW, CamB	$11 \cdot 10^3$	$3 \cdot 10^3$	0	–
LasC, 50 mW, CamA	$13 \cdot 10^3$	$14 \cdot 10^3$	$13 \cdot 10^3$	–
LasC, 50 mW, CamB	$14 \cdot 10^3$	$5 \cdot 10^3$	$0.4 \cdot 10^3$	–
LasC, 100 mW, CamA	$29 \cdot 10^3$	$14 \cdot 10^3$	–	$13 \cdot 10^3$
LasC, 100 mW, CamB	$31 \cdot 10^3$	$11 \cdot 10^3$	–	$1 \cdot 10^3$

The position distribution, a close-up of the light integral at low values as well as the cluster width is plotted for different values of the aperture setting of CamB and for different values of the intensity of the laser beam in figures 6.15-6.17. All plots are from measurements with pellets. The position distribution gets weaker and more uneven for higher aperture settings and the light integral gets narrower and peaks at lower values. The cluster width also gets narrower and peaks at lower values for higher values of the aperture settings. Since increasing the aperture setting corresponds to lowering the amount of light detected by the camera, these results make sense. The examples shown have been chosen in order to display the effects of the aperture settings as clearly as possible. *e.g.* the effects of the aperture settings on the position distribution are more prominent for lower intensities of the laser beam and since the smearing of the light integral is larger for higher intensities of the laser beam, the effects of the aperture settings are more visible in the plot in this case.

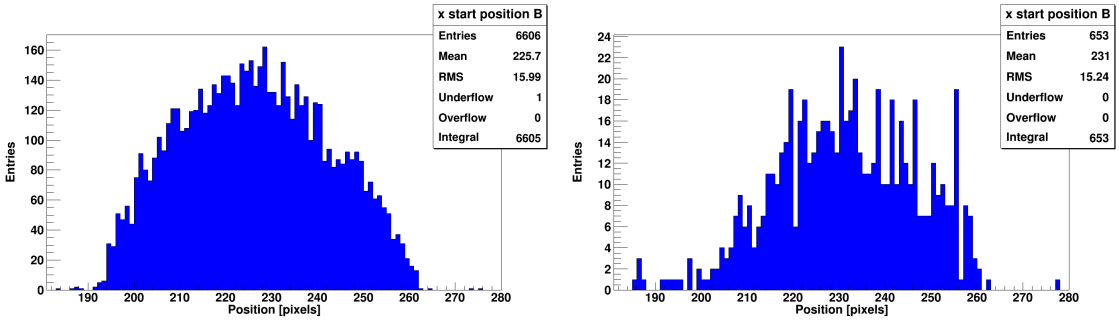

Figure 6.15: Position distributions as measured in CamB. The left plot is from measurements where the aperture setting of CamB is bl:5.6 and the right plot is from measurements with an aperture setting of bl:11. Note that the scale on the y-axis in the right plot is roughly 6 times smaller than that to the left. LasA, LasB and LasC are used with a power setting of 10 mW.

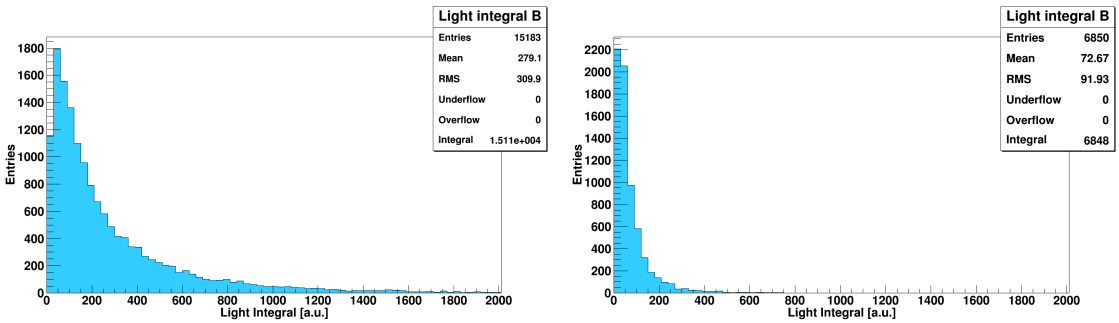

Figure 6.16: Light integral as measured in CamB. The left plot is from measurements where the aperture setting of CamB is bl:5.6 and the right plot is from measurements with an aperture setting of bl:16. LasA, LasB and LasC are used and a power setting of 100 mW.

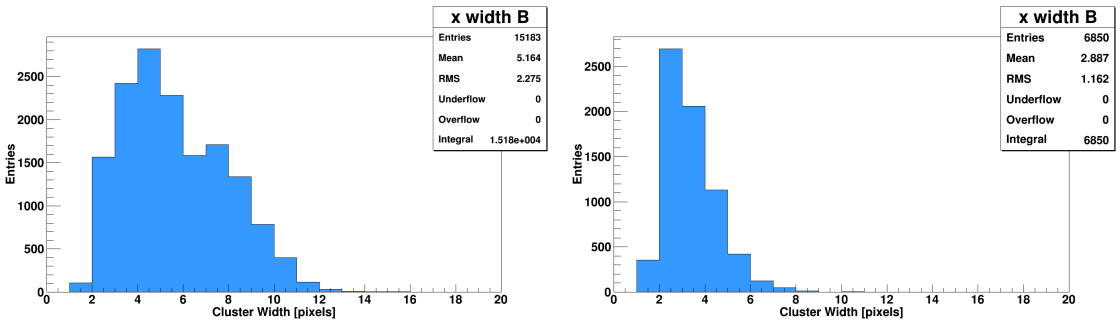

Figure 6.17: Cluster width as measured in CamB. The left plot is from measurements where the aperture setting of CamB is bl:5.6 and the right plot is from measurements with the aperture setting bl:16. LasA, LasB and LasC are used with a power setting of 100 mW.

6.4 Light Signal Length

The exposure cycle of the cameras is very short, 12.5 μs. There is a dead time of 2.5 μs included in this time which is a source of inefficiency. The theoretical inefficiency would be 20% for infinitely short light signals and for signals with an extension in time, there is still some inefficiency. Hence the dead time should be kept as short as possible to minimize this inefficiency. On the other hand, because of the short dead time, light signals slightly longer than the dead time or with a length comparable to the dead time risk being detected in two exposure cycles and thereby being counted twice. By keeping the exposure cycle and the exposure time constant, the effects of different light signal lengths is examined in the test bench setup by varying the light signal length of the pulsing lasers. The light signals counted twice are found from the number of signals with only one readout line between them since these are probably the same signal. Due to the long time between the light signals from the lasers in this investigation (>0.1 ms), the probability for two different light signals to accidentally be detected in two consecutive readout lines is very small. The rise and fall time of the laser pulse is less than 50 ns which constitute such a small part of the light signal length (in all measurements) and is negligible. The set light signal length is therefore used as the actual light signal length. One transparent fishing line of diameter 0.08 mm is used in the investigations. From the measurements it can be concluded what fraction of all detected light signals is counted twice for different light signal lengths.

The result of the investigations is shown in the plot in figure 6.18. Similar results have been obtained previously with a different setup with a LED (Light Emitting Diode) light instead of a laser in reference [5]. The light signal length is plotted against the fraction of light signals which are counted twice. For light signal lengths superseding 1.75 μs, corresponding to 70% of the dead time in this case, light signals start overlapping the dead time. In this particular case it means that light signals which are 0.75 μs shorter than the dead time can be detected in two exposure cycles in the same camera. At a light signal length below 3.5 μs the fraction of double counted signals are similar in both cameras but for signal lengths above this

light signal length, CamA starts detecting more double counted light signals than CamB.

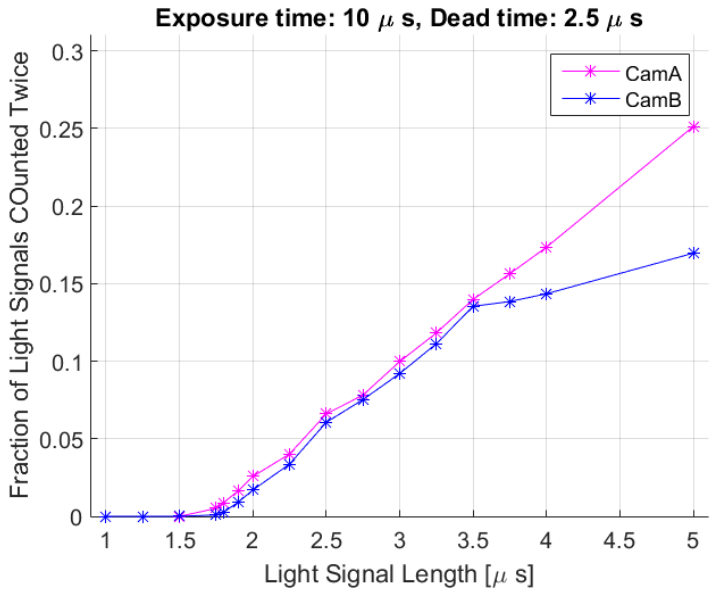

Figure 6.18: Light signal length vs the fraction of light signals counted twice.

6.5 Exposure Cycles

Measures can be taken to minimize the inefficiency due to the dead time. The cameras can be positioned opposite each other, as on the DM (Detection Module). The exposure cycle of one camera can be shifted with respect to the exposure cycle of the other camera such that the dead time in one exposure cycle occur at the exposure time of the exposure cycle of other camera. This way, at least one camera detects light signals at all times. A visualization of the shift between the exposure cycles can be seen in figure 6.19, for the case of a delay of the exposure cycle of CamB. The exposure times with the same label, *e.g.* n, occur at the same time for no delay of the exposure cycle. In order to examine the dependence on the relative delay between the exposure cycles of the two cameras, some series of measurements are performed. In these series of measurements the exposure cycle of CamB is delayed with respect to the exposure cycle of CamA throughout the exposure cycle in steps of 0.5 μs. For each measurement, information is obtained regarding how a signal detected in one camera is detected in the other camera. This is a test of the performance of the DM to see if the cameras detect signals in the way they should.

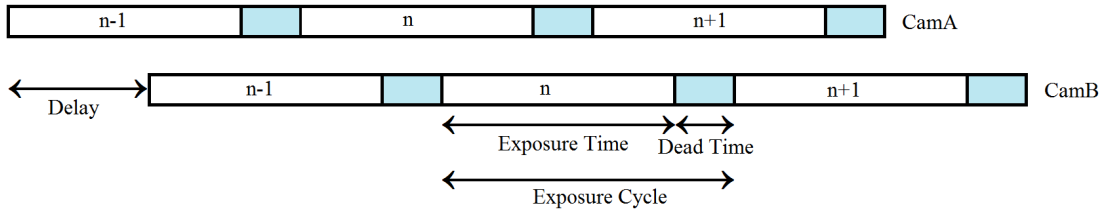

Figure 6.19: A visualization of the exposure cycles of the two cameras with some delay for the exposure cycle of CamB. The blue regions of the exposure cycles indicate the dead time.

In the analysis of the results from investigations with shifted exposure cycles, the detected light signals are referred to as pellets even in the case of measurements of light signals in the test bench setup with a fishing line because to how the analysis program treats the light signals in this analysis. Light signals within 5 pixels of each other (a user set value) in the same readout line are treated as coming from the same pellet. The analysis does not include the case of two pellets in the same readout line so in measurements in the test bench setup, only one fishing line is used.

The time of one exposure cycle, the exposure time and the set dead time are labeled t_{cyc}, t_{exp} and t_{dead} respectively. An effective dead time is used, denoted $t_{dead,eff}$, which is the actual dead time observed for a light signal of finite length. The effective dead time is defined as

$$t_{dead,eff} = max(t_{dead} - t_{signal} - t_{ineff}, 0), \tag{6.1}$$

where t_{dead}, is the dead time set on the NIM crate, t_{signal} is the light signal length and t_{ineff}, which may be positive or negative, is a shortening or elongation of the effective dead time by some electronic or camera inefficiency.

During the measurements with shifted cycles, three different classes are analyzed where pellets are categorized according to how they are detected in one camera as compared to in the other camera. In the analysis of the measurements in section 6.6, three classes of pellets are of interest.

1. **ABinSame** is the class consisting of all pellets detected in the same exposure cycle (readout line), *e.g.* n, in both cameras. For shorter delays of the exposure cycle of CamB, most pellets end up in this class since the temporal overlap of the same exposure cycle, is the largest for shorter delays. For no delay of the exposure cycle of CamB, all pellets should end up in this class. The fraction of pellets in this class decreases linearly with increasing delay until the delay is $t_{cyc} - t_{dead,eff}$ where it reaches zero since the temporal overlap between the exposure cycles n stop decreasing at this point and is zero.

2. **ABinPrevious** is the class consisting of the pellets detected by CamB in the previous readout line as compared to the readout line where CamA detects the same pellet. For no delay of the exposure cycle of CamB, the number of pellets in this class is zero since there is no temporal overlap between the exposure cycles $n-1$ in CamB and n in CamA. The fraction of pellets in this

class start increasing at a delay of $t_{dead,eff}$ of the exposure cycle of CamB since the overlap between the exposure cycles $n-1$ in CamB and n in CamA start increasing at this delay. The fraction of pellets in this class increases linearly with increasing delay of the exposure cycle of CamB until the delay is t_{cyc} where the fraction of pellets in this class is 1.

3. **AnoB** consists of the pellets detected by CamA but not by CamB in the same exposure cycle or in the previous. For no delay of the exposure cycle of CamB, the fraction of pellets in this class is zero. The fraction of pellets in this class increases linearly with increasing delay of the exposure cycle of CamB until the delay is $t_{dead,eff}$. The fraction of pellets is constant for delays of the exposure cycle longer than this time until the delay becomes $t_{cyc} - t_{dead,eff}$ where the fraction of pellets in this class once again start decreasing linearly and becomes zero at a delay of t_{cyc}. If the cameras detect a different number of pellets during one measurement this class may not contain the same number as $BnoA$, the class consisting of the pellets detected by CamB but not by CamA in the same exposure cycle or in the previous.

An example of the expected behavior of the fraction of pellets in the classes can be seen in figure 6.20 for an exposure cycle time of $12.5\mu s$ and effective dead time of $1.75\mu s$. The example values have been chosen to clearly illuminate the expected behavior of the classes. Checking how large fraction of the detected pellets end up in which of these classes for real measurements gives a measure of the detection efficiency.

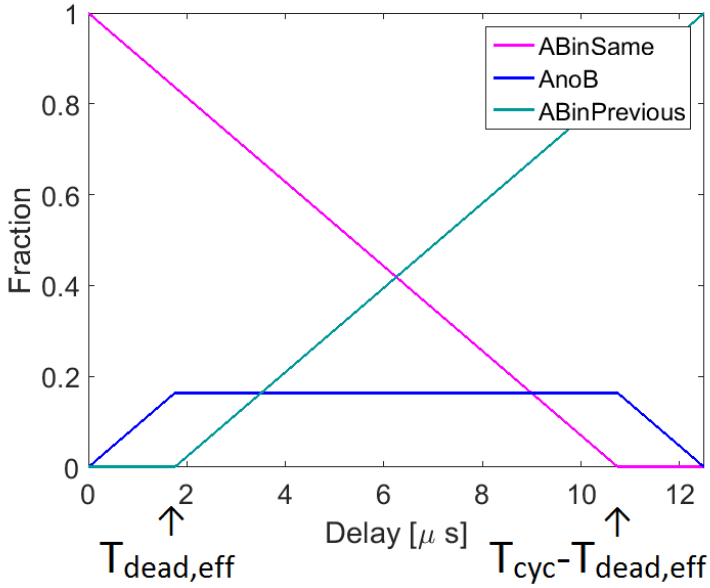

Figure 6.20: Example of the expected fraction of pellets in the three classes *ABinSame*, *AnoB* and *ABinPrevious* for different delay of the exposure cycle of CamB for an exposure cycle time of 12.5 μs and effective dead time of 1.75 μs.

6.6 Shifted Exposure Cycles

In order to test the performance of the setup of the DM, series of measurements with the exposure cycle of one camera successively delayed relative the exposure cycle of the other camera can be performed. In these measurements *e.g.* the fraction of pellets ending up in the classes *ABinSame*, *ABinPrevious* and *BnoA* if the exposure cycle of CamB is delayed relative the exposure cycle of CamA can be examined. The behavior of these fractions for different delays gives an idea of the performance of the DM. Eight series of measurements with the exposure cycle of CamB delayed relative the exposure cycle of CamA are performed with pellets and with different configurations of the lasers and different intensities of the laser beam. An exposure cycle of 12.5 μs and exposure time of 10 μs are used for these measurements. These types of measurements are also performed for different light signal lengths and frequencies with a fishing line in the test bench setup. In these measurements, different camera exposure times are used but constant exposure cycle time. As described in section 6.5, in this analysis the number of light signals is not of interest but the clusters of light signals within 5 pixels of each other (in the same readout line) being interpreted as one pellet. This means that in the measurements in the test bench setup where pellets are not actually used, the entries, *i.e.* the detected light signals, in the classes are still referred to as pellets.

As mentioned, if the light signal length is longer than or comparable to the dead time, some light signals will be counted twice. In order to deal with this problem in the analysis, the number of double counted pellets in each class is found in the analysis program and removed from the analysis. The class *AnoB* is in general not affected by the double counted pellets. The slope of the lines in the data consisting of the classes *ABinSame* and *ABinPrevious* changes drastically when double counted pellets are removed. In the cases with short light signal lengths compared to the dead time, the plots are hardly affected by the double counted pellets. Another issue for the analysis is the possibility of unsynchronized readout frames distorting the result making a too large number of pellets being added to the class *AnoB*. This problem is also taken care of by finding and removing the unsynchronized readout frames from the analysis in the analysis program. The results show that after removing the unsynchronized readout frames, a larger part of the class *AnoB* is removed for shorter delays of the exposure cycle of CamB. The longer the delay, the less number of pellets in the class *AnoB* is removed. This is due to the larger number of readout lines in all readout frames with signals in only one camera for longer delays of the exposure cycle of CamB which makes it harder to distinguish the unsynchronized readout frames for longer delays. Removing the unsynchronized readout frames smooths the lines made out of the three different classes in the original data.

The delay starts at 0.6 μs in all series of measurements with pellets because it is messy to set a shorter delay on the modules of the NIM crate. The delay starts at 0 μs for one series of measurements with a fishing line. The maximal delay of the exposure cycle of CamB is 10.5 μs in all measurements. This is the maximal delay allowed by the electronics.

6.6.1 Double Counted Pellets for Pellet Measurements

The plots in figure 6.21 show the fraction of double counted pellets in each class previously mentioned for different delays of the exposure cycle of CamB from measurements with pellets and with all lasers. The fraction of double counted pellets in each class is greater for a 100 mW power setting than a 10 mW power setting for the laser. The fraction of double counted pellets is greater for the class *ABinPrevious* the smaller the delay of the exposure cycle of CamB is. This is probably due to the small total number of pellets in this class for shorter delays of the exposure cycle making the double counted pellets more prominent.

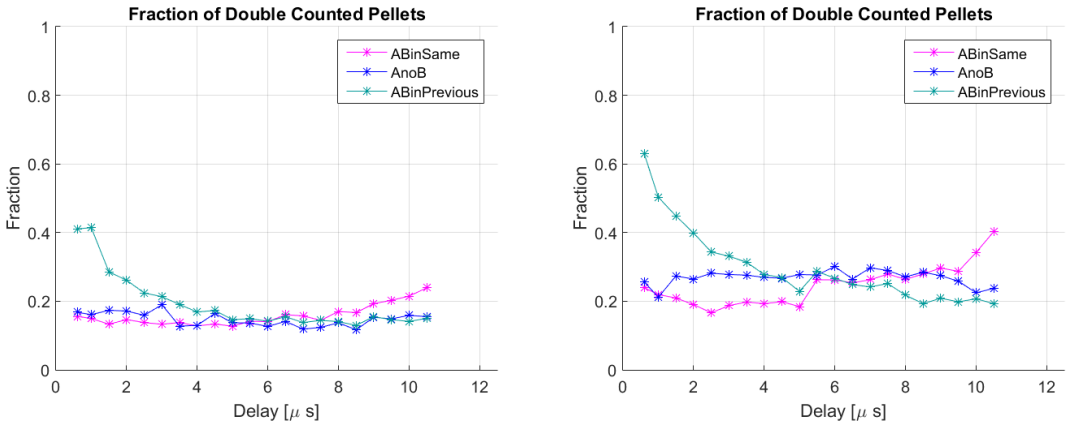

Figure 6.21: The fraction of double counted pellets in the three classes *ABinSame*, *AnoB* and *ABinPrevious* from measurements with pellets and with all three lasers with a power setting of 10 mW in the left plot and with a power setting of 100 mW in the right one.

6.6.2 Shifted Exposure Cycles for Pellet Measurements

The results from the series of measurements with pellets with a delayed exposure cycle of CamB relative the exposure cycle of CamA can be seen in figures 6.22-6.25. Additional results from this type of analysis from measurements with pellets but with only one laser in use can be seen in appendix C. After removing the unsynchronized readout frames, the fraction of detected pellets in the class *AnoB* drastically increases with increasing delay of the exposure cycle of CamB. As mentioned, this is because the unsynchronized readout frames are found by comparing the content of the readout lines in each readout frame of a measurement. If a readout frame contains such a large number of readout lines where the cameras do not detect light signals in the same readout line that it stands out amongst most other readout frames, it is considered unsynchronized. Since the number of readout lines containing light signals in only one camera increases with increasing delay of the exposure cycle of CamB, the unsynchronized readout frames get harder to distinguish for a longer delay. The delay starts at 0.6 μs in all series of measurements with pellets because it is messy to set a shorter delay on the modules of the NIM crate. The maximal delay of the exposure cycle of CamB is 10.5 μs in all measurements. This is the maximal delay allowed by the electronics.

The figures 6.22 and 6.23 show that the unsynchronized readout frames constitute a greater inefficiency than the double counted pellets for measurements with pellets and a 10 mW power setting to all lasers. The latter however constitute a small inefficiency. The figures 6.24 and 6.25 also show that the unsynchronized readout frames constitute a greater inefficiency than the double counted pellets for measurements with pellets and a 100 mW power setting to all lasers.. The latter however constitute a significant inefficiency. Figures 6.22-6.25 show that the effect of double counted pellets is greater for a 100 mW power setting to the lasers than for a 10 mW setting. This is expected from the results in figure 6.21.

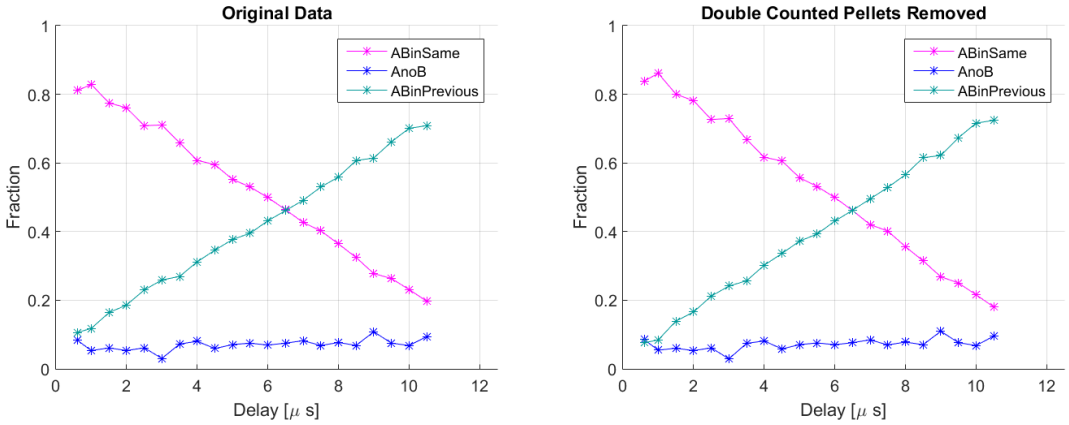

Figure 6.22: The fraction of pellets in the three classes *ABinSame*, *AnoB* and *ABinPrevious* from measurements with pellets and with all three lasers with a power setting of 10 mW. Original data (left) and with double counted pellets removed (right).

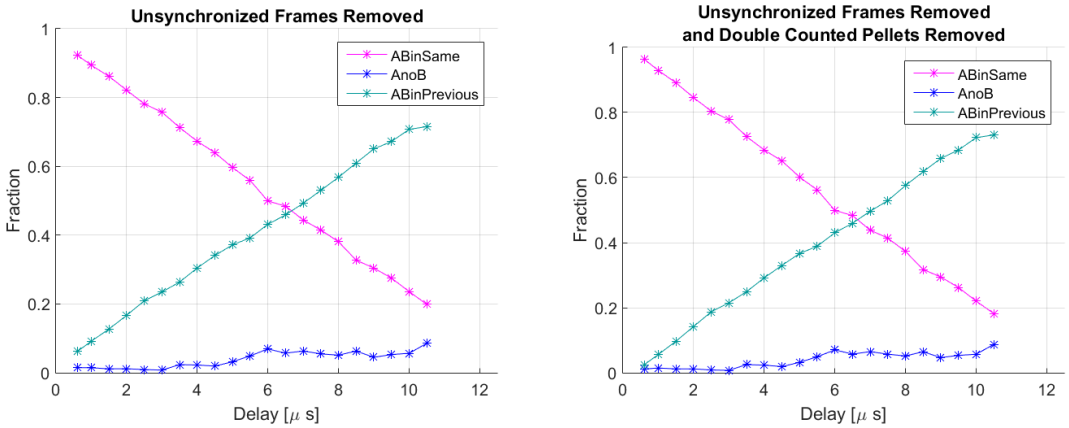

Figure 6.23: The fraction of pellets in the three classes *ABinSame*, *AnoB* and *ABinPrevious* from measurements with pellets and with all three lasers with a power setting of 10 mW. Original data with unsynchronized readout frames removed (left) and data with double counted pellets removed and unsynchronized readout frames removed (right).

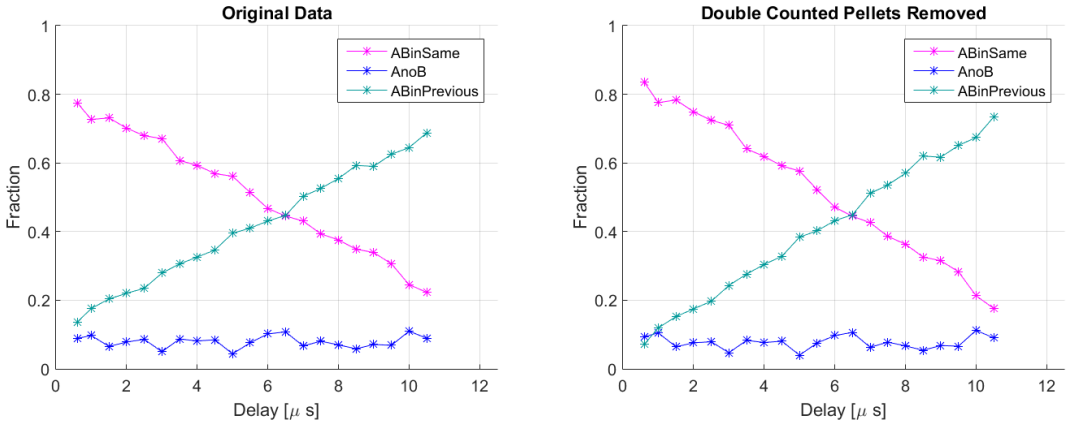

Figure 6.24: The fraction of pellets in the three classes *ABinSame*, *AnoB* and *ABinPrevious* from measurements with pellets and with all three lasers with a power setting of 100 mW. Original data (left) and with double counted pellets removed (right).

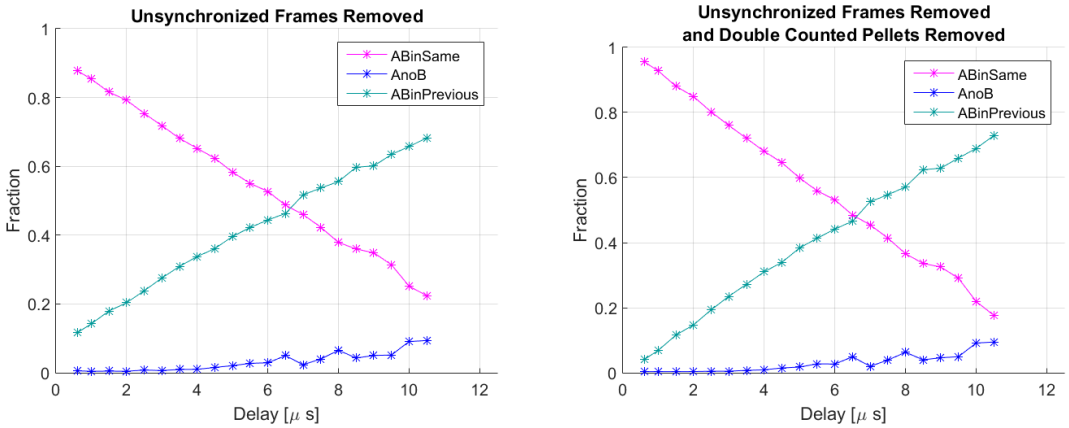

Figure 6.25: The fraction of pellets in the three classes *ABinSame*, *AnoB* and *ABinPrevious* from measurements with pellets and with all three lasers with a power setting of 100 mW. Original data with unsynchronized readout frames removed (left) and data with double counted pellets removed and unsynchronized readout frames removed (right).

6.6.3 Double Counted Pellets for Measurements in the Test Bench Setup

The fraction of double counted pellets in each of the classes *ABinSame*, *AnoB* and *ABinPrevious* from measurements with a fishing line can be seen in figures 6.26 and 6.27 for different light signal lengths and different exposure times. Exposure cycles of 12.5 μs are used throughout the measurements.

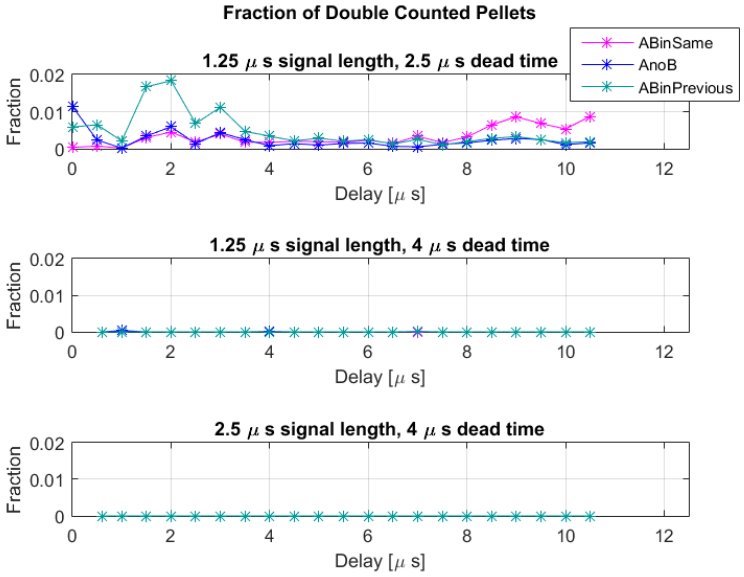

Figure 6.26: The fraction of double counted pellets in the three classes *ABinSame*, *AnoB* and *ABinPrevious* from measurements with fishing lines and with a 1.25 μs light signal length and a 2.5 μs dead time as well as 4 μs dead time in the upper and central plot respectively. The case of a signal length of 2.5 μs and 4 μs dead time is shown in the bottom plot. Note that the scale on the y-axes range between 0 and 0.02 corresponding to 2% of the total number of pellets in the class.

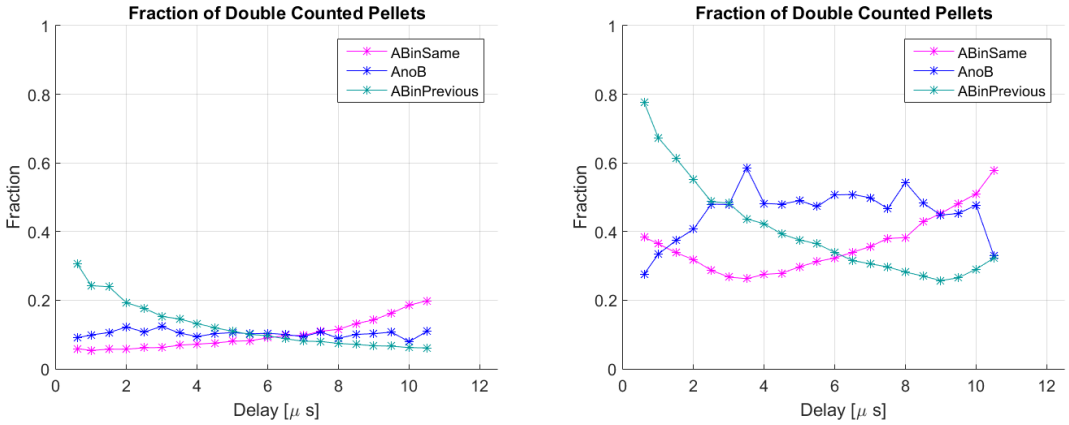

Figure 6.27: The fraction of double counted pellets in the three classes *ABinSame*, *AnoB* and *ABinPrevious* from measurements with fishing lines and with a 2.5 μs signal length and 2.5 μs dead time in the left plot and 5 μs signal length and 2.5 μs dead time in the right plot.

Hardly any light signals overlap the dead time and thereby gets counted twice for the cases of a light signal length of 1.25 μs and 2.5 μs, 1.25 μs and 4 μs dead time as well as the case of 2.5 μs signal length and 4 μs dead time as can be seen in figure 6.26.

Figure 6.27 show that in the case of a 2.5 μs signal length and dead time, a significant fraction of the pellets in the three classes originate from double counted pellets. In the case of 5 μs light signal length and 2.5 μs dead time a very large fraction of the pellets in the three classes originate from double counted pellets. In the cases where the double counted pellets constitute a significant part of the classes *i.e.* the cases shown in the plots in figure 6.27, the fraction of double counted pellets in the class *ABsame* increases with increasing delay of the exposure cycle of CamB and the fraction of double counted pellets in the class *ABinPrevious* decreases with increasing delay. In the left plot, the fraction of double counted pellets in the class *ABinSame* increases with increasing delay of the exposure cycle of CamB whereas the fraction of double counted pellets in the class *ABinPrevious* decreases with increasing delay of the exposure cycle of CamB. The fraction of double counted pellets in the class *AnoB* is not greatly affected by the delay of this exposure cycle and is approximately 10% throughout the series of measurement. A much larger fraction of double counted pellets can be seen in the right plot where the signal length is double the length of the dead time as opposed to in the left plot where the signal length and the dead time is the same. In the right plot the fraction of double counted pellets in the classes *ABinSame* and *ABinPrevious* is larger for both very short and very long delay of the exposure cycle of CamB. The fraction of double counted pellets in the class *AnoB* decreases for shorter and longer delays of the exposure cycle.

6.6.4 Shifted Exposure Cycles for Measurements in the Test Bench Setup

The results from the investigations with a fishing line where the exposure cycle of CamB is delayed relative the exposure cycle of CamA can be seen in figures 6.28-6.32. The fraction of pellets ending up in the classes *ABinSame*, *AnoB* and *ABinPrevious* are plotted as functions of the delay of the exposure cycle of CamB. The unsynchronized frames have been removed in all plots. As mentioned, the number of individual light signals is not used in the plots but rather the number of light signals in one readout line within 5 pixels of each other because these are together interpreted as one pellet. The delay starts at 0.6 μs in all cases but one. This is because it is messy to set a shorter delay on the modules of the NIM crate. The maximal delay of the exposure cycle of CamB is 10.5 μs in all measurements. This is the maximal delay allowed by the used electronics.

The effects of the double counted pellets on the data in figures 6.28-6.32 are in agreement with the results in figures 6.26-6.27 showing the fraction of double counted pellets in these cases. The shorter the light signal length is compared to the dead time, the smaller the effects of double counted pellets on the data.

Figure 6.28 shows that unsynchronized double counted pellets are a great sources of inefficiency in the analysis with shifted exposure cycles in this particular case since both plots in the figure are very similar. This is for the case of a light signal length of 2.5 μs and a 2.5 μs dead time as well. Figure 6.29 shows that double counted pellets do not constitute a great inefficiency in the case of a light signal length of 1.25 μs and a 2.5 μs dead time. This is because the plots are quite similar. Figure 6.30 shows that double counted pellets are a great source of inefficiency in the case of a light signal length of 5.0 μs and a 2.5 μs dead time. After removing the unsynchronized readout frames most entries in the class *AnoB* are zero. Since the light signal length is double the length of the dead time no signals are expected to be detected by only one camera so this result makes sense. Removing the double counted pellets drastically changes the slopes of the lines consisting of the classes *ABinSame* and *ABinPrevious* as can be seen by comparing the plots in figure 6.30. Figure 6.31 shows that the in the case of a 2.5 μs light signal length and a 4.0 μs dead time the effect of double counted pellets is negligible. Around 10% of all pellets in this analysis are detected in only CamA and end up in the class *AnoB*.

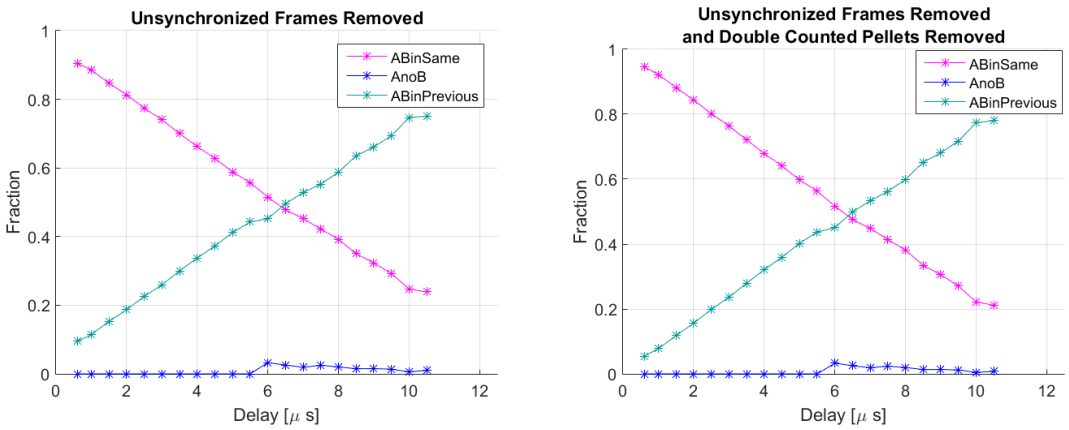

Figure 6.28: The fraction of pellets in the three classes *ABinSame*, *AnoB* and *ABinPrevious* from measurements with fishing lines and with a 2.5 μs light signal length and 2.5 μs dead time. Original data with unsynchronized readout frames removed (left) and data with double counted pellets removed and unsynchronized readout frames removed (right).

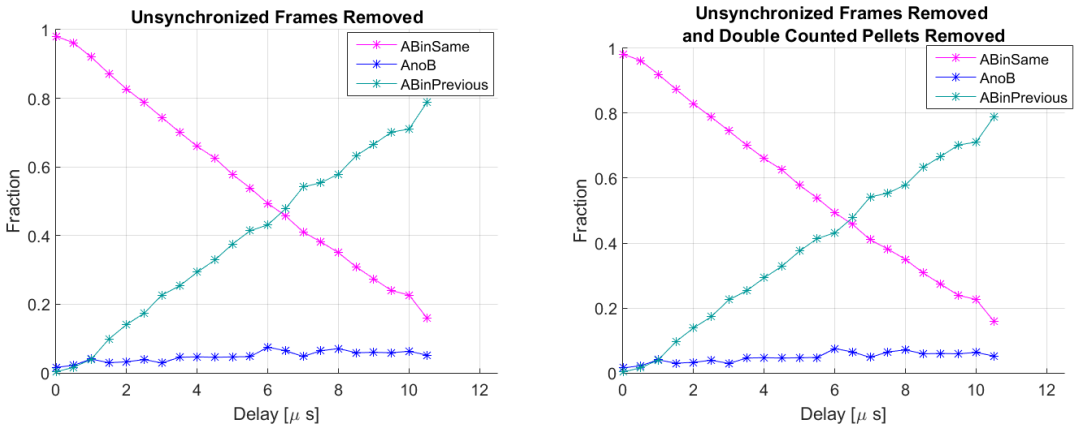

Figure 6.29: The fraction of pellets in the three classes *ABinSame*, *AnoB* and *ABinPrevious* from measurements with fishing lines and with a 1.25 μs light signal length and 2.5 a μs dead time. Original data with unsynchronized readout frames removed (left) and data with double counted pellets removed and unsynchronized readout frames removed (right)..

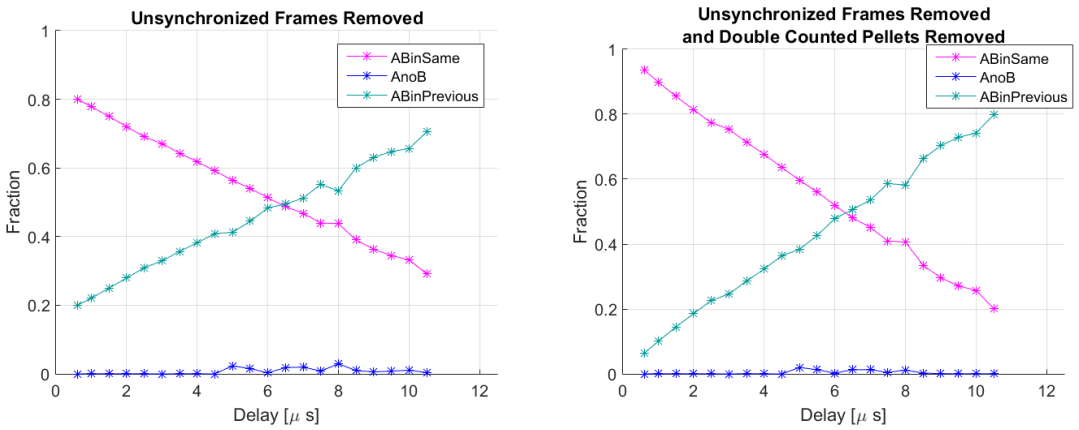

Figure 6.30: The fraction of pellets in the three classes *ABinSame*, *AnoB* and *ABinPrevious* from measurements with fishing lines and with a 5.0 μs light signal length and a 2.5 μs dead time. Original data with unsynchronized readout frames removed (left) and data with double counted pellets removed and unsynchronized readout frames removed (right).

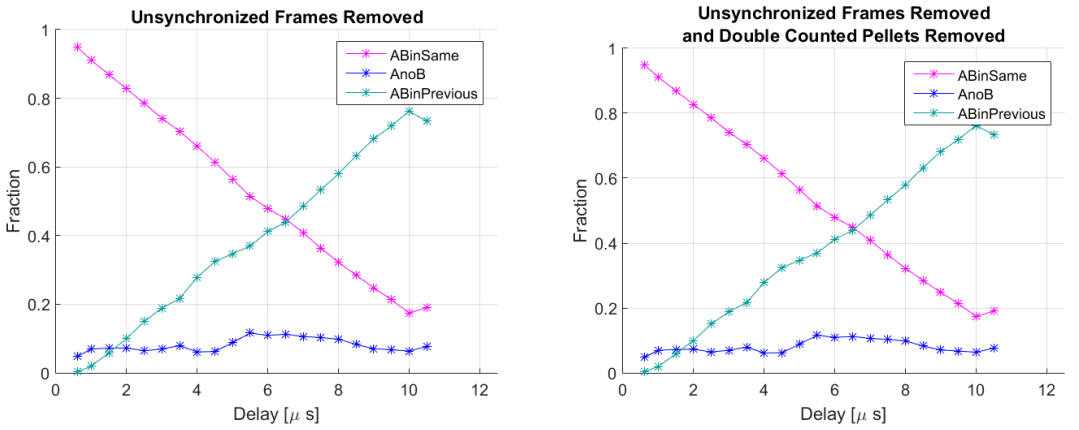

Figure 6.31: The fraction of pellets in the three classes *ABinSame*, *AnoB* and *ABinPrevious* from measurements with fishing lines and with a 2.5 μs light signal length and a 4.0 μs dead time. Original data with unsynchronized readout frames removed (left) and data with double counted pellets removed and unsynchronized readout frames removed (right).

Figure 6.32 shows that in the case of a 1.25 μs light signal length and 4.0 μs dead time, the effect of double counted pellets is negligible since both plots in this figure are very similar. There is a much larger fraction of pellets ending up in the class *AnoB* as compared to all previous cases where the light signal length is much longer compared to the dead time than in this case. Maximally 20% of all detected pellets in this analysis end up in the class *AnoB* after the unsynchronized readout frames have been removed. The fraction of pellets in this class increases until a delay of the exposure cycle of CamB of 2.0 μs has been reached. The expected value of the delay at which the increase should stop is the effective dead time. The expected effective dead time in this case is

$$t_{dead} - t_{signal} - t_{ineff} = 4.0 - 1.25 - t_{ineff} = 2.75 - t_{ineff}\mu s. \tag{6.2}$$

It is shown in figure 6.18 that light signals may overlap the dead time even when the light signal length is shorter than the dead time so this decreases the effective dead time. In particular, light signals start overlapping the dead time when they are 0.75 μs shorter than the set dead time giving $t_{ineff} = 0.75$. t_{ineff} is positive since it decreases the effective dead time. This gives an effective dead time of 2.0 μs in this case which is exactly the observed effective dead time in the data.

By the end of the series of measurements presented in figure 6.32, *i.e.* at long delays of the exposure cycle of CamB it appears as the fraction of pellets in the class *AnoB* starts decreasing at 10 μs delay which is 0.5 μs before expected delay which is at $t_{cyc} - t_{dead,eff} = 12.5 - 2 = 10.5\mu s$. This may be caused by some inefficiency and it is hard to determine if any real decrease actually occur since the decrease is only indicated by one measurement.

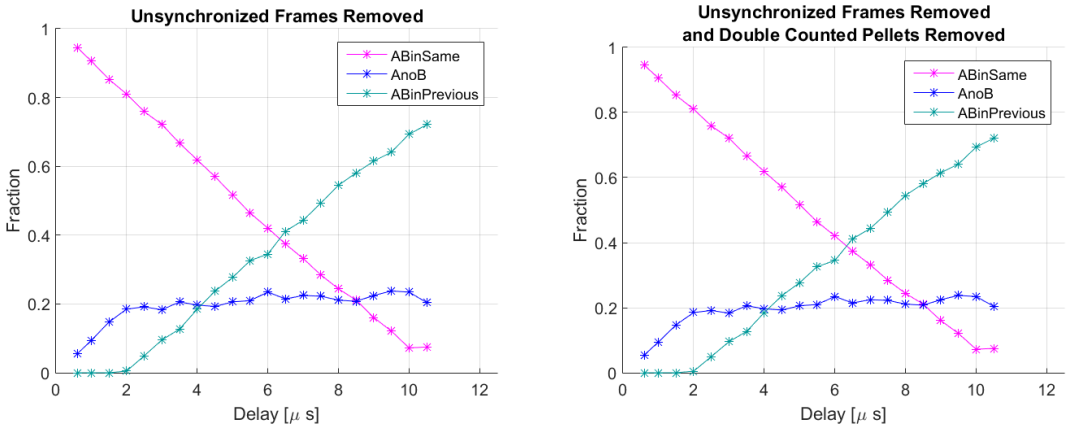

Figure 6.32: The fraction of pellets in the three classes *ABinSame*, *AnoB* and *ABinPrevious* from measurements with fishing lines and with a 1.25 μs light signal length and a 4.0 μs dead time. Original data with unsynchronized readout frames removed (left) and data with double counted pellets removed and unsynchronized readout frames removed (right).

6.7 Synchronization Diodes

In measurements with pellets, the synchronization of the cameras is crucial and needs to be monitored. In one measurement level, this can be done by comparing in which readout lines the cameras detect the same pellet. However, this technique is not possible to use for cameras at different measurement levels since these cameras detect the same pellet at different times. One technique of monitoring the synchronization which can be used for cameras on different levels is provided by so called synchronization diodes. The synchronization diode system consist of LEDs, one in front of each camera at the edge of the line of sight, flashing simultaneously at some given frequency and amplitude. This light is reflected into the cameras by white screens [6]. The synchronization diodes receive the same signal from a pulse generator ensuring their flashing to be completely simultaneous. Synchronization diodes have been installed at the DM for testing. The synchronization diodes as well as their positions in front of the cameras on the DM can be seen in figure 6.33. Due to the low aperture setting needed in order for the camera to detect a synchronization diode signal, the synchronization diodes can only (for the moment) be used for measurements with pellets where the biggest aperture is used, not with fishing lines where a smaller is generally used.

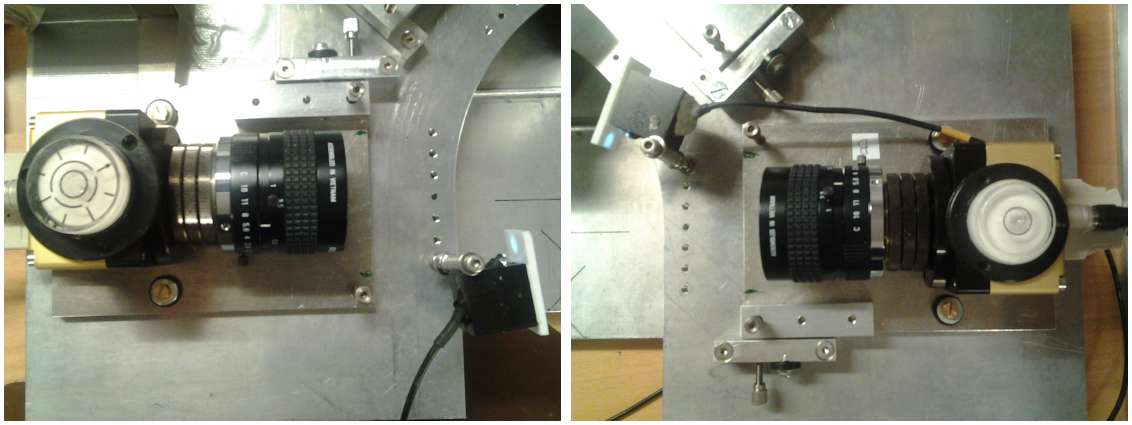

Figure 6.33: Synchronization diodes in front of CamA (left) and CamB (right). The synchronization diodes are the diodes placed in the square black boxes with a white screen reflecting the pulsed light into the cameras. The synchronization diodes can easily be rotated so that the angle with respect to the camera giving the best signal can be obtained.

In the analysis, information is given in terms of the number of readout lines between the detection of one synchronization diode signal in CamA and the detection of a synchronization diode signal in CamB. If the readout line difference is zero, the cameras detect the same synchronization diode signal in the same exposure cycle. This case is the most common for a small or no relative shift between the exposure cycles of the cameras. If the difference in readout lines corresponds to the number of readout lines between two synchronization diode pulses, CamB fails to detect the synchronization diode signal first detected by CamA and instead registers the next signal. This is possible since the analysis is made such that no two consecutive synchronization diode signals are registered in CamA unless one signal has been

registered in CamB in between. The analysis simply skips the synchronization diode signal from CamA if CamA also detected the previous signal. This case is most common with a long shift of the exposure cycles (>1/2 an exposure cycle).

The difference in readout lines between two consecutive synchronization diode signals can be calculated as

$$\Delta_{Lines} = \frac{\Delta t_{sync}}{t_{cyc}}, \tag{6.3}$$

where Δt_{sync} is the time between two synchronization diode signals and t_{cyc} is the time of one exposure cycle. The values used in the measurements with pellets are Δt_{sync}=2000 μs and t_{cyc}=12.5 μs giving Δ_{Lines}=160. Since the signal length of the synchronization diode signals, 3 μs, is longer than the dead time used in the measurements with pellets and most measurements with fishing lines, 2.5 μs, the problem of double counting some signals is present in this case as well. Since the synchronization diodes are only used for monitoring the synchronization of the cameras qualitatively, no adjustment for over-counting synchronization diode signals is made in this case.

The synchronization diodes are used throughout the measurements with pellets in order to monitor the synchronization of the cameras. This is particularly important in the series of measurements with the exposure cycle of CamB delayed relative the exposure cycle of CamA where the synchronization of the exposure cycles is crucial. Three examples of how the synchronization of the cameras is monitored using this technique can be seen in figures 6.34-6.36. The plots show the difference in readout lines in between the detection of a synchronization diode signal in the cameras for all times during one measurement. These examples are from a series of measurements with all three lasers with a power setting of 100 mW and for different delay for the exposure cycle of CamB. The exposure cycle is 12.5 μs and the exposure time is 10 μs. In the figures 6.34-6.36 two distinct lines consisting of detected synchronization diode signals can be seen corresponding to a difference in readout lines of 0 and 160. In figure 6.34 most synchronization diode signals end up in the line corresponding to a readout line difference of 0. This plot is from a measurement where the exposure cycle of CamB is delayed 0.6 μs relative the exposure cycle of CamA. In figure 6.35 the synchronization diode signals are quite evenly distributed between the two lines in the figure. This plot is from a measurement where the exposure cycle of CamB is delayed 6.5 μs relative the exposure cycle of CamA, about halfway through the exposure cycle. In 6.36 most synchronization diode signals end up in the line corresponding to a readout line difference of 160. This plot is from a measurement where the exposure cycle of CamB is delayed 10.5 μs relative the exposure cycle of CamA. The shorter the delay of the exposure cycle of CamB, the more synchronization diode signals are detected by both cameras in the same exposure cycle. In all figures 6.34-6.36 there are times when the cameras are not synchronized. This manifests itself by empty spaces in the lines of synchronization diode signals.

The synchronization diode signals have a signal length of 3.00 μs and come at a frequency of 500 Hz. 128 readout frames are used in the measurements with 2024

readout lines in each readout frame. This means that the total time for the measurement is 3.238 s and the expected number of synchronization diode signals detected during this time is more than 1619 (the expected number of detected synchronization diode signals in the absence of a dead time) since they always overlap the dead time. However some inefficiencies may occur resulting in less detected signals. As expected, a larger number of synchronization diode signals are detected in all three measurements presented.

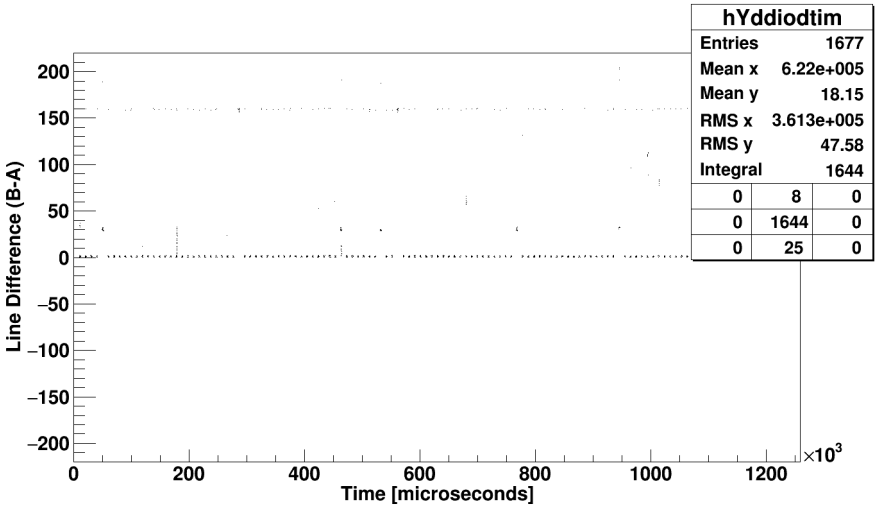

Figure 6.34: Time vs. the difference in readout lines (one line corresponding to one exposure cycle) for the synchronization diode signals. The measurements are made with a 0.6 μs delay of the exposure cycle of CamB relative the exposure cycle of CamA.

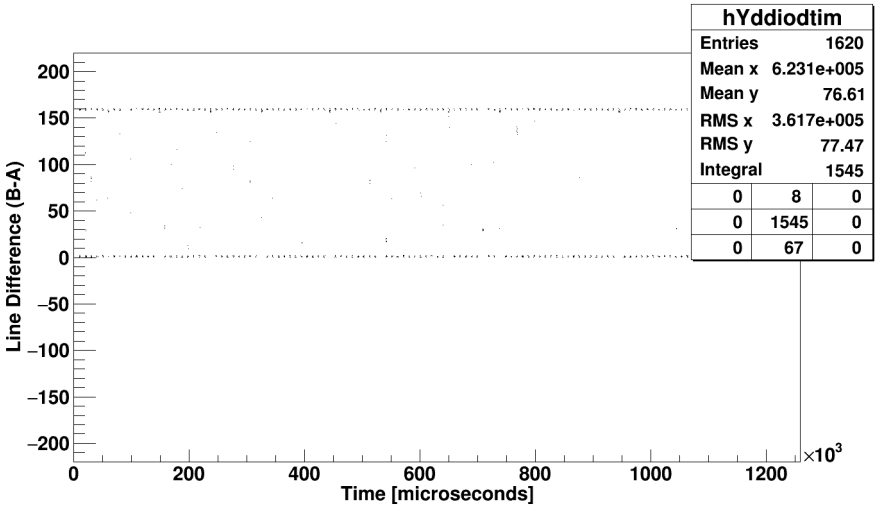

Figure 6.35: Time vs. the difference in readout lines (one line corresponding to one exposure cycle) for the synchronization diode signals. The measurements are made with a 6.5 μs delay of the exposure cycle of CamB relative the exposure cycle of CamA.

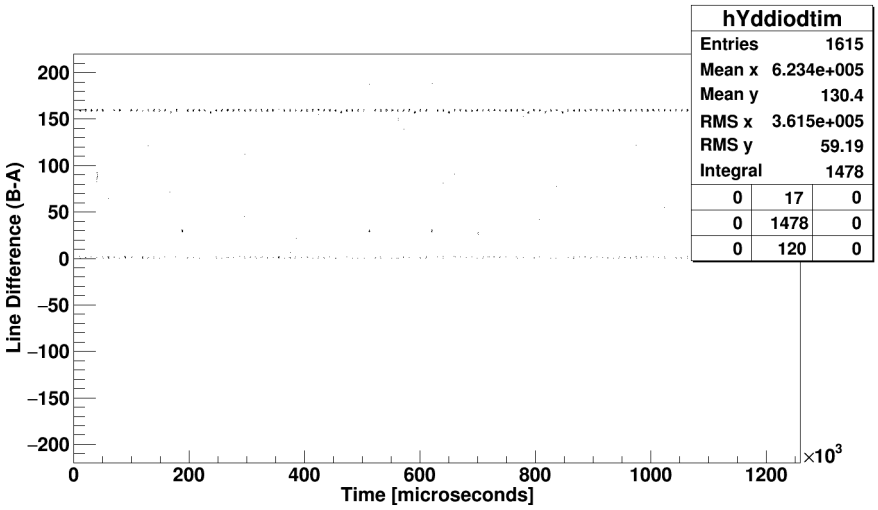

Figure 6.36: Time vs. the difference in readout lines (one line corresponding to one exposure cycle) for the synchronization diode signals. The measurements are made with a 10.5 μs delay of the exposure cycle of CamB relative the exposure cycle of CamA.

Chapter 7

Discussion and Conclusions

An alignment procedure has been developed for the cameras and lasers on the DM (Detection Module). A laser to simplify the alignment and make it more accurate has been installed. The stability of the alignment under certain conditions such as temperature changes, transportation of the DM and exposure to vibrations of the DM has been investigated. Alignment bench targets consisting of fishing lines, transparent, non-transparent and with different thickness and transparency have been investigated in order to determine which is the best target for alignment purposes. Optical effects affecting the measurements originating from camera aperture settings and focus settings have been investigated as well as the behavior of the system when the camera exposure cycles are shifted. In order to monitor the synchronization of the camera exposure cycles, synchronization diodes have been installed at the DM. Some aspects and conclusions regarding the alignment procedure and the investigations are discussed here.

7.1 Discussion

7.1.1 Alignment Procedure

Before the installation of LasC, CamA and LasA needed to be aligned with respect to each other and CamB needed to be aligned with LasB creating a plane A and a plane B. After the alignment was done, the planes needed to be aligned with respect to each other and cameras and lasers might have to be rotated further to get the planes properly aligned. Many adjustments and crosschecks of the alignment might be needed. The installation of LasC eliminates the need of a plane A and B since both cameras can first be aligned with respect to LasC and the other lasers can be aligned with respect to the cameras. After this is done only one crosscheck using reflected light should be necessary.

One complication when aligning the cameras with LasC is the angle at which the target holder needs to be placed in order for LasC to be used for alignment purposes since more than one fishing line needs to be used for alignment purposes in order to detect relative rotations between the laser and the camera. Any possible angle

will place some fishing lines closer to the camera than others and some closer to the laser than others. This change in distance leads to a slightly uneven disappearance of the image of the fishing lines when varying the height of the laser beam or the camera line of sight, uneven meaning that the camera image of the fishing lines do not disappear simultaneously. This effect is due to the geometrically larger overlap of the camera line of sight and the laser beam in the vertical direction at the position of fishing lines closer to the moving object than at the position of fishing lines further away. However, the effect of this is negligible for alignment purposes. The efficiency of the setup is not affected if this effect is simply ignored and it is made sure that the peaks in the camera image of the fishing lines simply disappear fairly evenly.

This effect is also present when aligning LasA and LasB with the cameras. If the fishing lines are placed on a row perpendicular to a camera, the most prominent feature of this effect is a slightly larger overlap region between the camera line of sight and the laser beam in the vertical direction when varying the height of the laser beam as compared to when varying the height of the camera line of sight. The opposite is true if the fishing lines are placed on a row perpendicular to a laser beam. This effect is so small it is hardly noticeable and there is no need for concern for the quality of the alignment if it is ignored. Additionally, in this case the target holder can simply be rotated such that the row of fishing lines is always perpendicular to the moving object.

When rotations of the target holder are performed, the fact that the center of the row of fishing lines is not placed perfectly in the central position and at perfect distances from the center needs to be taken in consideration. This only means that the fishing lines slightly changes position under 180° rotation. Depending on the horizontal position of the laser beam this can lead to very different images in the cameras since the horizontal width of the laser beam line profile in the central position is roughly 3 mm and the distance between the outermost fishing lines in the five fishing line holder is roughly 5 mm. All fishing lines can be illuminated though because of light spilling over at the edges of the laser beam and the fact that in certain configurations, the row of fishing lines is not perpendicular to the laser beam. Under rotations during the same alignment, rotations where any fishing line crosses from left to right in the camera images should not be performed. The outermost fishing lines should only cross the laser beam in order to always have comparable images.

7.1.2 Usage of the Pixel Correlation Plot

When using the pixel correlation plot to detect relative changes in the camera positions which may have occurred in between two measurements, the slope of the dotted line in figure 5.1 is not currently included in the analysis for fishing lines. The slope is impossible to determine for measurements with fishing lines where the distribution in the pixel correlation plot is basically a square or rectangle as opposed to in the case of pellet measurements where the dotted line is somewhat outlined by the distribution of signals in the pixel correlation plot. The slope of this dotted line for an object placed at an equal distance between the cameras is -1 but for all other placements, the slope of the dotted line is different from -1, it is unknown

and must be determined and should be included in the analysis. An improvement regarding this type of analysis is to include the slope of the dotted line for the pixel correlation plot with fishing lines for which it is not included at the moment. Several fishing lines can not be used to get a different distribution of several smaller square distributions from which a slope can be determined. Currently, when two light signals are detected in the same readout line, all light signals but the first one found in the line of pixels are removed from the analysis. This means that only the light signals corresponding to one fishing line found in one camera and the signals corresponding to another fishing line found in the other camera will be included in the pixel correlation plot if several fishing lines are used. This is because the cameras are placed opposite each other and the pixel line is read out from left to right (facing the cameras) for both cameras so the first signal encountered in the camera line of pixels will originate from different fishing lines. However, if the same setup of alignment targets is used for two measurements, the pixel correlation plots from these measurements are still comparable so they give a measure of the stability of the cameras relative each other.

In measurements with pellets, if the slope of the line made out by the distribution in the pixel correlation plot have changed in between two measurements the pellet stream have moved towards and away from the cameras. In such a case it is hard to determine if the cameras have moved relative each other as well. In order to separate these two cases, another measurement level with two cameras opposite each other and rotated by 90° relative the existing level is needed. By comparing the pixel correlation plots from both levels, the cases could be disentangled.

7.1.3 Effects of Different Temperatures

During the measurements at different temperatures, the lowest room temperature of 17.7°C was impossible to maintain throughout the series of measurements since the electronics immediately generates heat once switched on. However, the small temperature fluctuations throughout these measurements of less than 0.5°C are very small compared to the temperature change between the measurements at different temperatures differing about 5°C. It does not affect the qualitative comparisons. The highest temperature was also impossible to maintain. However, these fluctuations are only about 0.3°C.

A slightly greater concern regarding these measurements is the fact that the entire support material may not have reached the same temperature in preparation for the measurements at different temperatures. This means that the material may not have expanded or contracted as much as expected. However, since no detectable changes are expected from the room temperatures reached, this is not of any great concern either.

7.1.4 Investigations of Alignment Bench Targets and Effects at Different Laser Beam Intensities

A problem during investigations of the alignment bench targets is the inhomogeneous illumination of the fishing lines. The signals are heavily affected by the intensity of the laser beam. At low values of the power setting ($\lesssim$ 3.1 mW), the reflected light signals in the position distribution cannot be considered much more than noise. Additional, narrow peaks, which do not correspond to the position of a fishing line, appear in the position distribution for the refracted light at certain values of the power setting. Since the light signals making up this peak carry a low amount of light, these peaks can be eliminated by placing a cut on the light integral and thereby removing these light signals from the analysis. However, at even higher values of the power setting (on the order of 3.1 mW), the position distribution undergoes a smearing at which point the light integral for the refracted light becomes unreadable. In the range 2.7-3.3 mW for LasA and LasB with the system currently used, the light integral and the number of detected light signals is also temperature dependent. The effects appearing at slightly higher values of the power settings ($\gtrsim$ 3.1 mW) appear at lower values at lower temperatures. There is also reflection of light between the cameras distorting the position distribution at higher values ($\gtrsim$ 3.1 mW) of the power setting. When examining different fishing lines, the light distribution is therefore used instead of the position distribution. The peaks in the light distribution, corresponding to the positions of the fishing lines only get slightly wider for higher intensities of the laser beam. This makes the light distribution more fit to use for this purpose than the position distribution.

The fishing line found to be the most appropriate for alignment purposes is a transparent 0.08 mm diameter fishing line. Fishing lines of this thickness can be placed relatively close together with a smaller risk of optical effects distorting the light distribution or the light integral spectra as compared to thicker fishing lines.

7.1.5 Focus and Apertures of the Cameras

From the investigations of the focus of the cameras by the alignment bench it can be concluded that for the intensities of the laser beam used for the studies, the number of detected light signals is rather constant throughout the overlap between the line of sight of the camera and the laser beam in both the vertical direction and horizontal direction along the camera line of sight. It is also constant a bit outside this region where there is still some light from the laser beam. The light integral is the largest within a small region around the nominal center chosen in the alignment check. This means that the focus of the camera set using a camera monitoring program is quite accurate also for measurements with the analysis program. The detected light signals behave roughly as expected for different aperture settings of the cameras.

7.1.6 Camera Exposure Cycles and Shifted Exposure Cycles

A complication when doing the analysis with shifted exposure cycles is that for light signal lengths of the same length or longer or even slightly shorter than the dead time, the light signal might overlap the dead time giving rise to two light signals detected and being interpreted as pellets in two consecutive readout lines. However, the results of the investigations performed with shifted exposure cycles show that the greatest sources of inefficiency in this type of analysis originate from unsynchronized readout frames (in the setup used for the measurements presented in this report) and to a somewhat smaller extent from the double counted pellets. The latter effect appears from when the light signal length is 0.75 μm shorter than the dead time. By finding and removing all double counted pellets, this effect can be eliminated. However, the results from the checks with shifted exposure cycles presented in this report are only performed in order to check if the DM works as expected. When doing measurements with pellets, a detection efficiency of 100% is desired so no pellets should be removed from the analysis in that case. In such measurements, the double counted pellets can be found and placed *e.g.* in the dead time where they most likely belong if the light signal from these overlap the dead time. The fraction of double counted pellets depends on the intensity of the laser beam which can be concluded from the measurements with pellets.

The unsynchronized readout frames can be removed by successively searching all readout frames by checking all the readout lines in this readout frame to see in how many readout lines both cameras detect signals. For a readout frame to be considered unsynchronized, the number of readout lines where only one camera detects light signals must exceed a certain set number. This number is set for each individual measurement. Only the readout frames containing so many readout lines with a light signal in only one camera that is stands out against most other readout frames in the measurement can be considered unsynchronized. The longer the delay of the exposure cycle of CamB is with respect to the exposure cycle of CamA, the more readout frames of the measurement will contain a large amount of readout lines where a signal was detected in only one camera. Therefore it gets harder to distinguish unsynchronized readout frames the longer the delay of the exposure cycle of CamB with respect to the exposure cycle of CamA. This manifests itself in the fact that the fraction of pellets in the class $AnoB$ increases with increasing delay in the region where the fraction should be constant.

7.2 Conclusions

An alignment procedure for alignment of the lasers and cameras on the DM has been developed. The installation of a laser at 90° with respect to both cameras to simplify this procedure has been performed. Making use of this laser simplifies the alignment, saves time and effort and reduces the risk of mistakes. The most appropriate fishing line to use for alignment purposes in the alignment bench setup is a transparent fishing line of diameter 0.08 mm.

The alignment of the cameras and lasers on the DM is stable under reasonable changes in the room temperature (on the order of $\pm 3°C$). At a detector setup such as PANDA the expected variations in the room temperature is expected to be of this order of magnitude. The alignment of the cameras and lasers on the DM is stable under transportation between the alignment bench setup and the pellet tracking chamber by a pellet beam pipe. Since the need of the ability to align a tracking section in an alignment bench setup and moving it to the tracking chamber was one of the reasons why the DM was constructed in the first place, this is of vital importance. The alignment of the cameras and lasers on the DM is stable when the DM is subjected to vibrations from vacuum pumps during pellet runs.

In the measurements with shifted camera exposure cycles, the two main sources of inefficiency, double counted signals and unsynchronized readout frames has been identified and can be eliminated. The latter effect is present in the system currently used and is not expected to be present in general. In pellet measurements where a 100% detection efficiency is desired, the double counted signals can be placed in the dead time where they probably belong. During this type of measurements, synchronization diodes can be used to monitor the synchronization of the camera exposure cycles which is crucial.

Chapter 8

Outlook

Throughout this project, some improvements to the DM have been made such as the installation of a third laser simplifying the alignment and the installation of the synchronization diodes for monitoring the performance of the DM during measurements. However, there is always room for future improvements.

A second level with cameras and lasers will be added to the DM plate 60 mm above the plate present at the moment. This construction will be used in the alignment bench setup, by the pellet beam pipe the levels will be mounted separately 60 mm apart. 60 mm spacing is needed to fit the cameras and no more spacing is desired since the pellet identification efficiency in between two levels decreases with increasing distance between the levels. A good pellet identification efficiency is needed for the pellet track reconstruction. Having two different levels allows for control measurements by the test bench setup with more levels.

The DM is quite heavy with a weight of around 8 kg, so another improvement consists of drilling holes at suitable places, decreasing its weight by slightly more than 2 kg. This will simplify the transportation of the DM and decrease the risk of unintentional damages to the DM during transportation. Having holes drilled in the plate also simplifies and even enables a visual inspection of *e.g.* the cameras and lasers with two levels.

Another improvement includes simplifying measurement of the height of the camera plates and laser plates above the DM plate. At present, this is done using different tools such as a vernier caliper at three different locations on each plate. This method of using a vernier caliper can be improved by drilling small holes in the camera and laser plates at the places of measurements where the vernier caliper can be placed and stabilized.

There will be continued work on another readout system for the cameras. The work on optimizing the time resolution of the exposure cycles of the cameras will proceed as well as further investigations regarding the optics of the cameras and the lasers.

Chapter 9

Summary

Pellets are small spheres of frozen hydrogen used as internal targets at accelerators in hadron physics experiments. They have a diameter of roughly 20 μm. Pellets are planned to be used at the upcoming PANDA (anti-Proton ANnihilation at DArmstadt) experiment at the anti-proton accelerator HESR (High Energy Storage Ring), Darmstadt, Germany. They have previously been used as target at WASA (Wide Angel Shower Apparatus) first at the CELSIUS storage ring at TSL (The Svedberg Laboratoriet), Uppsala, Sweden and later at COSY (COoler SYnchrotron), Jülich, Germany. Pellets are currently being developed and investigated at the UPTS (Uppsala Pellet Test Station) at TSL. They constitute a good target *e.g.* due to their high density of target material of well above 10^{15} atoms/cm^2 of an individual pellet. Pellets are created some distance away from the accelerator beam, roughly 2.7 m and the pellet stream is directed within a pellet beam pipe to intersect the accelerator beam in an interaction region. Before and after the interaction region the pellets need to be tracked for the track and position reconstruction. The exact position of a pellet in the interaction region is highly desirable. It can be determined with an accuracy of 0.1 mm. Knowing the position of an individual pellet when reactions occur allows for knowing the reaction vertex and thereby allows for more accurate track reconstruction and knowledge of the four momenta of the reaction particles.

An optical tracking system making use of lasers illuminating the pellets and cameras detecting the light is currently being developed at the UPTS. Cameras and lasers are placed in planes with several planes making up a tracking section. There is an upper tracking section above the interaction region and a lower tracking section below the interaction region. LS (Line-Scan) cameras reading out one line of pixels at the time are used for pellet detection. This gives an advantage in speed as compared to a camera reading out a two dimensional image and there is no need for a two dimensional image for the pellet tracking. The effective pixel size at the working distance is 35×35 μm^2. STR (Structured-Light-Pattern) diode lasers are used for illuminating the pellets. These lasers can be set to have a thin horizontal beam line profile with a width of roughly 3 mm and a height of less than 50 μm in the pellet stream region. The camera line of sight and the laser beam line profile need to converge in a plane within 10 μm in the pellet stream region and the pellet detection efficiency need to be 20 μm. With these requirements fulfilled the position

of a single pellet in the interaction region can be reconstructed with an accuracy better than 0.1 mm. This puts high demands on the alignment of the cameras and lasers. Cameras and lasers in a plane are aligned mechanically with each other. The measurement planes are aligned with each other in the track reconstruction process. The alignment of the measurement levels with respect to the accelerator beam is done by including the frequency of reactions as a function of pellet position.

Due to lack of space and poor sight conditions by the pellet beam pipe at experiments, the mechanical alignment need to be performed away from the pellet beam pipe. Since the pellet stream have a spatial spread in the horizontal plane perpendicular to the pellet stream direction, it is unsuitable to use as an alignment target. Another alignment target which is simpler to set up than to start a pellet run and whose position is more fixed should be used. Since no other alignment target apart from a pellet beam can be used by the pellet beam pipe, alignment with another target needs to be performed away from the pellet beam pipe. The optics of the cameras and lasers as well as the readout from the cameras also needs to be investigated with another target. To meet these three needs, a DM (Detection Module) has been designed. The DM currently consists of a DM plate with two cameras mounted to it as well as two lasers for pellet detection and one laser mainly for alignment purposes. The cameras and lasers are fastened to camera- and laser-plates which can be adjusted vertically, horizontally and rotated using adjustment screws with a micrometer precision. The alignment can be performed in an alignment bench setup and the entire construction can be transported to a pellet beam pipe for pellet measurements.

Investigations have been made regarding the stability of the alignment of the cameras and lasers on the DM under certain conditions such as smaller changes in the room temperature, transportation and exposure to vibrations. Together with exposure to magnetic fields, these are the main sources of expected changes or distortions of the alignment. The alignment is found to be stable under changes in the room temperature, transportation and exposure to vibrations. Magnetic fields have previously been show not to affect the optics of the cameras or lasers. Alignment bench targets consisting of different fishing lines of different thicknesses and transparency have been investigated in order to find the most appropriate target for the alignment in the alignment bench setup. Additionally, an alignment procedure for the cameras and lasers on the DM has been developed.

Camera effects originating from the aperture settings and the focus of the cameras have been examined both with fishing lines in the alignment bench setup and with pellets. In these cases, especially the number of detected light signals giving a measure of the detection efficiency of the cameras has been examined.

The cameras operate continuously with an exposure cycle of 12.5 μs consisting of an exposure time of 10 μs when light is collected and a dead time of 2.5 μs when the collected charge is transferred. Since the cameras do not collect any light during the dead time, this constitutes a theoretical source of inefficiency of roughly 20% for infinitely short light signals. For very short light signals there is also an inefficiency. In order to deal with this, the cameras on the DM have been placed opposite each other facing the central position corresponding to the pellet stream region. The exposure cycle of one camera can be delayed relative the exposure cycle

of the other camera such that the dead time of one camera always end up in the exposure time of the other camera. This way it can be ensured that at least one camera detects light signals and thereby pellets at all times. Examining how the cameras detect light signals for different relative shifts of the exposure cycles gives a measure of the alignment of the cameras and lasers. This is examined with pellets and in the alignment bench setup. It is shown that if the light signal length is $t_{signal} = t_{dead} - 0.75\ \mu s$, where t_{dead} is the set dead time, the light signal may be detected in two consecutive exposure cycles of one camera. This leads to double counting of light signals and these cases can be found and placed in the dead time where they probably belong if they overlap the dead time. From this, an effective dead time, $t_{dead,eff} = t_{dead} - t_{signal} - 0.75\ \mu s$, can be calculated. This is the dead time experienced for light signals of finite length.

Chapter 10

References

[1] The PANDA Collaboration (2012), *Technical Design Report for the PANDA Internal Targets* Available: http://www.fair-center.eu/for-users/publications/experiment-collaboration-publications.html [2017-01-02]

[2] Pyszniak, A. (2014), *Development and Applications of Tracking of Pellet Streams*. Diss. Uppsala University, Sweden. Uppsala: Acta Universitatis Upsaliensis. Available: http://urn.kb.se/resolve?urn=urn:nbn:se:uu:diva-235671 [2016-12-12]

[3] Research Programme-Department of Physics and Astronomy http://www.physics.uu.se/research/nuclear-physics/research-projects/panda/forskningsprogram/ [2017-01-08]

[4] Activities-Department of Physics and Astronomy http://www.physics.uu.se/research/nuclear-physics/research-projects/panda/pagaende-aktiviteter/ [2017-01-08]

[5] Torgersen, S and Wallin, A (2015), *Investigation of Improvement of Pellet Tracking System*, Uppsala University, Uppsala, Sweden. Available: http://urn.kb.se/resolve?urn=urn:nbn:se:uu:diva-255123 [2016-12-12]

[6] Calén, H., Fransson, K., Hellbeck,E. and Fridén,K-J., (2009), *Design ideas for pellet tracking systems for PANDA and WASA*, Dept. of Physics and Astronomy, Uppsala University, Uppsala, Sweden. Available: http://physics.uu.se/research/nuclear-physics/research-projects/panda/reports/ [2016-12-11]

[7] A. Pyszniak et al., (2013), *Simulation studies for design of pellet tracking systems*, Dept. of Physics and Astronomy, Uppsala University, Uppsala, Sweden. Available: http://physics.uu.se/research/nuclear-physics/research-projects/panda/reports/ [2017-01-08]

[8] Nordling, A and Österman, J; *Physics Handbook for Science and Engineering*, Studentlitteratur, Edition 8:5, 2010. (p. 28)

[9] The PANDA Collaboration (2009), *Technical Design Report for the PANDA Solenoid and Dipole Spectrometer Magnets* (Figure 3.58, p

67) Available: `http://www.fair-center.eu/for-users/publications/experiment-collaboration-publications.html` [2017-01-02]

[10] CERN (2008) *ROOT*. Geneva: CERN.

[11] MathWorks (2015) *MATLAB*. N.A: The MathWorks, Inc.

[12] MATRIX VISION GmbH (2012) *wxPropView*. Oppenweiler: MATRIX VISION GmbH.

[13] e2v technologies Ltd. *AVIIVA SM2 CL Camera Link Line Scan Camera* (2009). Essex

[14] Coherent, Inc. *Coherent StingRay Structured Light Pattern Generating Laser* (2013). Santa Clara

Appendix A

Distributions at Different Levels of the Tracking Section

In order to check the behavior of the pellet stream, measurements are made with pellets at the UPTS with one camera at PTRup and with CamB at the detection module at PTRlow 60 cm below. Figures A.1-A.3 show some of the results of measurements at PTRup (left plots) and by CamB at the DM at PTRlow (right plots). Both cameras are facing the same direction. The plots in figure A.1 show the spatial distribution of the pellet stream at the different levels, the distributions are quite similar. The measured width of the pellet stream is approximately 70 pixels corresponding to approximately 2.6 mm both at PTRup and at PTRlow. In previous tests [2] the width of the pellet stream was found to be 70 pixels wide at PTRup and 80 pixels wide at PTRlow corresponding to 2.6 and 3 mm respectively. The light integrals in figure A.2 have quite different shape, likely due to different intensities of the laser beam of the lasers on the different levels. LasB on the DM is used in the measurements and have a power setting of 10 mW whereas the laser used on the PTRup level have a power setting of 50 mW. This probably also accounts for the differences between the plots of the cluster width in figure A.3. Both LasB and the laser used on PTRup makes an angle of 135° with respect to the camera on the respective level.

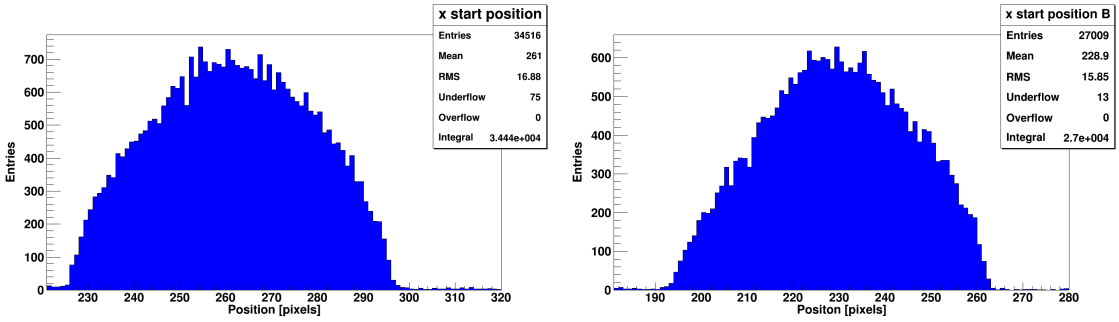

Figure A.1: Position distributions. The left plot shows the position distribution of the pellet stream as measured at PTRup. The right plot shows the position distribution as measured by CamB at the DM. The measured width of the pellet stream is approximately 70 pixels corresponding to approximately 2.6 mm at both PTRup and at PTRlow.

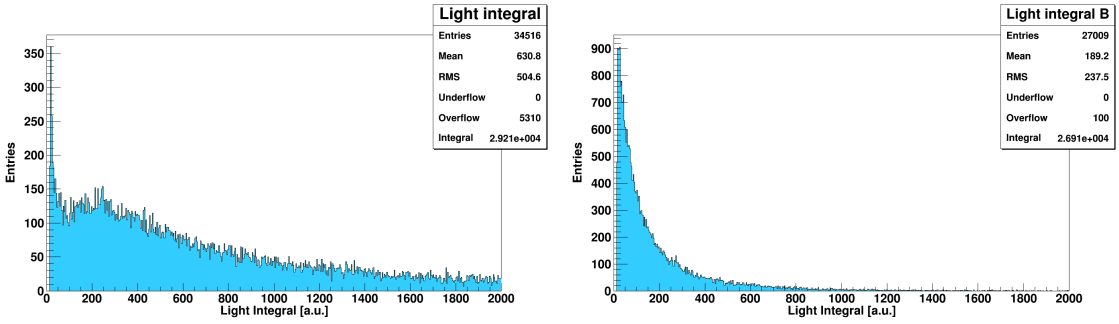

Figure A.2: Light integral as measured at PTRup (left) and by CamB on the DM at PTRlow (right). The light integral as measured at PTRup peaks at lower values of the light integral than the more smeared out distribution as measured at PTRup. The latter has an extremely narrow peak at very low values. This very narrow peak is also slightly present in the left plot but less prominent.

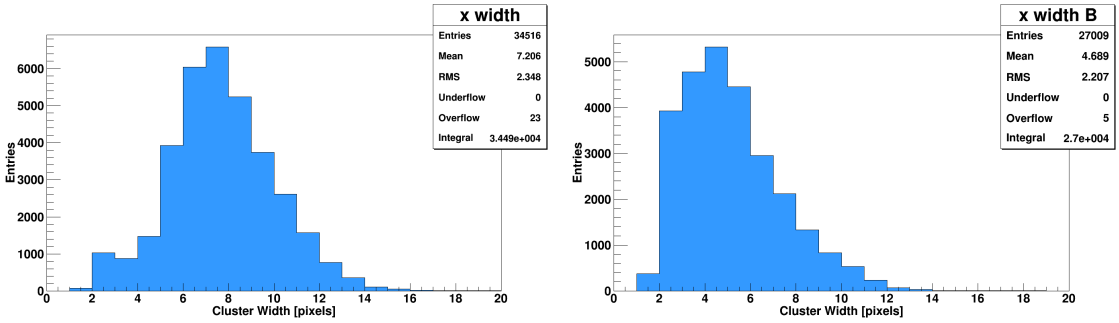

Figure A.3: Cluster width as measured at PTRup (left) with a mean value of roughly 7 pixels and by CamB on the DM at PTRlow (right) with a mean value of roughly 5 pixels.

Appendix B

Additional Light Integrals

The light integral from measurements with pellets and with different intensities of the laser beam to all three lasers (10 mW, 30 mW, 50 mW and 100 mW) can be seen in figures B.1-B.12. The entire light integral as well as a close a close up of the light integral for low values are plotted for all cases for CamA and CamB. For a power setting of 10 mW to the lasers, the light integral displays a narrow peak at low values. This peak gets thicker and more smeared out for higher values of the power setting. Its height decreases and it peaks at higher values for higher values of the power setting. At a power setting of 100 mW an additional narrow peak appears at low values in the light integral.

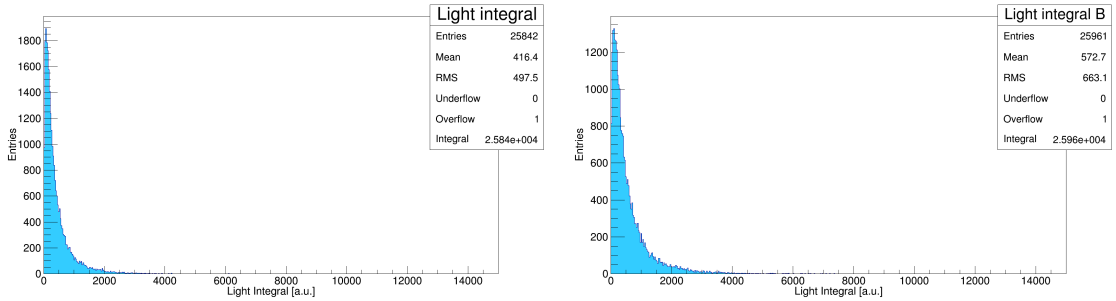

Figure B.1: Light integral as measured in CamA in the left plot and in CamB in the right plot. LasA, LasB and LasC are used with a 10 mW power setting.

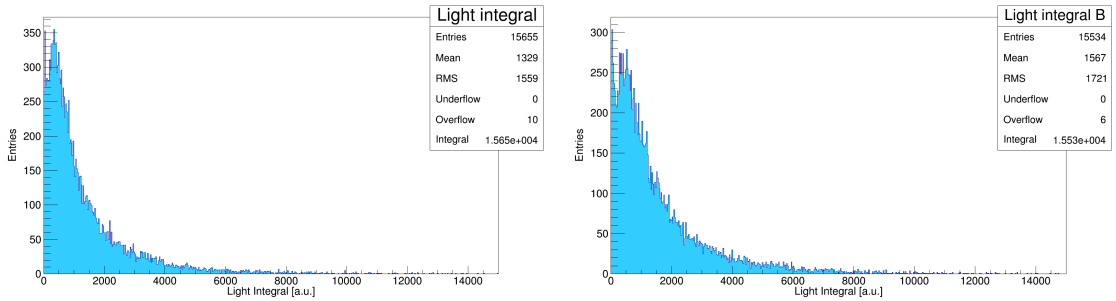

Figure B.2: Light integral as measured in CamA in the left plot and in CamB in the right plot. LasA, LasB and LasC are used with a power setting of 30 mW.

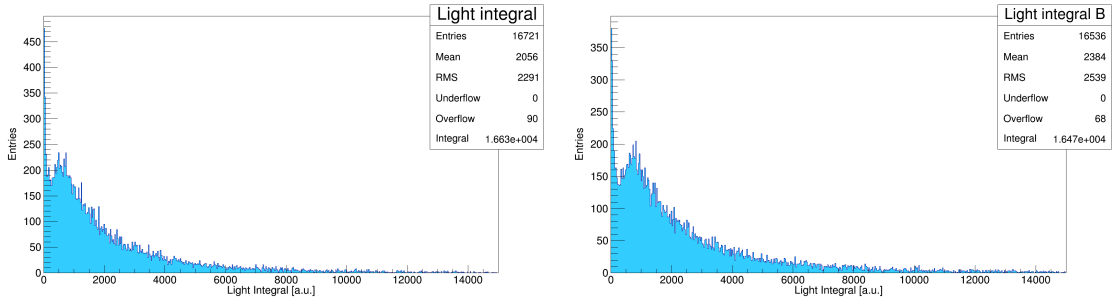

Figure B.3: Light integral as measured in CamA in the left plot and in CamB in the right plot. LasA, LasB and LasC are used with a power setting of 50 mW.

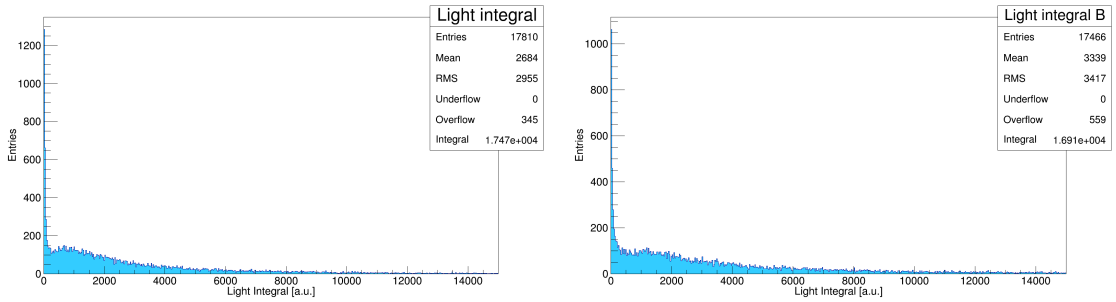

Figure B.4: Light integral as measured in CamA in the left plot and in CamB in the right plot. LasA, LasB and LasC are used with a power setting of 100 mW.

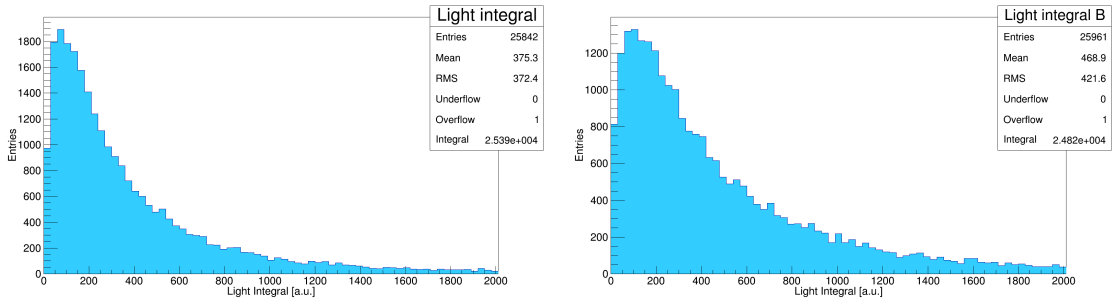

Figure B.5: Close up on the light integral as measured in CamA in the left plot and in CamB in the right plot. LasA, LasB and LasC are used with a power setting of 10 mW.

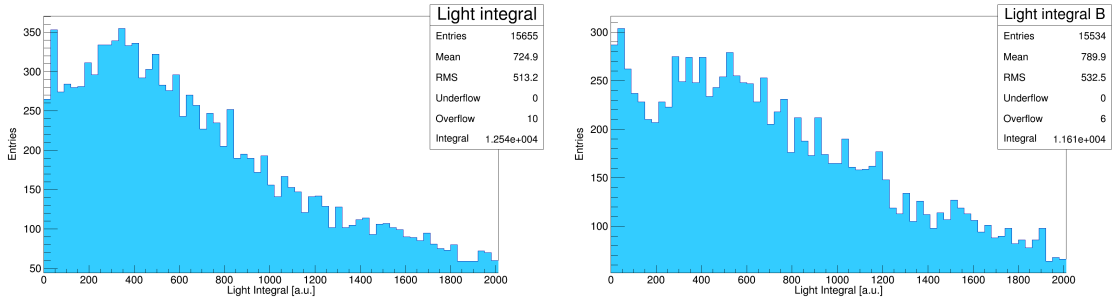

Figure B.6: Close up on the light integral as measured in CamA in the left plot and in CamB in the right plot. LasA, LasB and LasC are used with a power setting of 30 mW.

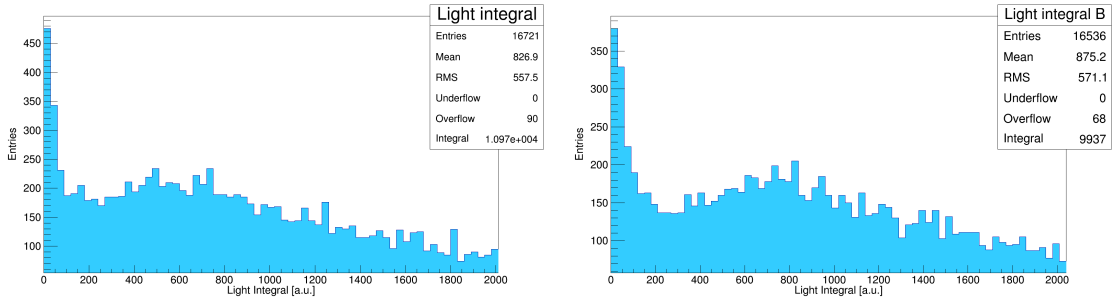

Figure B.7: Close up on the light integral as measured in CamA in the left plot and in CamB in the right plot. LasA, LasB and LasC are used with a power setting of 50 mW.

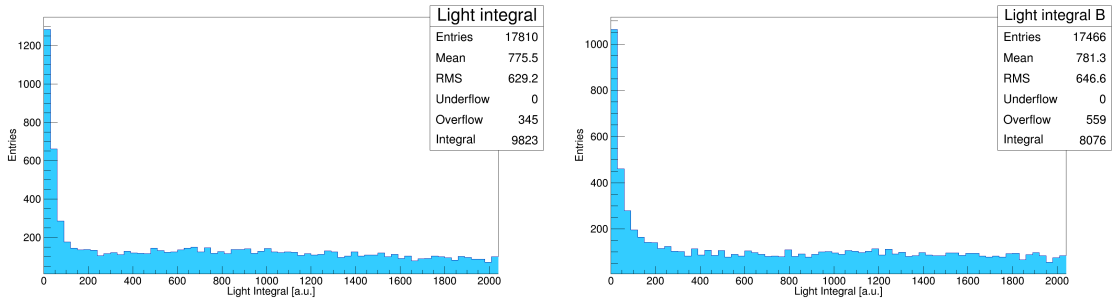

Figure B.8: Light integral as measured in CamA in the left plot and in CamB in the right plot. LasA, LasB and LasC are used with a power setting of 100 mW.

Figures B.9-B.12 are from measurements where only LasA is used. This means that CamA detects refracted light and CamB detects reflected light. The light integrals in B.9 and B.11 are from measurements where a 10 mW power setting is used for LasA and the light integrals in figures B.10 and B.12 are from measurements where a 100 mW power setting is used for LasA. For a 10 mW power setting for the laser, the light integral for refracted and reflected light look very similar and consist of a narrow peak at low values which decreases rapidly for increasing values. The height of the peaks in the light integrals is roughly the same. For 100 mW, the light integral for refracted light also exhibits a peak at low values of the light integral but in this case, the peak decreases more slowly for increasing values. The light integral for reflected light in the case of measurements with a 100 mW power setting for the laser exhibits a very narrow peak at low values and a slightly broader peak at slightly higher values than in the case of refracted light. The broader peak in the light integral spectra for reflected light decreases much slower than that in the light integral spectra for refracted light. The peak in the light integral for refracted light is roughly twice the height of the peaks in the light integral for reflected light.

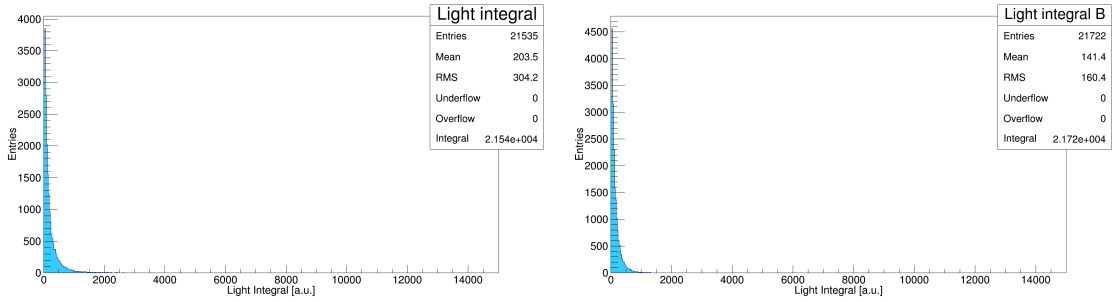

Figure B.9: Light integral as measured in CamA in the left plot and in CamB in the right plot. LasA is used with a power setting of 10 mW. CamA detects transmitted light and CamB detects reflected light.

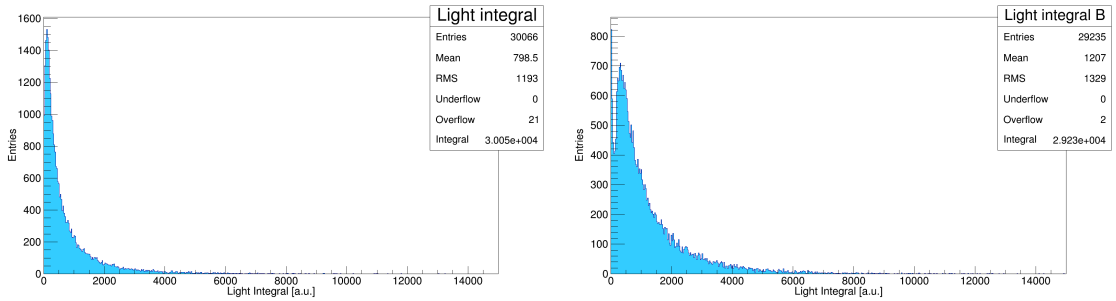

Figure B.10: Light integral as measured in CamA in the left plot and in CamB in the right plot. LasA is used with a power setting of 100 mW. CamA detects transmitted light and CamB detects reflected light.

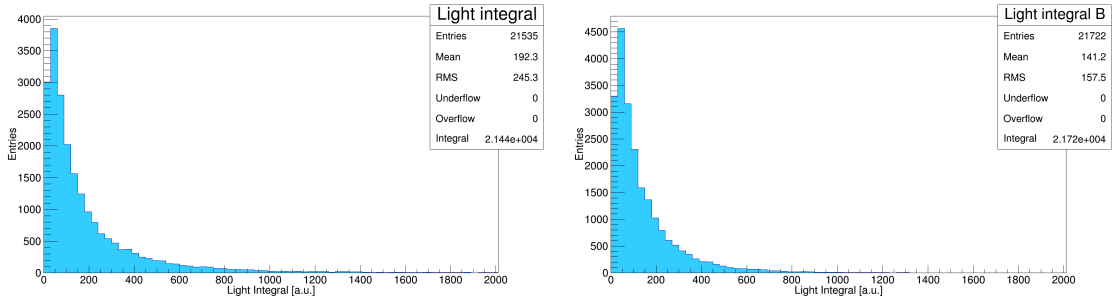

Figure B.11: Close up on the light integral as measured in CamA in the left plot and in CamB in the right plot. LasA is used with a power setting of 10 mW. CamA detects transmitted light and CamB detects reflected light.

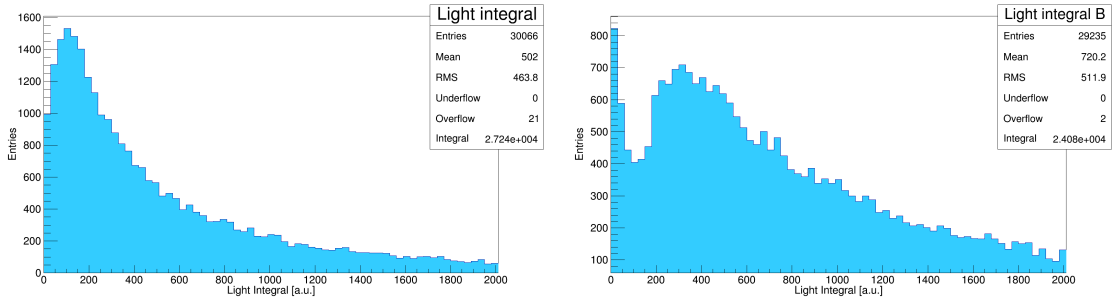

Figure B.12: Close up on the light integral as measured in CamA in the left plot and in CamB in the right plot. LasA is used with a power setting of 100 mW so CamA detects transmitted light and CamB detects reflected light.

Appendix C

Shifted Exposure Cycles

Additional results from series of measurements with shifted exposure cycles can be seen in figures C.1-C.9. Figure C.1 shows the fraction of double counted pellets in each of the classes *ABinSame*, *AnoB* and *ABinPrevious* for LasA with a power setting of 10 mW (left plot) and 100 mW (right plot) as a function of the delay of the exposure cycle of CamB. Figure C.2 shows the fraction of double counted pellets in each of the classes *ABinSame*, *AnoB* and *ABinPrevious* for LasB with a power setting of 10 mW (left plot) and 100 mW (right plot) as a function of the delay of the exposure cycle of CamB. Figure C.3 shows the fraction of double counted pellets in each of the classes *ABinSame*, *AnoB* and *ABinPrevious* for LasC with a power setting of 10 mW (left plot) and 100 mW (right plot) as a function of the delay of the exposure cycle of CamB. Figures C.1-C.3 show that the fraction of double counted pellets is larger for a 100 mW power setting for all lasers as compared to a 10 mW power setting.

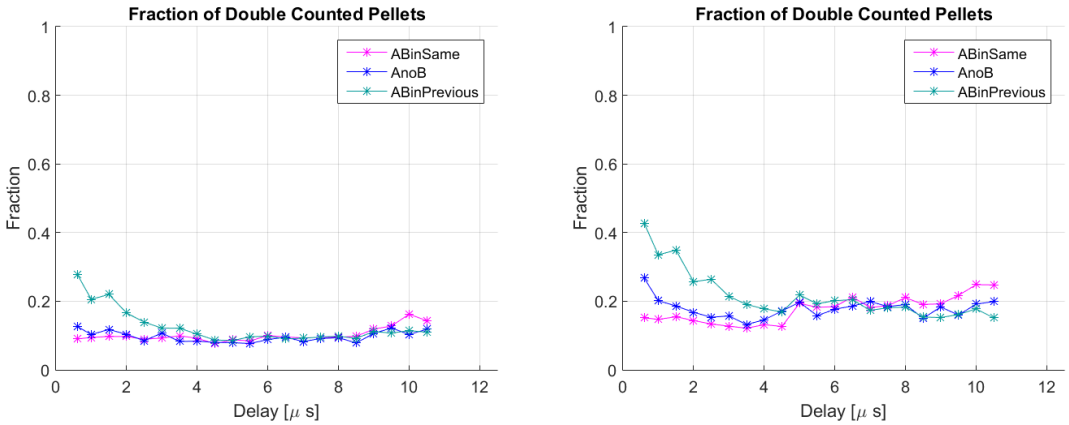

Figure C.1: The fraction of double counted pellets in the three classes *ABinSame*, *AnoB* and *ABinPrevious* from measurements with pellets and with LasA with a 10 mW power setting in the left plot and with a 100 mW power setting in the right plot. The plots show the fraction of detected signal in each class (in the original data) which were counted twice and interpreted as two pellets.

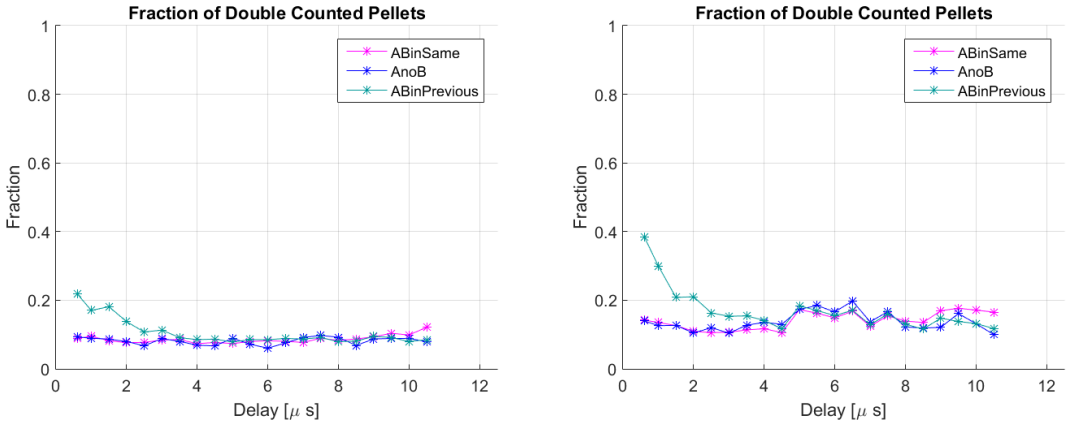

Figure C.2: The fraction of double counted pellets in the three classes *ABinSame*, *AnoB* and *ABinPrevious* from measurements with pellets and with LasB with a 10 mW power setting in the left plot and with a 100 mW power setting in the right plot. The plots show the fraction of detected signal in each class (in the original data) which were counted twice and interpreted as two pellets.

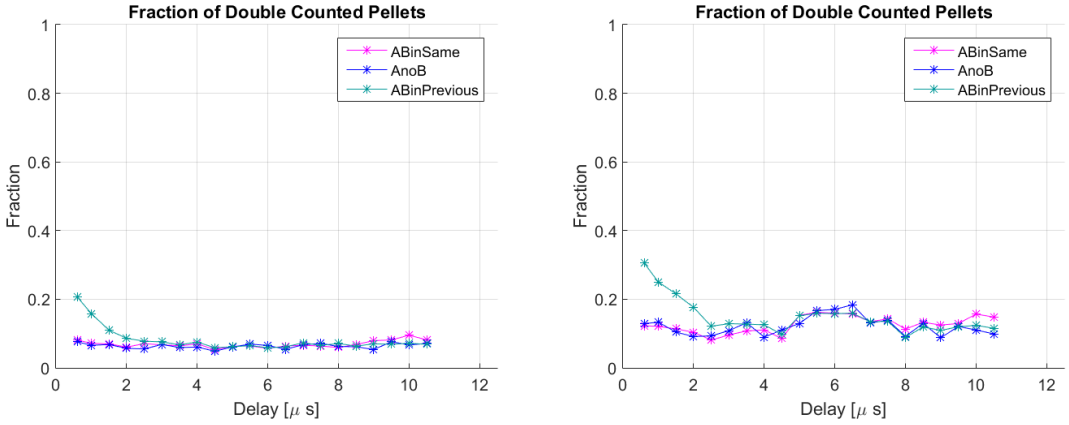

Figure C.3: The fraction of double counted pellets in the three classes *ABinSame*, *AnoB* and *ABinPrevious* from measurements with pellets and with LasC with a 10 mW power setting in the left plot and a 100 mW power setting in the right plot. The plots show the fraction of detected signal in each class (in the original data) which were counted twice and interpreted as two pellets.

The fraction of double counted pellets in each class for all cases shown in figures C.1-C.3 are quite similar (within the same plot) for all classes for a delay of around half an exposure cycle of the exposure cycle of CamB. However, for short delays of the exposure cycle of CamB, the fraction of double counted pellets in the class *ABinPrevious* is noticeably larger than the fraction of double counted pellets in the other two classes this is probably due to the low amount of pellets in total in the class *ABinPrevious* for shorter delays of the exposure cycle of CamB. There are indications that the fraction of double counted pellets in the class *ABinSame* is greater than the fraction of double counted pellets in the other two classes for a long delay of the exposure cycle of CamB.

The fraction of pellets in the class *ABinSame*, *AnoB* and *ABinPrevious* are shown in figures C.4-C.9 as a function of the delay of the exposure cycle of CamB for LasA, LasB and LasC separately and for a 10 mW and 100 mW power setting to the lasers. Both original data and data with the double counted pellets removed are presented. In all presented data, unsynchronized frames have been removed. For all measurements, the fraction of pellets detected by only CamA is greater for 10 mW input power than for 100 mW input power. This is the case for all lasers. This is also expected since the light signals from a higher intensity of the laser beam gets more intense and thereby more likely to be detected outside the dead time due to the light signal spilling over.

Figure C.4 shows that the signals counted twice and being interpreted as two pellets do not constitute a great inefficiency since the left and right plot with the double counted pellets removed look quite the same. However it does constitute a small inefficiency. Figures C.5 and C.6 show that the pellets counted twice do not constitute a great inefficiency since the left and right plot with the double counted pellets removed look quite the same in both figures. Figures C.7, C.8 and C.9 show that the double counted pellets do not constitute a great inefficiency since the left and right plot with the double counted pellets removed look quite the same in all figures. However, the plots differ somewhat for short values the delay of the exposure cycle of CamB in all figures.

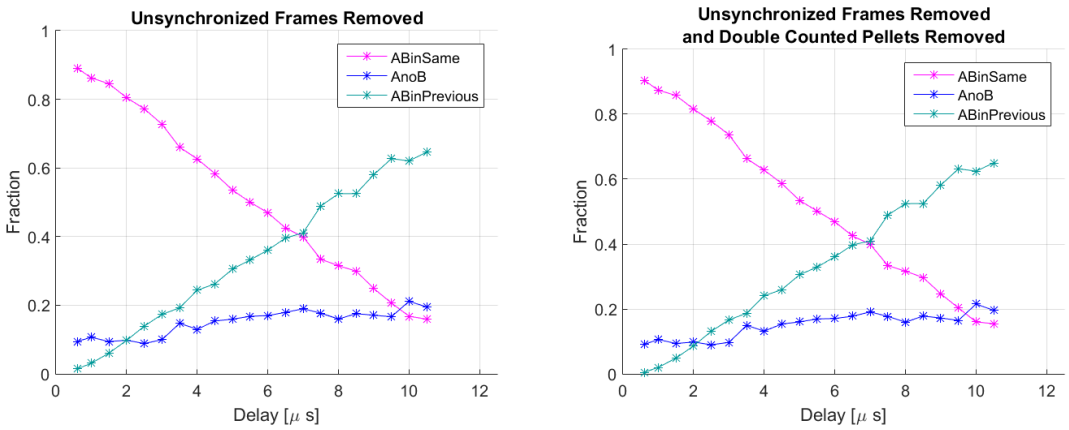

Figure C.4: The fraction of pellets in the three classes *ABinSame*, *AnoB* and *ABinPrevious* from measurements with pellets and with LasA with a 10 mW power setting. Original data with unsynchronized readout frames removed (left) and data with double counted pellets removed and unsynchronized readout frames removed (right).

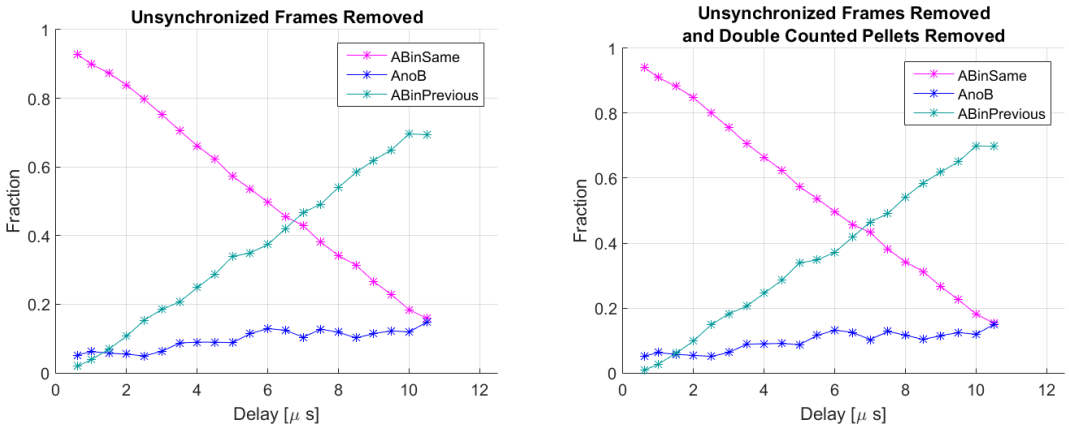

Figure C.5: The fraction of pellets in the three classes *ABinSame*, *AnoB* and *ABinPrevious* from measurements with pellets and with LasB with a 10 mW power setting. Original data with unsynchronized readout frames removed (left) and data with double counted pellets removed and unsynchronized readout frames removed (right).

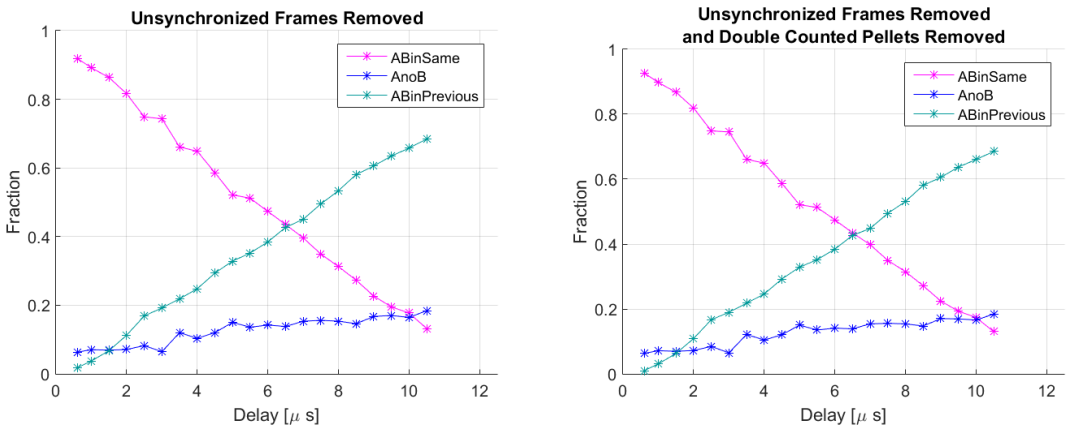

Figure C.6: The fraction of pellets in the three classes *ABinSame*, *AnoB* and *ABinPrevious* from measurements with pellets and with LasC with a 10 mW power setting. Original data with unsynchronized readout frames removed (left) and data with double counted pellets removed and unsynchronized readout frames removed (right).

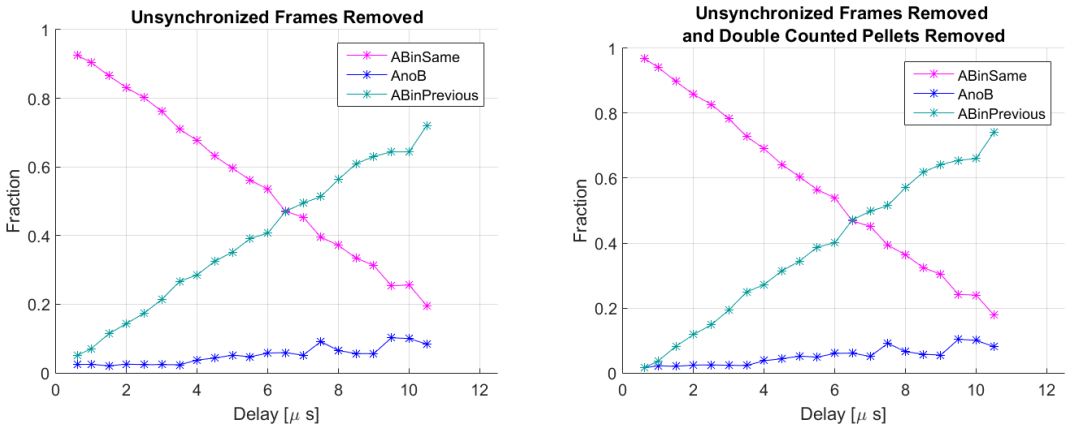

Figure C.7: The fraction of pellets in the three classes *ABinSame*, *AnoB* and *ABinPrevious* from measurements with pellets and with LasA with a 100 mW power setting. Original data with unsynchronized readout frames removed (left) and data with double counted pellets removed and unsynchronized readout frames removed (right).

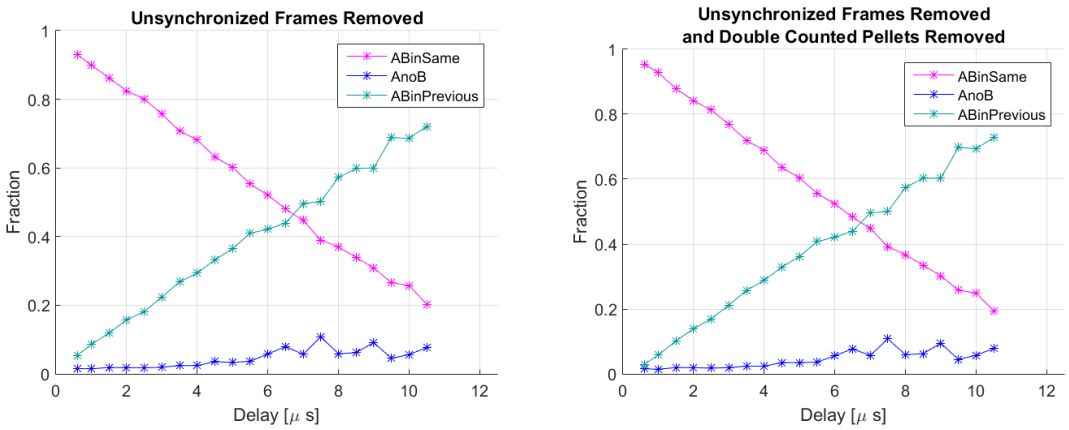

Figure C.8: The fraction of pellets in the three classes *ABinSame*, *AnoB* and *ABinPrevious* from measurements with pellets and with LasB with a 100 mW power setting. Original data with unsynchronized readout frames removed (left) and data with double counted pellets removed and unsynchronized readout frames removed (right).

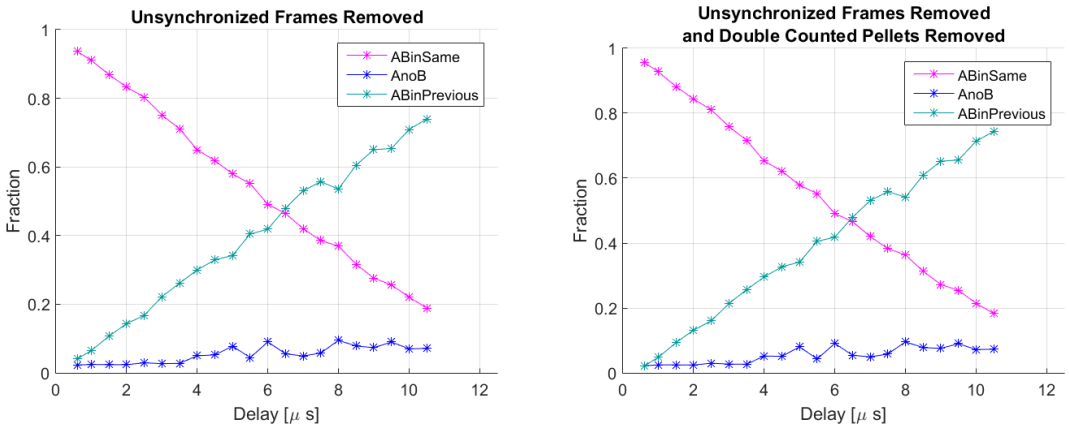

Figure C.9: The fraction of pellets in the three classes *ABinSame*, *AnoB* and *ABinPrevious* from measurements with pellets and with LasC with a 100 mW power setting. Original data with unsynchronized readout frames removed (left) and data with double counted pellets removed and unsynchronized readout frames removed (right).

Appendix D

List of Acronyms and some Abbreviations

ABinPrevious	Class in the shifted exposure cycles analysis consisting of the cases when CamB detect the same light signal in the previous readout line as compared to the readout line when CamA detects the light signal.
ABinSame	Class in the shifted exposure cycles analysis consisting of the cases when both cameras detect the same light signal in the same readout line (the lines which coincides in time when these is no relative shift).
AnoB	Class in the shifted exposure cycles analysis consisting of the cases when only CamA detects a light signal.
bl:	Camera lens aperture (bländare)
CamX	Name of camera X on the DM (as seen in figure 3.1)
CCD	Charge Coupled Device (a type of sensor widely used in cameras)
CELSIUS	(an accelerator and storage ring at TSL -2005)
COSY	COoler SYnchrotron (cooler synchrotron and storage ring at FZJ)
CYC	exposure cycle signal (signal defining the exposure cycles of the cameras)
DC	Droplet Chamber (chamber where the droplets are formed and travel)
DM	Detection Module
FAIR	Facility for Antiproton and Ion Research (research center in Darmstadt)
FG	Frame Grabber (used for reading out the camera images)

Frame	A set of camera images (typically 2024 lines)
FZJ	Forschungszentrum Jülich (research center in Jülich)
GSI	Gesellschaft für Schwerionenforschung (Centre for Heavy Ion Research in Darmstadt)
HESR	High Energy Storage Ring (storage ring at FAIR in Darmstadt)
LasX	Name of laser X on the DM (as seen in figure 3.1)
LED	Light Emitting Diode
LS camera	Line-Scan camera (CCD-cameras with one readout line of pixels)
MATLAB	MATrix LABoratory (Numerical computing environment)
NIM	Nuclear Instrument Module
PANDA	anti-Proton ANnihilation at DArmstadt (upcoming detector system at HESR)
PelletCounter	Computer analysis program used for analyzing data from pellet measurements
PC	Personal Computer
PTR	Pellet Tracking and where PTRxxx=pellet measurement level xxx (described in section 2.3)
PTS	Pellet Tracking Section
QCD	Quantum Chromodynamics (theory of the strong interaction)
ROOT	A data analysis framework
STR	Structured-Light-Pattern diode laser (a type of laser used on the DM)
TRIG	Trigger signal (signal which triggers the start of reading out a frame)
TSL	The Svedberg Laboratoriet (in Uppsala)
UPTS	Uppsala Pellet Test Station (at TSL)
VIC	Vacuum Injection Capillary (where the pellets are formed and injected into (high) vacuum)
WASA	Wide Angel Shower Apparatus (detector system built in Uppsala)
wxPropView	Camera monitoring program used for alignment of the cameras and lasers on the DM